UNIVERSITY OF CALIFORNIA, SAN DIEGO

The Effects of Ocean Acidification on the Development, Behavior and Survival of Marine Fish Eggs and Larvae Inferred from Laboratory and Natural Experiments

A dissertation submitted in partial satisfaction of the
requirements for the degree
Doctor of Philosophy

in

Oceanography

by

Sara Shen

Committee in charge:

Professor David Checkley, Jr., Chair
Professor Todd Martz
Professor Kaustuv Roy
Professor Stuart Sandin
Professor Martin Tresguerres

2016

The dissertation of Sara Shen is approved, and it is acceptable in quality and form for publication on microfilm and electronically:

_____

_____

_____

_____

Chair

University of California, San Diego

2016

DEDICATION

For my grandparents, Daniel and Sarah McCue, with love

TABLE OF CONTENTS

LIST OF FIGURES

LIST OF TABLES

ACKNOWLEDGEMENTS

The willpower, strength, and self-belief that have carried me through the completion of my undergraduate career and PhD come from the two greatest, loving, and self-giving people I know: my parents, Geraldine and Paul Walkup. All of my accomplishments, past and future, are possible because they have taught me the importance of setting goals and enduring the hardship it takes to achieve those goals. For this, and for teaching me love, empathy, and compassion, I am so grateful. I could not ask for a better friend than my sister, Nola Walkup. She has been a constant source of encouragement and has kept me tethered to the real world.

My life would not be the adventure it is today without my loving and brilliant husband, Brian Shen. Ten years ago, he introduced himself to me during the Davidson Dormitory Orientation, as I sat on the couch, sad that my parents had left and anxious about what the next four years at UC Berkeley would bring. From that moment forward, he has loved and supported me, traveled the world and shared in new experiences with me, and challenged me to think differently. He brings endless joy and happiness to my life and I love him so much. His family, Kathryn Wang, Christopher Sheng and David Shen, have welcomed me into their lives, and traveling to see them has provided many much-needed breaks over the years.

My friends have helped to keep me happy and motivated during my years in undergraduate and graduate school: Theresa Mongelluzzo, Alexandra Freibott, Tessa Pierce, Stacy Aguilera, Hadley McIntosh, Amanda Netburn, Elizabeth Sibert, Catherine Nickels, Ewa Gassmann, William Jones, Rebecca Asch, Sarah Parish, Helen Lockett, Karen Kim, Hannah Gelb, Stephen Awbrey, and so many others. I am thankful for the kindness and camaraderie of the 2010 cohort, especially during our two years of coursework and preparing for the departmental. I admire so many of the students at Scripps and thank them all for sharing their friendship and scientific expertise.

My advisor, Dave Checkley, has taught me most of what I know about biological and fisheries oceanography, and everything I know about being a good scientist. Although distressing at times, I am grateful that Dave continually challenged me to ask better questions, think more critically, consider other ways to interpret my data, find the greater importance of my work, be concise in my writing, and to be passionate in my speaking- all while 'KIS: Keeping It Simple.' Lastly, I am thankful that he trusted me to find my way through all of the challenges I encountered, and to emerge having learned so much more than just the story my data told. Much of what I have learned from trying to replicate his careful and thoughtful approach to science has helped me both professionally and personally. He has been a great mentor to me, and I am so grateful for his wisdom, expertise, and friendship.

My committee, Todd Martz, Kaustuv Roy, Stuart Sandin, and Martin Tresguerres have provided me with valuable insight and guidance. Their patience, expertise, and feedback on manuscripts, are immensely appreciated. I am especially grateful for the continual lessons in statistics and fish physiology provided by Stuart Sandin and Martin Tresguerres, respectively, over the years. Martin graciously allowed me unrestricted access to his laboratory resources, and his contribution to my third chapter was invaluable. I am thankful for the many informative conversations with professors at Scripps that opened my eyes to the breadth of exciting research.

Many organizations and institutions helped to fund my graduate studies and research, including the National Science Foundation Graduate Research Fellowship Program, Michael M. Mullin fellowship, Doherty fellowship, Teledyne RDI Instruments Academic Product Grant, SIO Department Graduate Student Excellence Research Award, and a SIO Teaching Assistant stipend. This financial support enabled me to travel to several conferences to present my data, and to spend two months on a fisheries research cruise off Peru collecting data for my dissertation. The staff of the Graduate Office and Integrative Oceanography Division helped with everyday logistics, and made travel arrangements and funding proposals

much easier: Gilbert Bretado, Hanna Choe, Iris Isla, Adam Peterson, Maureen McGreevy, Maureen McCormack and Christine Co.

Lastly, I must thank my coauthors: Patricia Ayón, Dave Checkley, Fangyi Chen, Jonathan Correa, Peer Fietzek, Garfield Kwan, David Schoppik, Andrew Thompson and Martin Tresguerres. All of these people helped me to gain a better understanding of the various aspects of my research. I especially want to thank Andrew for his friendship and mentorship. He was a constant source of inspiration and motivation. Garfield became a great friend while spending many hours together as I learned the physiological techniques for my third chapter. Collaborating with Paty and Jonathan at the Instituto del Mar del Perú and spending a month at sea was an unforgettable experience. I witnessed how data collected by government scientists formed the foundation of management actions at the federal level, and it was truly inspirational.

Chapter 2, in full, is a reprint of materials as they appear in Shen, S.G., Chen, F., Schoppik, D.E., and Checkley, D.M., Jr. (2016) Otolith size and the vestibulo-ocular reflex of larvae of white seabass *Atractoscion nobilis* at high pCO_2. Marine Ecology Progress Series, 553:173-183. The dissertation author was the primary investigator and author of this manuscript.

Chapter 3, in full, is in review as Shen, S.G., Thompson, A.R., Correa, J., Fietzek, P., Ayón, P., and Checkley, D.M., Jr. Spawning and mortality of Anchoveta *Engraulis ringens* eggs and larvae in relation to pCO_2. The dissertation author was the primary investigator and author of this manuscript.

Chapter 4, in full, is in preparation for publication as Shen, S.G., Kwan, G., Tresguerres, M., and Checkley, D.M., Jr. Physiological resilience of white seabass *Atractoscion nobilis* larvae to ocean acidification. The dissertation author was the primary investigator and author of this manuscript.

VITA

2010	Bachelor of Art, Earth and Planetary Science: Marine Science, University of California, Berkeley
2013	Master of Science, Marine Biology, Scripps Institution of Oceanography at the University of California, San Diego
2016	Doctor of Philosophy, Oceanography, Scripps Institution of Oceanography at the University of California, San Diego

PUBLICATIONS

Shen, S.G., Chen, F., Schoppik, D.E., and Checkley, D.M., Jr. (2016) Otolith size and the vestibulo-ocular reflex of larvae of white seabass *Atractoscion nobilis* at high pCO_2. Marine Ecology Progress Series, 553:173-183.

Shen, S.G., Thompson, A.R., Correa, J., Fietzek, P., Ayón, P., and Checkley, D.M., Jr. Spawning and mortality of Anchoveta *Engraulis ringens* eggs and larvae in relation to pCO_2. In Review.

ABSTRACT OF THE DISSERTATION

The Effects of Ocean Acidification on the Development, Behavior and Survival of Marine Fish Eggs and Larvae Inferred from Laboratory and Natural Experiments

by

Sara Shen

Doctor of Philosophy in Oceanography

University of California, San Diego, 2016

Professor David Checkley, Jr., Chair

The physiology, development, behavior and survival of the early life history stages of marine fish are challenged by increasing carbon dioxide concentrations in the ocean, known as ocean acidification. A widespread effect of elevated pCO_2 on fish larvae is increased otolith size. To understand the functional consequences of larger otoliths on the vestibular system of fish larvae, Chapter 2 investigated the vestibulo-ocular reflex (VOR) of white seabass (*Atractoscion nobilis*) larvae reared at $\sim$2500 µatm pCO_2. The VOR is an otolith-dependent response in fish that stabilizes vision during body movement. Larvae reared at high pCO_2 possessed saccular and utricular otoliths that were $\sim$ 17% and $\sim$ 38%

larger in size. Despite the increased otolith size, the gain of the VOR, which describes the ratio of eye to head amplitude, was not statistically different between treatment (0.39 ± 0.05, $n = 28$) and control (0.30 ± 0.03, $n = 20$) larvae.

Fish spawning habitat and survival of offspring are greatly influenced by environmental conditions. In Chapter 3, the effects of pCO_2 on the spawning habitat of Anchoveta (*Engraulis ringens*) and mortality of eggs and early stage larvae were investigated. Eggs, larvae, and oceanographic data, were collected across an onshore-offshore gradient in pCO_2 that ranged from 167-1392 µatm. pCO_2 was statistically significant in explaining egg presence. The abundance of eggs and relative absence of larvae at high pCO_2 suggests that Anchoveta preferentially spawned at high pCO_2 (>800 µatm) and that these eggs had lower survival.

Fish living in a high-pCO_2 world may have to spend more energy on acid-base balance. Chapter 4 explores the effects of elevated pCO_2 on the oxygen consumption rate (OCR) and abundance of Na^+-K^+-ATPase (NKA) proteins in white seabass larvae reared at $\sim$2000 µatm pCO_2. OCR, a proxy for aerobic metabolic rate, did not differ significantly between larvae reared at present-day (0.18 ± 0.03 µL O_2 individual^{-1} h^{-1}, $n = 80$) and future (0.19 ± 0.03 µL O_2 individual^{-1} h^{-1}, $n = 80$) pCO_2. Consistent with this finding, the relative abundance of NKA proteins that fuel important ion exchangers for acid-base balance did not differ between control and treatment larvae in Western blot and immunohistochemistry analyses. Mass and length were also unchanged at high pCO_2, suggesting larvae were physiologically robust in these variables to ocean acidification conditions.

Chapter 1

Introduction

1.1 Ocean Acidification

Humans are altering the state of our planet in unprecedented ways through deforestation, fossil fuel burning, and other consumptive activities that add carbon dioxide (CO_2) to the atmosphere and cause significant climate change. Furthermore, because the ocean constitutes approximately 70% of the Earth's surface area, increasing atmospheric CO_2 acts to increase the partial pressure of CO_2 (pCO_2) and alter the inorganic carbon chemistry of the ocean through a process known as ocean acidification (Orr *et al.* 2005, Doney *et al.* 2009).

As CO_2 enters the ocean, it reacts with water (H_2O) to form carbonic acid (H_2CO_3), which dissociates into bicarbonate (HCO_3^-) and hydrogen ions (H^+). The increase in the concentration of H^+ causes a reduction in pH, a measure of acidity, and gives rise to the term 'ocean acidification.' HCO_3^- dissociates into H^+ and carbonate ions (CO_3^{2-}), further reducing pH and calcium carbonate saturation state ($\Omega CaCO_3$), a thermodynamic property that describes the degree of saturation of seawater with respect to the mineral calcium carbonate (Doney *et al.* 2009).

Atmospheric CO_2 has increased from 278 to >400 parts per million (ppm) since

the industrial revolution (Orr *et al.* 2005, Doney *et al.* 2009) and is projected to exceed 1000 ppm by the end of the century and 1900 ppm by the year 2250 (IPCC 2013). The ocean has absorbed approximately 30% of current anthropogenic carbon emissions (Sabine *et al.* 2004) and the rate of absorption is outpacing that of the Earth's natural buffering from weathering and the preservation of seafloor $CaCO_3$sediments (Hönish *et al.* 2012). As a result, ocean pH has already declined 0.1 units and is expected to decline 0.3-0.32 units by 2100 (IPCC 2013).

While it is true that the concentration of CO_2 in the atmosphere has been much higher in the past than it is today, with estimates of 5000 µatm during the Triassic-Jurassic (T/J) boundary approximately 200 million years ago, it is the combination of the magnitude of increase and rate at which we are adding CO_2 that is unparalleled in Earth history (Hönish *et al.* 2012). During the T/J mass extinction, atmospheric CO_2 doubled over 20 thousand years, magnitudes slower than what is occurring presently (Hönish *et al.* 2012). Therefore, we are disrupting the equilibrium of the ocean carbon cycle in a way that has never occurred over the past 300 million years of Earth history (Hönish *et al.* 2012).

1.1.1 Effects on Young Fish

The multitude of correlated changes that occur in the carbonate chemistry during ocean acidification make it difficult to assess which variables are most severely affecting biota. The reduction in Ω may be the culprit for the decline in growth, calcification, abundance, and survival of many calcifying organisms (Kleypas *et al.* 1999, Kroeker *et al.* 2010, Bednaršek and Ohman 2015). Conversely, it is more likely that the increase in pCO_2 is the largest contributing factor to the effects of ocean acidification on marine fish because a reduced outward diffusion of CO_2 can lower the pH of internal fluids and disrupt pH homoeostasis (Hayashi *et al.* 2004, Ishimatsu *et al.* 2008, Esbaugh *et al.* 2012, Heuer and Grosell 2014).

Several physiological and behavioral differences between the early life history stages (i.e., eggs and larvae) of marine fish and juveniles and adults may increase the susceptibility of the former to ocean acidification. Briefly, this includes the lack of functional gills that are important for ion regulation, reliance on cutaneous diffusion for gas exchange (Rombough *et al.* 1988), and passive existence as plankton. The latter means that young larvae cannot escape exposure to poor environmental conditions. Importantly, high and variable mortality during the early life history stages, often related to environmental conditions, may be decisive in generating recruitment variability (Houde 2009).

The effects of elevated pCO_2 on marine fish eggs and larvae are diverse and variable (reviewed in Heuer and Grosell 2014). Elevated pCO_2, ranging from 800 to 5000 µatm can result in developmental abnormalities of larvae, such as tissue and organ damage, and changes to fatty acid composition (Chambers *et al.* 2013, Díaz-Gil *et al.* 2015, Frommel *et al.* 2016, others reviewed in Heuer and Grosell 2014). Larvae of some species experience an increase in size-at-hatch and growth rate (Munday *et al.* 2009a, Chambers *et al.* 2014, Bignami *et al.* 2014), while others experience a reduction or no change. Perhaps one of the most widespread developmental changes is the hypercalcification of otoliths (Checkley *et al.* 2009, Munday *et al.* 2011b, Bignami *et al.* 2013, Maneja *et al.* 2013, Réveillac *et al.* 2015, Shen *et al.* 2016). All bony fish possess three pairs of $CaCO_3$ otoliths that play a vital role in the auditory and vestibular systems, the latter providing vertebrates with information about orientation and acceleration (Platt 1983, Goldberg *et al.* 2012). A 49% increase in otolith size of larval cobia (*Rachycentron canadum*) reared at 2100 µatm was predicted to increase hearing range by 50% (Bignami *et al.* 2013). In Chapter 2, I explore the effects of elevated pCO_2 and hypercalcification on the vestibular system of white seabass larvae (*Atractoscion nobilis*).

The impairment of numerous sensory systems and general cognitive function of the larvae and juveniles of several species of fish is indicative of an effect of pCO_2 on central

neural processing. Exposure to elevated pCO_2 reverses the attraction of young (mostly tropical) fish to the odors and sounds of predators (Dixson *et al.* 2010, Simpson *et al.* 2011) and favorable settlement habitats (Munday *et al.* 2009b, Devine *et al.* 2012, Rossi *et al.* 2015). The larvae of some species also demonstrate a reduction in anti-predator responses (Ferrari *et al.* 2011), lateralization (Domenici *et al.* 2012) and learning capacity (Ferrari *et al.* 2012). The alteration of the γ-aminobutyric acid ($GABA_A$) neurotransmitter receptor in the brain is thought to be the primary cause of the reversal of these sensory preferences and behavioral changes (Nilsson *et al.* 2012, Hamilton *et al.* 2014). However, there are also many species of fish that do not experience any negative effects of elevated pCO_2 on growth, development, behavior and survival during the egg and larvae stages (Munday *et al.* 2009a, 2011a, 2015, Franke and Clemmesen 2011, Frommel *et al.* 2013, Bignami *et al.* 2014 Hurst *et al.* 2012).

The effects of high CO_2 on the mortality of the early life history stages and the consequences for larger-scale population and ecosystem structure are hard to predict, especially given the fact that some species of fish are affected by ocean acidification conditions more than others. Settlement-stage damselfish (*Pomacentrus wardi*) larvae reared at elevated pCO_2 (700-850 μ) with a compromised olfactory system and reduced anti-predator response behavior experienced 5-9 times higher mortality than control larvae (Munday *et al.* 2010, Ferrari *et al.* 2011). On the contrary, attraction to predator odor, inability to differentiate among odors of different habitats, and bold behavior observed for damselfish and cardinalfish at natural CO_2 seeps did not result in any changes to fish abundance (Munday *et al.* 2014). Furthermore, while elevated pCO_2 increases the mortality of eggs and larvae of some species (Baumann *et al.* 2012, Forsgren *et al.* 2013, Chambers *et al.* 2013), presumably through direct effects on physiology, it can also increase the reproductive output (number of clutches and eggs per clutch) and survival of eggs for other (mostly benthic spawning) species (Miller *et al.* 2013, Welch and Munday 2016). In Chapter 3, I investigate

whether high pCO_2 affects the spawning and mortality of pelagic eggs and young larvae of Anchoveta (*Engraulis ringens*) off the coast of Peru.

Ocean acidification can present a physiological challenge for marine fish because the reduced outward diffusion gradient of CO_2 from the body to the seawater can result in higher CO_2 and lower pH in the blood plasma and intracellular fluids (Perry and Gilmour 2006). Much literature exists for freshwater fish documenting that juveniles and adults compensate for this acid-base disruption through the uptake or retention of HCO_3^- and export of H^+ using a variety of ion-transporters that are fueled by ion gradients created by Na^+-K^+-ATPase (NKA) in the mitochondria-rich cells of the gills (Perry and Gilmour 2006, Melzner *et al.* 2009a). Mechanisms for saltwater fish are less understood but likely include similar transporters in the exchange of acid-base equivalents. Maintaining pH homeostasis is an energetically costly process, but an important one as changes in pH can impact cellular function, metabolism, and eventually the growth and reproduction of fish (Putnam and Roos 1997, Pörtner *et al.* 2005). For example, NKA pumping for NaCl excretion can account for as much as $\sim$25% of the oxygen consumption of the gills in marine fish (Stagg and Shuttleworth 1982, Morgan *et al.* 1997). The gradients generated by NKA are used in the transport of acid-base equivalents. Therefore, the additional cost of maintaining ion and acid-base regulation at elevated pCO_2 may be reflected in an increased oxygen consumption rate (OCR), a proxy for the metabolic rate (Munday *et al.* 2009c, Enzor *et al.* 2013), as well as increased abundance of NKA proteins (Deigweiher *et al.* 2008, Melzner *et al.* 2009b). In Chapter 4, I investigate how the OCR and abundance of NKA proteins in larval white seabass are affected by elevated pCO_2.

1.2 Outline of the Dissertation

The research in this dissertation furthers our understanding of the effects of ocean acidification on the early life history stages of marine fish through multiple experiments

performed at various scales, from an investigation of cellular to whole-animal behavioral responses in laboratory experiments to that of a large fish population in a high-pCO_2 upwelling system and natural experiment.

In Chapter 2, I focused on the effects of elevated pCO_2 on otolith morphology and functionality in larval white seabass (*Atractoscion nobilis*). There are several studies that have documented larger otoliths in larvae reared under acidified conditions (Checkley *et al.* 2009, Munday *et al.* 2011b, Bignami *et al.* 2013, Réveillac *et al.* 2015, Shen *et al.* 2016), but the effects on the vestibular system have not been explored. I hypothesized that elevated pCO_2 would increase the size of the utricular otoliths of white seabass larvae and this would affect vestibular functioning. To test these hypotheses, I reared white seabass eggs and larvae at 2500 atm pCO_2, determined the area of the utricular otoliths, and tested an otolith-dependent response, the vestibulo-ocular reflex (VOR). The VOR is a compensatory eye rotation that is stimulated by otolith movement and allows fish and other vertebrates to maintain their visual acuity during self-movement (Bianco *et al.* 2012, Goldberg *et al.* 2012). From these results, I made inferences about the potential effects of larger-sized otoliths on the vestibular function and survival of marine fish larvae.

In Chapter 3, eggs and larvae of Anchoveta (*Engraulis ringens*) and oceanographic data were collected off the coast of Peru during a cruise by the Instituto del Mar del Perú (Imarpe) in August and September 2013. The cruise study area spanned 10° latitude (1,112 km) and occurred during the peak season for upwelling and Anchoveta spawning. In this chapter, I used the natural onshore-offshore gradient in pCO_2 to investigate the relationship of Anchoveta eggs and larvae to pCO_2, and make inferences about the effects of ocean acidification on coastal marine fish. Anchoveta are an ideal study organism because they constitute the world's largest single-species fishery (FAO 2015), live in one of the highest pCO_2 regions in the world's ocean (Takahashi *et al.* 2009), and have a similar life history to other pelagic fish species. The relative importance of environmental variables in explaining

egg presence, an index of spawning, and larva abundance were explored using generalized linear mixed models. Furthermore, the distributions of the largest egg and larva samples were analyzed in pCO_2-salinity space to investigate the potential mortality of eggs and larvae in high pCO_2 waters.

In Chapter 4, the physiological effects of elevated pCO_2 on larval white seabass (*Atractoscion nobilis*) were investigated to gain insight into the possible underlying causes of the wide range of behavioral and developmental abnormalities in fish exposed to ocean acidification conditions (reviewed in Heuer and Grosell 2014). Although the mechanisms of acid-base regulation for larvae are unknown, they are assumed to be similar to those of juveniles and adults (Rombough *et al.* 1988). I hypothesized that white seabass larvae reared at elevated pCO_2 would experience an increase in OCR and abundance of NKA proteins to compensate for internal acid-base disruption. To test these hypotheses, I reared white seabass eggs and larvae at 2000µatm pCO_2, measured the oxygen consumption of larvae at 5 days post-fertilization (dpf), and used Western Blot and immunohistochemistry analysis to quantify the abundance of NKA proteins. These data provide insight into the energetic costs of maintaining acid-base balance and the physiological resiliency of fish larvae to elevated pCO_2.

1.3 References

Baumann H, Talmage SC, Gobler CJ (2012) Reduced early life growth and survival in a fish in direct response to increased carbon dioxide. Nature Climate Change, 2:38-41.

Bednaršek N, Ohman MD (2015) Changes in pteropod distributions and shell dissolution across a frontal system in the California Current System. Marine Ecology Progress Series, 523:93-103.

Bianco IH, Ma LH, Schoppik D, Robson DN, Orger MB, Beck JC, Li JM, Schier AF, Engert F, Baker R (2012) The tangential nucleus controls a gravito-inertial vestibulo-ocular reflex. Current Biology, 22:1285-1295.

Bignami S, Enochs IC, Manzello DP, Sponaugle S, Cowen RK (2013) Ocean acidification alters the otoliths of a pantropical fish species with implications for sensory function. Proceedings of the National Academy of Sciences, 110:7366-7370.

Bignami S, Sponaugle S, Cowen RK (2014) Effects of ccean acidification on the larvae of a high-value fisheries species, Mahi mahi *Coryphaena hippurus*. Aquatic Biology, 21:249260.

Chambers RC, Candelmo AC, Habeck EA, Poach ME, Wieczorek D, Cooper KR, Greenfield CE, Phelan BA (2014) Effects of elevated CO_2 in the early life stages of summer flounder, *Paralichthys dentatus*, and potential consequences of ocean acidification. Biogeosciences, 11:1613-1626.

Checkley DM Jr, Dickson AG, Takahashi M, Radich JA, Eisenkolb N, Asch R (2009) Elevated CO_2 enhances otolith growth in young fish. Science, 324:1683-1683.

Deigweiher K, Koschnick N, Pörtner HO, Lucassen M (2008) Acclimation of ion regulatory capacities in gills of marine fish under environmental hypercapnia. American Journal of Physiology-Regulatory, Integrative and Comparative Physiology, 295:R1660-R1670.

Devine BM, Munday PL, Jones GP (2012) Rising CO_2 concentrations affect settlement behaviour of larval damselfishes. Coral Reefs, 31:229238.

Díaz-Gil C, Catalán IA, Palmer M, Faulk CK, Fuiman LA (2015). Ocean acidification increases fatty acids levels of larval fish. Biology Letters, 11:20150331.

Dixson DL, Munday PL, Jones GP (2010) Ocean acidification disrupts the innate ability of fish to detect predator olfactory cues. Ecology Letters, 13:68-75.

Domenici P, Allan B, McCormick MI, Munday PL (2012) Elevated carbon dioxide affects behavioural lateralization in a coral reef fish. Biology Letters, 8:78-81.

Doney SC, Fabry VJ, Feely RA, Kleypas JA (2009) Ocean acidification: the other CO_2 problem. Annual Review of Marine Science, 1:169-192.

Enzor LA, Zippay ML, Place SP (2013) High latitude fish in a high CO_2 world: synergistic effects of elevated temperature and carbon dioxide on the metabolic rates of Antarctic notothenioids. Comparative Biochemistry and Physiology Part A: Molecular and Integrative Physiology, 164:154-161.

Esbaugh AJ, Heuer R, Grosell M (2012) Impacts of ocean acidification on respiratory gas exchange and acidbase balance in a marine teleost, *Opsanus beta*. Journal of Comparative Physiology B, 182:921-934.

Ferrari MC, Dixson DL, Munday PL, McCormick MA, Meekan MG, Sih A, Chivers DP (2011) Intrageneric variation in antipredator responses of coral reef fishes affected by ocean acidification: implications for climate change projections on marine communities. Global Change Biology, 17:2980-2986.

Ferrari MC, Manassa RP, Dixson DL, Munday PL, McCormick MI, Meekan MG, Sih A, Chivers DP (2012) Effects of ocean acidification on learning in coral reef fishes. PLoS One, 7:e31478.

Fisheries and Aquaculture topics. The State of World Fisheries and Aquaculture (SOFIA). Topics Fact Sheet. Text by Jean-Francois Pulvenis. In: FAO Fisheries and Aquaculture Department (online. Rome. Updated 19 May 2015).

Forsgren E, Dupont S, Jutfelt F, Amundsen T (2013) Elevated CO_2 affects embryonic development and larval phototaxis in a temperate marine fish. Ecology and Evolution, 3:3637-3646.

Franke A, Clemmesen C (2011) Effect of ocean acidification on early life stages of Atlantic herring (*Clupea harengus* L.). Biogeosciences, 8:3697-3707.

Frommel AY, Schubert A, Piatkowski U, Clemmesen C (2013) Egg and early larval stages of Baltic cod, *Gadus morhua*, are robust to high levels of ocean acidification. Marine Biology, 160:1825-1834.

Frommel AY, Margulies D, Wexler JB, Stein MS, Scholey VP, Williamson JE, Bromhead D, Nicol S, Havenhand J (2016) Ocean acidification has lethal and sub-lethal effects on larval development of yellowfin tuna, *Thunnus albacares*. Journal of Experimental Marine Biology and Ecology, 482:18-24.

Goldberg JM, Wilson VJ, Cullen KE (2012) The Vestibular System: A Sixth Sense, PP. 560,

Oxford University Press, New York.

Hamilton TJ, Holcombe A, Tresguerres M (2014) CO_2induced ocean acidification increases anxiety in Rockfish via alteration of $GABA_A$ receptor functioning. Proceedings of the Royal Society B: Biological Sciences, 281:20132509.

Hayashi M, Kita J, Ishimatsu A (2004) Comparison of the acid-base responses to CO_2 and acidification in Japanese flounder (*Paralichthys olivaceus*). Marine Pollution Bulletin, 49:1062-1065.

Heuer RM, Grosell M (2014) Physiological impacts of elevated carbon dioxide and ocean acidification on fish. American Journal of Physiology-Regulatory, Integrative and Comparative Physiology, R1061-R1084.

Hönisch B, Ridgwell A, Schmidt DN, Thomas E, Gibbs SJ, Sluijs A, Zeebe R, Kump L, Martindale RC, Greene SE, Kiessling W, Ries J, Zachos JC, Royer DL, Barker S, Marchitto TM Jr., Moyer R, Pelejero C, Ziveri P, Foster GL, Williams B (2012) The geological record of ocean acidification. Science, 335:10581063.

Houde ED (2009) Recruitment variability. In Fish Reproductive Biology: Implications for Assessment and Management, PP.91-171, Wiley-Blackwell, West Sussex, UK.

Hurst TP, Fernande ER, Mathis JT, Miller JA, Stinson CM, Ahgeak EF (2012). Resiliency of juvenile walleye pollock to projected levels of ocean acidification. Aquatic Biology, 17:247259.

IPCC (2013) Climate change 2013: the physical science basis, Chapter 6. In: Stocker TF, Qin D, Plattner GK, Tignor M and others (Eds.), Contribution of working group 1 to the fifth assessment report of the Intergovernmental Panel on Climate Change, PP. 465-544, Cambridge University Press, Cambridge.

Ishimatsu A, Hayashi M, Kikkawa T (2008) Fishes in high-CO_2, acidified oceans. Marine Ecology Progress Series, 373:295-302.

Kleypas JA, Buddemeier RW, Archer D, Gattuso JP, Langdon C, Opdyke BN (1999) Geochemical consequences of increased atmospheric carbon dioxide on coral reefs. Science, 284:118-120.

Kroeker KJ, Kordas RL, Crim R, Hendricks IE, Ramajo L, Singh GS, Duarte CM, Gattuso J-P (2013) Impacts of ocean acidification on marine organisms: quantifying sensitivities and interaction with warming. Global Change Biology, 19:1884-1896.

Maneja RH, Frommel AY, Geffen AJ, Folkvord A, Piatkowski U, Chang MY, Clemmesen C

(2013) Effects of ocean acidification on the calcification of otoliths of larval Atlantic cod *Gadus morhua*. Marine Ecology Progress Series, 477:251-258.

Melzner F, Gutowska MA, Langenbuch M, Dupont S, Lucassen M, Thorndyke MC, Bleich M, Portner H-O (2009a) Physiological basis for high CO_2 tolerance in marine ectothermic animals: pre-adaptation through lifestyle and ontogeny. Biogeosciences, 6:2313-2331.

Melzner F, Göbel S, Langenbuch M, Gutowska MA, Pörtner HO, Lucassen M (2009b) Swimming performance in Atlantic Cod (*Gadus morhua*) following long-term (4-12 months) acclimation to elevated seawater pCO_2. Aquatic Toxicology, 92:30-37.

Miller GM, Watson SA, Donelson JM, McCormick MI, Munday PL (2012) Parental environment mediates impacts of increased carbon dioxide on a coral reef fish. Nature Climate Change, 2:858-861.

Miller GM, Watson SA, McCormick MI, Munday PL (2013) Increased CO_2 stimulates reproduction in a coral reef fish. Global Change Biology, 19:3037-3045.

Morgan JD, Iwama GK, Wilson JM (1997) Oxygen consumption and Na^+, K^+-ATPase activity of rectal gland and gill tissue in the spiny dogfish, *Squalus acanthias*. Canadian Journal of Zoology, 75:820-825.

Munday PL, Donelson JM, Dixson DL, Endo GGK (2009a) Effects of ocean acidification on the early life history of a tropical marine fish. Proceedings of the Royal Society B: Biological Sciences, 276:32753283.

Munday PL, Dixson DL, Donelson JM, Jones GP, Pratchett MS, Devitsina GV, Doving KB (2009b) Ocean acidification impairs olfactory discrimination and homing ability of a marine fish. Proceedings of the National Academy of Sciences, 106:1848-1852.

Munday PL, Crawley NE, Nilsson GE (2009c) Interacting effects of elevated temperature and ocean acidification on the aerobic performance of coral reef fishes. Marine Ecology Progress Series, 388:235-242.

Munday PL, Dixson DL, McCormick MI, Meekan M, Ferrari MC, Chivers DP (2010) Replenishment of fish populations is threatened by ocean acidification. Proceedings of the National Academy of Sciences, 107:12930-12934.

Munday PL, Gagliano M, Donelson JM, Dixson DL, Thorrold SR (2011a) Ocean acidification does not affect the early life history development of a tropical marine fish. Marine Ecology Progress Series, 423:211-221.

Munday PL, Hernaman V, Dixson DL, Thorrold SR (2011b) Effect of ocean acidification

on otolith development in larvae of a tropical marine fish. Biogeosciences, 8:1631-1641.

Munday PL, Cheal AJ, Dixson DL, Rummer JL, Fabricius KE (2014) Behavioural impairment in reef fishes caused by ocean acidification at CO_2 seeps. Nature Climate Change 4, 487-492.

Munday PL, Watson S-A, Parsons DM, King A (2015) Effects of elevated CO_2 on early life history developmnet of the yellowtail kingfish, *Seriola lalandi*, a large pelagic fish. ICES Journal of Marine Science 73, 641-649.

Nilsson GE, Dixson DL, Domenici P, McCormick MI, Sorensen C, Watson SA, Munday PL (2012) Near-future carbon dioxide levels alter fish behavior by interfering with neurotransmitter function. Nature Climate Change, 2:201-204.

Orr JC, Fabry VJ, Aumont O, Bopp L, Doney SC, Feely RA, Gnanadesikan A, Gruber N, Ishida A, Joos F, Key RM, Lindsay K, Maier-Reimer E, Matear R, Monfray P, Mouchet A, Najjar RG, Plattner G-K, Rodgers KB, Sabine CL, Sarmiento JL, Schiltzer R, Slater RD, Totterdell IJ, Weirig M-F, Yamanaka Y, Yool A (2005) Anthropogenic ocean acidification over the twenty-first century and its impact on calcifying organisms. Nature, 437:681-686.

Perry SF, Gilmour KM (2006) Acid-base balance and CO_2 excretion in fish: unanswered questions and emerging models. Respiratory Physiology and Neurobiology, 154:199-215.

Pimentel MS, Faleiro F, Dionísio G, Repolho T, Pousão-Ferreira P, Machado J, Rosa R (2014a) Defective skeletogenesis and oversized otoliths in fish early stages in a changing ocean. Journal of Experimental Biology, 217:2062-2070.

Pimentel M, Pegado M, Repolho T, Rosa R (2014b) Impact of ocean acidification in the metabolism and swimming behavior of the dolphinfish (*Coryphaena hippurus*) early larvae. Marine Biology, 161:725-729.

Platt C (1983) The peripheral vestibular system of fishes. Fish Neurobiology, 1:89-123.

Pörtner HO, Langenbuch M, Michaelidis B (2005) Synergistic effects of temperature extremes, hypoxia, and increases in CO_2 on marine animals: from Earth history to global change. Journal of Geophsyical Research, 110:C09S10.

Putnam RW, Roos A (1997) Intracellular pH. In Handbook of Physiology, Cell Physiology, PP. 389-440, Oxford University Press, New York

Réveillac E, Lacoue-Labarthe T, Oberhänsli F, Teyssié J-L, Jeffree R, Gattuso J-P, Martin S (2015) Ocean acidification reshapes the otolith-body allometry of growth in juvenile seabream. Journal of Experimental Marine Biology and Ecology, 463:87-94.

Rombough P (1988) Respiratory gas exchange, aerobic metabolism, and effects of hypoxia during early life. In: The Physiology of Developing Fish, PP.59-161, Academic Press, San Diego, CA.

Rossi T, Nagelkerken I, Simpson SD, Pistevos JC, Watson SA, Merillet L, Fraser P, Munday PL, Connell SD (2015) Ocean acidification boosts larval fish development but reduces the window of opportunity for successful settlement. Proceedings of the Royal Society B: Biological Sciences, 282:20151954.

Sabine CL, Feely RA, Gruber NA, Key RM, Lee K, Bullister JL, Wanninkhof R, Wong C, Wallace DW, Tilbrook B, Millero FJ (2004) The oceanic sink for anthropogenic CO_2. Science, 305:367-371.

Shen SG, Chen F, Schoppik DE, Checkley Jr DM (2016) Otolith size and the vestibulo-ocular reflex of larvae of white seabass *Atractoscion nobilis* at high pCO_2. Marine Ecology Progress Series, 553:173-183.

Simpson SD, Munday PL, Wittenrich ML, Manassa R, Dixson DL, Gagliano M, Yan HY (2011) Ocean acidification erodes crucial auditory behaviour in a marine fish. Biology Letters, 7:917-920.

Stagg RM, Shuttleworth TJ (1982) The effects of copper on ionic regulation by the gills of the seawater-adapted flounder (*Platichthys flesus* L.). Journal of Comparative Physiology, 149:83-90.

Takahashi T, Sutherland SC, Wanninkhof R, Sweeney C, Feely RA, Chipman DW, Hales B, Friederich G, Chavez F, Sabine C, Watson A (2009) Climatological mean and decadal change in surface ocean pCO_2, and net sea-air CO_2 flux over the global oceans. Deep Sea Research Part II: Top Studies in Oceanography, 56:554-577.

Welch MJ, Munday PL (2016) Contrasting effects of ocean acidification on reproduction in reef fishes. Coral Reefs, 35:485-493.

Chapter 2

Otolith size and the vestibulo-ocular reflex of larvae of white seabass (*Atractoscion nobilis*) at high pCO_2

Vol. 553: 173–183, 2016
doi: 10.3354/meps11791

MARINE ECOLOGY PROGRESS SERIES
Mar Ecol Prog Ser

Published July 14

Otolith size and the vestibulo-ocular reflex of larvae of white seabass *Atractoscion nobilis* at high pCO_2

Sara G. Shen[1,*], Fangyi Chen[2], David E. Schoppik[3], David M. Checkley Jr.[1]

[1]Scripps Institution of Oceanography, University of California San Diego, La Jolla, CA 92093, USA
[2]Department of Biology, South University of Science and Technology of China, Shenzhen, Guangdong 518055, PR China
[3]Department of Physiology and Neuroscience, New York University School of Medicine, New York, NY 10016, USA

ABSTRACT: We investigated vestibular function and otolith size (OS) in larvae of white seabass *Atractoscion nobilis* exposed to high partial pressure of CO_2 (pCO_2) The context for our study is the increasing concentration of CO_2 in seawater that is causing ocean acidification (OA). The utricular otoliths are aragonitic structures in the inner ear of fish that act to detect orientation and acceleration. Stimulation of the utricular otoliths during head movement results in a behavioral response called the vestibulo-ocular reflex (VOR). The VOR is a compensatory eye rotation that serves to maintain a stable image during movement. VOR is characterized by gain (ratio of eye amplitude to head amplitude) and phase shift (temporal synchrony). We hypothesized that elevated pCO_2 would increase OS and affect the VOR. We found that the sagittae and lapilli of young larvae reared at 2500 µatm pCO_2 (treatment) were 14 to 20% and 37 to 39% larger in area, respectively, than those of larvae reared at 400 µatm pCO_2 (control). The mean gain of treatment larvae (0.39 ± 0.05, n = 28) was not statistically different from that of control larvae (0.30 ± 0.03, n = 20), although there was a tendency for treatment larvae to have a larger gain. Phase shift was unchanged. Our lack of detection of a significant effect of elevated pCO_2 on the VOR may be a result of the low turbulence conditions of the experiments, large natural variation in otolith size, calibration of the VOR or mechanism of acid–base regulation of white seabass larvae.

KEY WORDS: Ocean acidification · Fish larvae · Otolith · Vestibulo-ocular reflex · pCO_2

INTRODUCTION

Humans are disrupting the equilibrium of the ocean carbon cycle at a greater magnitude and rate than nature has achieved over the past 300 million years of Earth history (Hönisch et al. 2012). Ocean acidification (OA) is the increase in surface seawater partial pressure of CO_2 (pCO_2) and decrease in pH and calcium carbonate saturation state (Ω) caused by the imbalance in the rates of addition to the ocean of carbon by the burning of fossil fuels and alkalinity by weathering (Doney et al. 2009, Hönisch et al. 2012). Humans have released 555 Pg of carbon into the atmosphere through fossil fuel burning since the Industrial Revolution, increasing atmospheric pCO_2 from 278 to >400 ppm today and decreasing pH by 0.10 units (Doney et al. 2009, IPCC 2013). Atmospheric pCO_2 is projected to exceed 1000 ppm by the end of the century and 1900 ppm by the year 2250 under the Intergovernmental Panel on Climate Change (IPCC) business-as-usual (Representative Concentration Pathway 8.5) scenario, further decreasing pH by 0.30 to 0.77 units (Caldeira & Wickett 2003, IPCC 2013).

The effects of OA on marine fish are diverse (see review by Heuer & Grosell 2014), variable and most severe during the early life-history stages (Rombough 1988, Tseng et al. 2013). The dynamics of these stages are critical in determining future population size and recruitment success (Houde 1997). Experiments show that elevated pCO_2 can influence growth (Munday et al. 2009a, Baumann et al. 2012), condition (Franke & Clemmesen 2011, Frommel et al.

*Corresponding author: sgshen@ucsd.edu

Publisher: Inter-Research · www.int-res.com

2012) and mortality (Baumann et al. 2012, Chambers et al. 2014) of fish eggs and larvae. Altered auditory (Simpson et al. 2011), olfactory (Munday et al. 2009b, Devine et al. 2012) and visual (Forsgren et al. 2013, Chung et al. 2014) sensory abilities that have resulted in behavioral changes are thought to be the result of modifications to the γ-aminobutyric acid ($GABA_A$) neurotransmitter receptor in the brain (Nilsson et al. 2012, Hamilton et al. 2014). Another widespread effect of elevated pCO_2 is the increase in otolith size (OS) (Checkley et al. 2009, Munday et al. 2011, Bignami et al. 2013a, Réveillac et al. 2015).

Otoliths are aragonitic structures underlain by sensory hair cells located in the inner ear of fish, and play a vital role in the auditory and vestibular systems (Platt 1983, Popper et al. 2005). The vestibular system provides vertebrates with information about orientation and acceleration (Goldberg et al. 2012). Fish have 3 pairs of otoliths: the sagittae, lapilli and asterisci. The saccular otoliths (sagittae) are generally thought to be involved in hearing and the utricular otoliths (lapilli) in vestibular function (Platt 1983, Riley & Moorman 2000, Straka & Dieringer 2004). Otoliths are approximately 3 times denser than the fish body, causing them to lag the movement of the underlying sensory epithelium during acceleration. Movement of the otolith relative to the hair cells causes the latter to bend and send mechanically induced signals related to orientation and acceleration to the brainstem (Popper et al. 2005).

Fish have evolved with otoliths optimized for their motor activity and environment. Mathematical models of otolith displacement by Lychakov & Rebane (2000) suggest that there are ecomorphological adaptations to otolith morphology that are a result of the ecology and behavior of fish. For example, the otoliths of pelagic fish are relatively small and the fish only moderately sensitive to acceleration, because they experience a limited and relatively uniform range of acceleration while swimming in an unobstructed environment. Conversely, darting demersal fish that accelerate rapidly have larger otoliths and the fish are more sensitive to acceleration. In general, models predict that larger otoliths move more and with a longer lag than smaller otoliths in response to stimuli.

Given the ecological constraints on otolith morphology for optimal functioning, deviations from the ideal morphology can negatively affect fish. For example, fish with naturally asymmetric otoliths experience impaired auditory (Gagliano et al. 2008) and vestibular (Helling et al. 2003) functioning. Furthermore, experimentally enlarged utricular otoliths of zebrafish *Danio rerio* acquired the sense of sound (Inoue et al. 2013). In the context of OA, larval cobia *Rachycentron canadum* reared at 2100 µatm pCO_2 and possessing larger sagittae are predicted to experience a 50% increase in hearing range compared to control larvae (Bignami et al. 2013a). Therefore, it might be expected that changes to the lapilli would result in altered vestibular functioning.

The vestibulo-ocular reflex (VOR) is a compensatory eye rotation used to maintain visual acuity during self-motion (Goldberg et al. 2012). The precision of VOR performance is commonly measured by 2 variables: gain, the ratio of eye amplitude to head amplitude, and phase shift, the temporal synchrony between head and eye movements (Goldberg et al. 2012). The VOR is stimulated by the movements of the otoliths and endolymph in the semi-circular canals. It comprises a '3-neuron arc', in which primary afferent neurons convey signals from sensory hair cells to secondary vestibular neurons in the vestibular nuclei in the brainstem, which in turn project to ocular motoneurons that innervate the extraocular muscles of the eyes (Szentagothai 1950, Goldberg et al. 2012). The result is a counter-rotation of the eyes of equal amplitude and opposite velocity to head movement, in order to stabilize images on the retina in relation to the Earth's geoid.

The VOR is plastic, meaning that it can maintain a modified state for long periods of time without reinforcement (Miles & Lisberger 1981). For example, when head movement results in image motion, the visual system sends error messages in the form of retinal slip signals (Miles & Lisberger 1981). Together with the vestibular signals, these signals are processed in the cerebellum to adjust the activity of the vestibular nuclei neurons in order to modify the gain (Miles & Lisberger 1981). In this way, the VOR operates as an open-loop system and requires calibration by the visual system (Miles & Lisberger 1981). It is not until 3 d post-fertilization (dpf) that zebrafish begin to demonstrate a VOR in response to rotation around an Earth-horizontal axis at a range of frequencies (Riley & Moorman 2000, Mo et al. 2010, Bianco et al. 2012). The gain of the VOR is low (<0.5) for newly hatched animals and increases through ontogeny, eventually approaching a value of 1 (full compensation) for adult goldfish (Wallman et al. 1982, Pastor et al. 1992). The VOR of fish may be more plastic than most other vertebrates (Pastor et al. 1992) as, unlike other vertebrates, fish possess otoliths that grow continuously throughout their lifetime (Pannella 1971). This fact requires that the VOR be constantly recalibrated during otolith growth.

Young fish larvae provide the opportunity to study the utricular otoliths as independent transducers of vestibular information because the semi-circular canals are not functional due to their small size (Beck et al. 2004, Lambert et al. 2008). Therefore, the VOR is solely activated by the utricular otoliths. Furthermore, the contribution of the vestibular system to the VOR can be studied in isolation from that of the visual system by performing experiments in the dark (Beck et al. 2004).

The VOR may be a particularly important behavioral response for first-feeding fish larvae. Many species of temperate fish, including white seabass *Atractoscion nobilis*, spawn pelagic eggs that hatch within a few days and produce yolk-bearing larvae (Moser et al. 1983). Soon after yolk absorption, larvae must find abundant and suitable planktonic prey, or starve (Hjort 1926). Ingestion of prey is the end result of encounter, pursuit, attack and capture processes (MacKenzie & Kiørboe 1995). The dynamics of these processes are influenced by small-scale turbulence due to the small size of the larvae and their prey (MacKenzie & Kiørboe 1995). Therefore, the VOR may play an important role in the ability of larvae to assume and maintain an attack position, and successfully capture prey in a turbulent environment.

We hypothesized that elevated pCO_2 would increase the size of the utricular otoliths. A schematic of our experiment and hypotheses is shown in Fig. 1. Assuming that larger otoliths experience a larger displacement and lag than smaller otoliths (Lychakov & Rebane 2000, Bignami et al. 2013a), we hypothesized that the gain and phase shift of the VOR are increased under elevated pCO_2. We tested these hypotheses by rearing larval white seabass under elevated pCO_2 (2500 µatm) and measuring the area of the utricular otoliths, and the gain and phase shift of the VOR.

MATERIALS AND METHODS

Data collection

Fish

Fertilized eggs of white seabass *Atractoscion nobilis* were obtained the morning after spawning occurred from the Hubbs-SeaWorld Research Institute Leon Raymond Hubbard, Jr., Marine Fish Hatchery in Carlsbad, California, USA, during 2012 to 2015. Eggs that appeared healthy (undamaged, single oil globule) upon microscopic inspection were

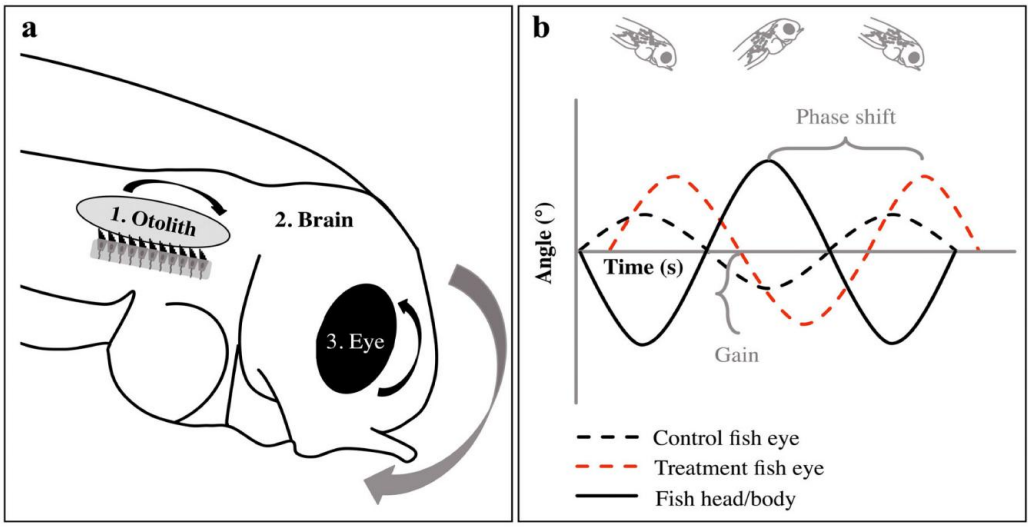

Fig. 1. Schematic of larval fish vestibulo-ocular reflex (VOR) and our hypotheses. (a) Fish larvae are rotated about an Earth-horizontal axis (gray arrow). The denser otolith lags the larva body, including the macula with sensory hair cells on which it rests. This causes the hair cells to bend posteriorly (1 and black arrow). Signals from the hair cells are transmitted to the vestibular nuclei in the brainstem (2). These signals are relayed to the extraocular muscles of the eye, resulting in a counter-rotation (3 and black arrow). (b) Angles of the body/head and eye. See 'Introduction' for definitions of gain and phase shift. We hypothesize that larvae reared at 2500 µatm pCO_2 (treatment) would have increased gain and phase shift compared to larvae reared at 400 µatm pCO_2 (control)

selected for experiments. Eggs hatch at ~2 dpf and larvae deplete their yolk sac and begin to feed at ~4 to 5 dpf (Moser et al. 1983).

Experimental system

The experimental system from Checkley et al. (2009) was used and includes 2 (1 control, 1 treatment) or 4 (2 control, 2 treatment) water-jacketed, 5 l glass vessels with jacket water maintained at 18.0°C. Vessels were bubbled with gas certified to contain a known mixture of air and CO_2 at a rate of 60 ml min^{-1} and equilibrated 1 to 2 d before experiments commenced. In each experiment, 200 eggs were introduced into fully equilibrated control (400 µatm pCO_2) or treatment (2500 µatm pCO_2) vessels at ~12 h post-fertilization.

At the termination of each experiment, seawater samples from each vessel were collected in 250 ml polyethylene terephthalate bottles and fixed with 100 µl of saturated mercuric chloride for the analysis of total alkalinity (A_T) and dissolved inorganic carbon (DIC) by open-cell potentiometric titration and coulometry, respectively. Conductivity-based salinity was also measured. The software CO2Calc (http://cdiac.ornl.gov/ftp/co2sys) was used to estimate pH and pCO_2 from measured A_T and DIC.

OS experiments

Two OS experiments, OS 1 and OS 2, were performed to investigate the effects of elevated pCO_2 on the size of the saccular and utricular otoliths of larvae at 7 dpf. In each experiment, there was 1 control (400 µatm pCO_2) and 1 treatment (2500 µatm pCO_2) vessel.

At 7 dpf, larvae were preserved in 95% ethanol for otolith removal. Sagittae and lapilli were removed with minuten needles under cross-polarized light with the aid of a dissecting microscope. Otoliths were mounted using double-sided black carbon tape onto scanning electron microscopy (SEM) stubs, sputter-coated with iridium for 8 s and imaged at high magnification (×1500 to 3000) and high resolution (2 nm) using SEM (Phillips XL30 ESEM). Otoliths in SEM images, calibrated to magnification, were traced using ImageJ (National Institutes of Health), and area and circularity ($4\pi \times \text{area/perimeter}^2$) estimated. Otolith identity was masked during measurements. Estimates of otolith mass were obtained assuming that otolith density is constant and that volume is proportional to $\text{area}^{1.5}$ (Checkley et al. 2009).

VOR experiments

Three VOR experiments, VOR 1, VOR 2 and VOR 3, were performed to test for effects of elevated pCO_2 on the VOR of larvae at 4 dpf. VOR 1 had 1 control (400 µatm pCO_2) and 1 treatment (2500 µatm pCO_2) vessel, while VOR 2 and VOR 3 each had 2 control and 2 treatment vessels. However, high mortality or the inability to analyze some of the VOR videos, due to larva movement or poor lighting, led to data from larvae in only 1 of the treatment vessels for VOR 2 and only 1 of the control vessels for VOR 3 (see Table S1 in the Supplement at www.int-res.com/articles/suppl/m553p173_supp/).

At 4 dpf, a fish larva was removed by pipette from a vessel and partially immobilized in a Pasteur pipette by embedding the posterior end (pectoral fins to caudal fin) in 2% low-gelling-temperature agarose, while the anterior end (head to pectoral fins) was surrounded by seawater. This process allowed unrestricted eye movement while restricting body movement during video recording. Several drops of food coloring were added to the agarose to aid in visual confirmation that no agarose hardened around the eye. Embedding was done with the aid of a dissecting microscope.

The pipette containing the embedded larva was then mounted on a micromanipulator attached to an automatic test tube rocker (Barnstead M48725) that was repurposed as a tilting platform. Using the micromanipulator, the pipette was positioned so that the head of the larva was aligned near the axis of rotation, and the anterior–posterior axis of the larva was perpendicular to the axis of rotation. Positioning of the larva slightly above the center of rotation of the platform resulted in a small amount of translation in addition to rotation of the larva.

Larvae were pitch-tilted (i.e. nose up and down) 24.4 ± 0.8° (mean ± SD) at 0.28 Hz, consistent with prior studies of goldfish (Pastor et al. 1992) and zebrafish (Mo et al. 2010, Bianco et al. 2012). A gyroscope (Sparkfun LPY503AL) was attached to the platform along its axis of rotation to measure angular velocity, which was recorded by an Arduino Duo microcontroller.

A USB 2.0 monochrome digital video camera (Point Grey CMLN-13S2M-CS) mounted to a Mitutoyo 5× long working distance lens (Edmund Optics 46-143) was used to record movement of the left eye of the larva at 15 frames s^{-1} for a total of 500 frames, or ~33 s. Larvae were trans-illuminated with four 980 nm infrared LEDs. Since larvae are mostly transparent, this illumination increased the contrast be-

tween the eye and body for optimal image processing. All experiments were conducted in a dark box.

Data analysis

Platform

The platform was sinusoidally rotated 24° in each direction with constant peak velocity of 5° s^{-1} at a frequency of 0.28 Hz. The gyroscope measured angular velocity (° s^{-1}) of the platform every 0.2 s. Relative angular position was calculated by cumulatively summing angular velocity. Relative angular position was multiplied by a conversion factor, calculated as the ratio of the maximum angle of the platform (±24°) to the maximum angular position value, to obtain the angular position of the platform.

Fish eye

Variation in the quality of the video recordings necessitated an approach to eye angle quantification different from that previously used (Beck et al. 2004, Mo et al. 2010). Video analysis was performed using custom software written in MATLAB (Mathworks).

Briefly, images were converted from grayscale to binary using a threshold value that demarcated the eye from the remaining fish body as well as possible. A section of the eye with a clear edge was selected as the region of interest, and the angle of rotation of this section was calculated using Radon transform (Deans 1993). This angle represents the angle of the entire eye. For more information and an illustration of the image analysis process using a sample video frame see Fig. S1 and the corresponding full video (Video S1, both in the Supplement at www.int-res.com/articles/suppl/m553p173_supp/) for more information.

Gain and phase shift

The VOR was measured by calculating the gain and phase shift of the eye of the fish larvae during movement of the platform. An example of the platform and eye data for a larva is shown in Fig. 2. The eye and platform data were fitted with a sinusoidal function in a least-squares framework. Nonlinear optimization was performed using the function 'fminsearch' in MATLAB, which outputs the values of amplitude, period and phase that parameterized the best-fit sinusoidal model. Depending on the initial direction of the platform, 180° were added to the phase, so that a phase shift of 0° was equal to the fish eye and platform moving 180° out of phase. This was necessary, given the coordinates we defined for the movement of the platform and fish. By convention, phase shifts are expressed relative to 180°. Gain was calculated as the ratio of the absolute value of the amplitude of the eye sinusoid to that of the platform sinusoid. Phase shift was calculated as the difference between the phase of the eye sinusoid and the phase of the platform sinusoid, constrained between –90 and 270° by additions or subtractions of 360°. Positive values of phase shift are termed phase lags and negative values are termed phase leads.

Statistics

OS and VOR experiments were analyzed using 2-way analysis of variance (ANOVA) with either otolith area, otolith circularity, gain or phase shift as the response variable, and pCO_2 and experiment as the 2 factors. We acknowledge that observations within each control or treatment group of each experiment are not independent because larvae in each group were from either 1 or 2 experimental containers. Thus, our result that the ANOVA did not show significant effects of either pCO_2 or experiment on either gain or phase shift is conservative.

Gain data of VOR experiments and otolith circularity data of OS experiments were log-transformed to satisfy the assumption of normality required for ANOVA. Normality and homoscedasticity of data were tested using Shapiro-Wilks and Bartlett's tests. Results were considered significant at $p < 0.05$.

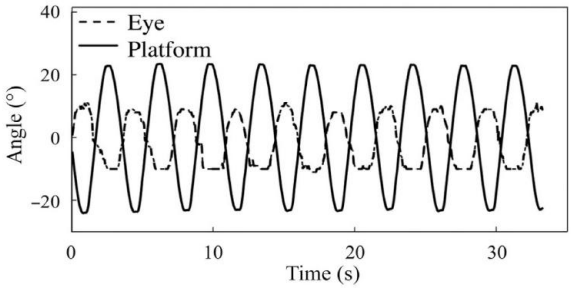

Fig. 2. Example of the platform and eye data for a fish larva reared at 2500 µatm pCO_2. Solid and dashed sinusoids represent the movement of the platform and thus fish body/head, and eye of the fish larva, respectively. These data are from the fish larva in Video S1 in the Supplement at www.int-res.com/articles/suppl/m553p173_supp/

Empirical cumulative distribution functions (CDFs) of the gain of control and treatment larvae were calculated, and differences in the CDFs were tested using a Kolmogorov-Smirnov (K-S) test. Statistical analyses were performed in MATLAB (Mathworks). Summary statistics are reported as mean ± SE.

RESULTS

Seawater carbonate chemistry

In general, control and treatment vessels in OS and VOR experiments accurately represented target pCO_2. Mean A_T, DIC and salinity were consistent among control and treatment vessels within and between OS and VOR experiments (Table 1).

OS experiments

pCO_2 significantly affected the size of saccular and utricular otoliths at 7 dpf (Fig. 3, Table 2). Sagittae and lapilli were 14 to 20% and 37 to 39% larger in area for treatment larvae than control larvae, respectively (Table 2). Two-way ANOVAs showed an effect of experiment on saccular and utricular OS (ANOVA, $p < 0.001$; Table 3). There was a weak, but significant, interaction between pCO_2 and experiment (ANOVA, $p = 0.02$; Table 3) for sagittae. Residuals of the area of saccular otoliths were non-normal (Shapiro-Wilks, $p < 0.001$) due to 1 small value, but variance was homoscedastic (Bartlett's, $p > 0.05$). Residuals of the area of utricular otoliths were normal (Shapiro-Wilks, $p > 0.05$) and variance was homoscedastic (Bartlett's, $p > 0.05$). Circularity of saccular and utricular otoliths was unaffected by pCO_2 (ANOVA, $p > 0.05$), so that otolith area was increased for treatment larvae compared to control larvae, while shape was unchanged.

Table 1. Seawater carbonate chemistry measurements for otolith size (OS) and vestibulo-ocular reflex (VOR) experiments. Values are measured salinity, temperature, total alkalinity (A_T) and dissolved inorganic carbon (DIC). Partial pressure of CO_2 (pCO_2) was estimated using the software CO2Calc

Expt	Salinity	Temperature (°C)	A_T (µmol kg^{-1})	DIC (µmol kg^{-1})	pCO_2 (µatm)
Control					
OS 1	33.61	18.0	2245	2025	416
OS 2	33.68	18.0	2246	2030	426
VOR 1	33.61	18.1	2233	2029	450
VOR 2	33.63	18.0	2255	2053	465
VOR 2	33.62	18.0	2256	2056	468
VOR 3	33.62	18.0	2249	2045	455
Treatment					
OS 1	33.60	18.0	2242	2274	2468
OS 2	33.65	18.0	2248	2279	2465
VOR 1	33.57	18.0	2239	2258	2230
VOR 2	33.63	18.0	2254	2282	2407
VOR 3	33.65	18.0	2251	2287	2543
VOR 3	33.65	18.1	2251	2278	2400

VOR experiments

Turbulence

We calculated the turbulent dissipation rate equivalent to that of the environment of the larvae as they were pitch-tilted during experiments to relate our experimental conditions to the turbulent conditions that pelagic larvae experience in the upper surface ocean. Using the Kolmogorov time scale equation $\tau = (\nu/\varepsilon)^{1/2}$, where τ is approximately half of the period of the platform (2 s), and ν is the kinematic viscosity of seawater (10^{-6} m^2 s^{-1}), we calculated a turbulent dissipation rate, ε, of 2.5×10^{-7} m^2 s^{-3}.

Gain and phase shift

Gain of larvae reared at 2500 µatm pCO_2 was consistently larger, but not significantly so, than larvae reared at 400 µatm pCO_2 (Table 4). Gain and phase shift data for individual fish in each VOR experiment are available (see Table S1 in the Supplement). A comparison of the CDFs for control and treatment larvae revealed that 90% of control larvae had a gain <0.6, whereas this value was 0.9 for treatment larvae. A single treatment larva overcompensated for head movement with a gain >1. Despite the tendency for treatment larvae to exhibit a larger gain compared to control larvae, a 2-way ANOVA yielded non-significant results for pCO_2 (ANOVA, $p > 0.05$; Table 5) and a K-S test found non-significant differences in the CDFs (K-S, $p > 0.1$). There was no effect of experiment (ANOVA, $p > 0.05$) or the interaction of experiment and pCO_2 (ANOVA, $p > 0.05$; Table 5) on gain. Residuals for gain approximated a normal distribution (Shapiro-Wilks, $p > 0.05$) and variance was homoscedastic (Bartlett's, $p > 0.05$).

Phase shift did not differ significantly between control and treatment larvae (Table 4).

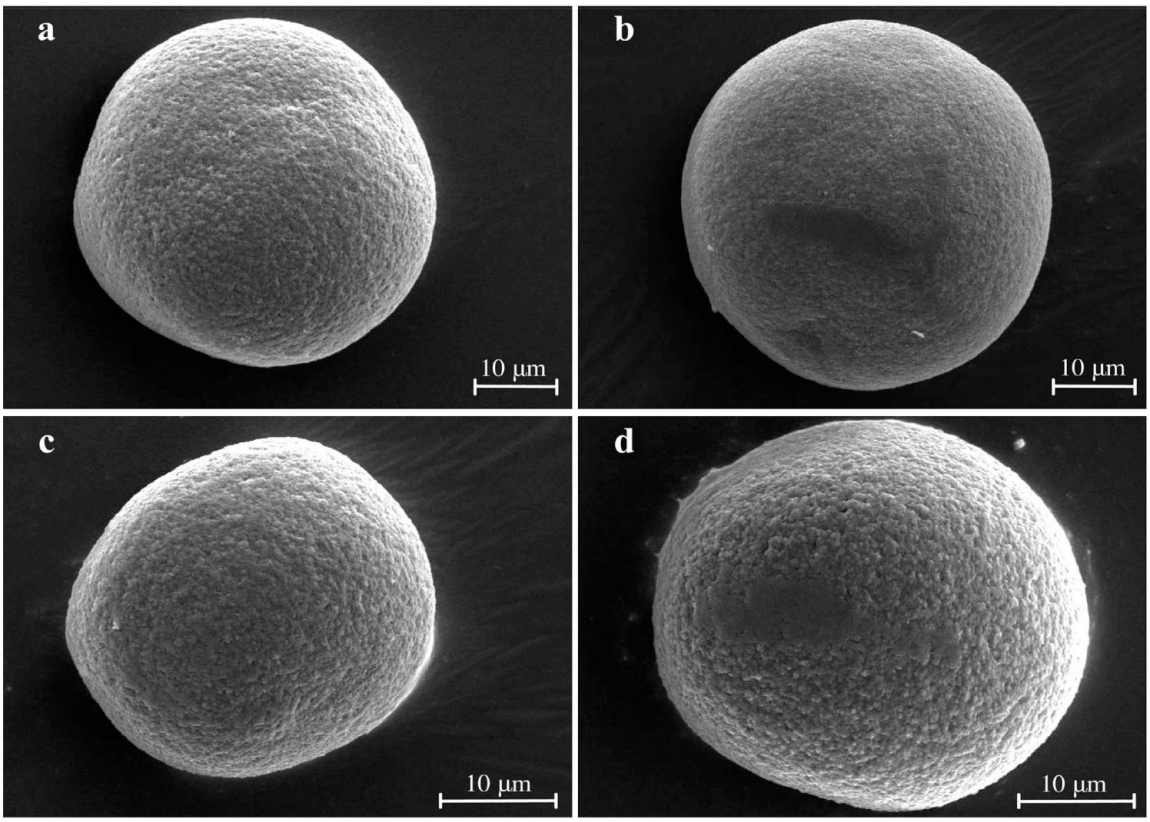

Fig. 3. SEM images of the saccular and utricular otoliths of 7 d post-fertilization (dpf) white seabass larvae reared at control (400 µatm) and treatment (2500 µatm) pCO_2. (a) Control sagittae. (b) Treatment sagittae. (c) Control lapilli. (d) Treatment lapilli. Saccular and utricular otoliths were imaged at ×1750 and ×2500, respectively

Table 2. Results of otolith size (OS) experiments on 7 d post-fertilization (dpf) larvae. Values are target pCO_2, number of otoliths measured (N), mean otolith area ± SE and the ratio of otolith areas of treatment (2500 µatm) to control (400 µatm) larvae. *$p < 0.05$

Expt	pCO_2 (µatm)	N	Mean otolith area (µm^2)	Ratio of otolith areas
Sagittae				
OS 1	400	13	715 ± 19	
OS 1	2500	12	982 ± 17	1.14*
OS 2	400	18	762 ± 19	
OS 2	2500	20	1061 ± 17	1.20*
Lapilli				
OS 1	400	15	1454 ± 18	
OS 1	2500	15	1663 ± 18	1.37*
OS 2	400	15	1609 ± 27	
OS 2	2500	16	1936 ± 29	1.39*

In general, phase shifts were smaller for treatment larvae compared to control larvae. Both control and treatment larvae experienced phase leads and lags, although the mean across experiments was a small phase lead (Table 4). There was no effect of pCO_2, experiment, or the interaction of experiment and pCO_2 (ANOVA, $p > 0.05$) on phase shift (Table 5). Residuals of phase shift were non-normal (Shapiro-Wilks, $p = 0.04$) and variance was homoscedastic (Bartlett's, $p > 0.05$).

DISCUSSION

We reared white seabass larvae at present (400 µatm) and future (2500 µatm) pCO_2 to investigate the effects of elevated pCO_2 on otolith morphology and functionality. We found a significant effect

Table 3. Results of 2-way ANOVA tests for otolith size (OS) experiments. The response variables are saccular and utricular otolith areas of 7 d post-fertilization larvae. Factors are pCO_2 with 2 levels (400 and 2500 µatm) and experiment with 2 levels (OS 1 and OS 2). Values are degrees of freedom (df), mean squares (MS), *F*-statistic and p-value

	df	MS	*F*	p
Sagittae				
pCO_2	1	1 090 000	126.68	<0.001
Expt	1	694 000	80.47	<0.001
pCO_2 × Expt	1	53 500	6.20	<0.05
Error	57	8630		
Total	60			
Lapilli				
pCO_2	1	1 200 000	226.21	<0.001
Expt	1	60 000	11.27	<0.01
pCO_2 × Expt	1	3990	0.75	0.39
Error	59	5320		
Total	62			

Table 4. Results of vestibulo-ocular reflex (VOR) experiments for 4 d post-fertilization larvae. Values are target pCO_2, number of larvae tested (N), mean gain and phase shift ± SE

Expt	pCO_2 (µatm)	N	Mean gain	Mean phase shift (µm^2)
Control				
VOR 1	400	5	0.30 ± 0.09	7.4 ± 9.3
VOR 2	400	6	0.30 ± 0.04	−10.8 ± 4.4
VOR 3	400	9	0.30 ± 0.05	−7.6 ± 8.2
Treatment				
VOR 1	2500	5	0.37 ± 0.13	−3.0 ± 11.4
VOR 2	2500	9	0.39 ± 0.10	1.6 ± 5.4
VOR 3	2500	14	0.40 ± 0.05	−6.1 ± 9.0

Table 5. Results of 2-way ANOVA tests for vestibulo-ocular reflex (VOR) experiments. The response variables are gain and phase shift of 4 d post-fertilization larvae. Factors are pCO_2 with 2 levels (400 and 2500 µatm) and experiment with 3 levels (VOR 1, VOR 2 and VOR 3). Values are degrees of freedom (df), mean squares (MS), *F*-statistic and p-value

	df	MS	*F*	p
Gain				
pCO_2	1	0.85	3.00	0.09
Expt	2	0.39	1.39	0.26
pCO_2 × Expt	2	0.29	1.04	0.36
Error	42	0.28		
Total	47			
Phase shift				
pCO_2	1	14.35	0.02	0.88
Expt	2	285.64	0.45	0.64
pCO_2 × Expt	2	382.45	0.61	0.55
Error	42	632.11		
Total	47			

of pCO_2 on otolith area and non-significant effect on VOR. Our study provides new insight into the functional consequences of larger otoliths in the larvae of several species of fish reared at high pCO_2.

The sagittae and lapilli of 7 dpf larvae reared at elevated pCO_2 were 14 to 20% and 37 to 39% larger in area, respectively, and estimated to be 21 to 30% and 55 to 59% greater in mass than those of control larvae. We did not measure the dry mass of larvae, but assumed it to be similar for control and treatment larvae, based on the results of Checkley et al. (2009), which showed that the dry mass of white seabass larvae at 7 to 8 dpf and reared at 380 µatm pCO_2 was not statistically significantly different from that of those reared at 2500 µatm CO_2. Our results are consistent with the increase in saccular otolith area of 7 to 17% and estimated mass of 10 to 26% reported by Checkley et al. (2009). Similarly, the otoliths of cobia (Bignami et al. 2013a,b), Atlantic cod (Maneja et al. 2013a), clownfish (Munday et al. 2011) and seabream (Réveillac et al. 2015) are 10 to 46% larger when larvae are raised under acidified conditions (700 to 4653 µatm).

We characterized the VOR of white seabass, a previously untested species, at the time of first feeding (4 dpf). Larval fish–prey dynamics are influenced by turbulence due to the small size of both larvae and planktonic prey (MacKenzie & Kiørboe 1995). The integrity of the VOR may be most important during the 'critical period' when first-feeding larvae must locate and capture prey. The mean gain (0.30) and phase shift (–4.8°) we observed for 4 dpf white seabass are comparable to those of 4 dpf zebrafish (gain, 0.33; phase shift, approximately –5°) as reported by Bianco et al. (2012). A higher mean gain of 0.49 was reported by Mo et al. (2010), also for zebrafish larvae. Given the small size of white seabass larvae at 4 dpf (3.7 mm standard length), it is likely that the VOR at this stage is driven solely by the sensory input of the utricular otoliths (Beck et al. 2004, Lambert et al. 2008).

pCO_2 did not significantly affect the VOR of larvae. We offer 4 possible explanations for the non-significant treatment effect. First, the VOR of larvae was tested under conditions that reflect a relatively calm surface ocean. We estimated the turbulent dissipation rate equivalent to that of the environment of the larvae in our experiments to be 2.5×10^{-7} m^2 s^{-3}. Turbulence dissipation rates in the surface water of the ocean where pelagic larvae reside span several orders of magnitude, from 10^{-8} to 10^{-2} m^2 s^{-3} (Mackenzie & Leggett 1993, Horne et al. 1996). Therefore, our stimulus may not have produced the accelera-

tions to which larvae are adapted and which cause significant otolith displacement. Subjecting larvae to more turbulent conditions with greater accelerations will increase otolith stimulation. The difference between otolith displacement for control and treatment larvae with different sized otoliths, and thus resulting VOR, may be greater at higher stimulus velocities. Therefore, the VOR of white seabass larvae, and the larvae of other species, should be tested under a range of turbulence conditions that fish larvae may experience in nature in future experiments.

Second, the larger-sized otoliths of treatment larvae may be within the natural range of variation of otoliths that allows for normal functioning of the VOR. OS is known to vary with species (Paxton 2000) and in response to environmental conditions (Marshall & Parker 1982, Mosegaard et al. 1988). The natural variation in OS could also explain the lack of pCO_2 effect on the swimming kinetics and performance of larval cobia (Bignami et al. 2013b) and Atlantic cod (Maneja et al. 2013b) with enlarged otoliths, and of Atlantic herring with smaller otoliths (Maneja 2012, Maneja et al. 2015). Because the VOR is calibrated to OS and displacement, as occurs during development, it is perhaps not surprising that the gain and phase shift of the VOR were unchanged for larvae with enlarged otoliths.

Third, it is possible that the pCO_2 has not affected OS by 4 dpf. Owing to the small size of the otoliths (<50 µm) at 4 dpf, removal and manipulation onto an SEM stub was not possible. For this reason, we were unable to measure OS at the same age as we performed VOR experiments. It is also possible that larvae compensated for the negative effects of pCO_2, thereby maintaining a normal VOR at an energetic cost. A reduction in the size of the yolk sac or oil globule of fish larvae when reared at elevated pCO_2, as experienced by yellowtail kingfish *Seriola lalandi*, orange clownfish *Amphiprion percula* and summer flounder *Paralichthys dentatus*, is one example of an increased energetic cost (Munday et al. 2016).

Lastly, it was suggested by Munday et al. (2016) that the slow growth and delayed development of gills and branchial acid–base regulation of temperate, pelagic spawned fish may predispose them to morphological and energetic effects of high pCO_2 earlier during the larval stages than for tropical species. Behavioral effects may not manifest until the later larval stages, after the development of gills and acid–base regulation. The many negative effects of elevated pCO_2 on the sensory systems and behavior of tropical reef fish larvae has been attributed to the disruption of the GABA and $GABA_A$ neurotransmitter and receptors (Nilsson et al. 2012, Hamilton et al. 2014, Heuer & Grosell 2014). The resiliency of the VOR to elevated pCO_2 despite the role of GABA as the primary inhibitory neurotransmitter (Spencer & Baker 1992) suggests that white seabass larvae, and perhaps the larvae of other fish, may utilize Na^+/H^+ exchangers for acid–base regulation prior to the development of branchial Cl/HCO_3^- exchange (Munday et al. 2016).

Subtle changes in the VOR were discernible in our experiments. There was a marginally significant tendency (ANOVA, $p = 0.09$) for treatment larvae to have increased gain compared to control larvae. Further studies should explore the influence of stimulus intensity, representative of turbulence conditions, on the VOR and test other vestibular-related behaviors (e.g. counter-rolling) in the larvae of different fish species. Future studies may show effects of elevated pCO_2 on the vestibular function of fish larvae.

Acknowledgements. We are grateful to Hubbs-SeaWorld Research Institute Leon Raymond Hubbard, Jr., Marine Fish Hatchery for providing fertilized white seabass eggs. This research would not have been possible without its contribution. We thank Peter Franks, Peng Sun, Sammie Wang, Stuart Sandin, Ryan Anderson and David Cervantes for assistance with turbulent dissipation rate calculations, image analysis, gyroscope data, statistics, use of SEM and carbonate chemistry analyses. We thank Martin Tresguerres, William Jones and Rebecca Asch for comments that improved the manuscript. We also thank 3 anonymous reviewers for providing us with suggestions to improve the manuscript. Animal handling and experimental procedures were approved by the University of California San Diego Institutional Animal Care and Use Committee under protocol S12161. Funding in support of this research was provided by the Academic Senate of the University of California, San Diego (UCSD) to D.M.C. and the Scripps Institution of Oceanography at UCSD to S.G.S. Support was provided from the National Science Foundation Graduate Research Fellowship Program to S.G.S. The authors declare no conflicts of interest.

LITERATURE CITED

Baumann H, Talmage SC, Gobler CJ (2012) Reduced early life growth and survival in a fish in direct response to increased carbon dioxide. Nat Clim Change 2:38–41

Beck JC, Gilland E, Tank DW, Baker R (2004) Quantifying the ontogeny of optokinetic and vestibuloocular behaviors in zebrafish, medaka, and goldfish. J Neurophysiol 92:3546–3561

Bianco IH, Ma LH, Schoppik D, Robson DN and others (2012) The tangential nucleus controls a gravito-inertial vestibulo-ocular reflex. Curr Biol 22:1285–1295

Bignami S, Enochs IC, Manzello DP, Sponaugle S, Cowen RK (2013a) Ocean acidification alters the otoliths of a pantropical fish species with implications for sensory function. Proc Natl Acad Sci USA 110:7366–7370

Bignami S, Sponaugle S, Cowen RK (2013b) Response to ocean acidification in larvae of a large tropical marine fish, *Rachycentron canadum*. Glob Change Biol 19: 996–1006

Caldeira K, Wickett M (2003) Anthropogenic carbon and ocean pH. Nature 425:365

Chambers RC, Candelmo AC, Habeck EA, Poach ME and others (2014) Effects of elevated CO_2 in the early life stages of summer flounder, *Paralichthys dentatus*, and potential consequences of ocean acidification. Biogeosciences 11:1613–1626

Checkley DM Jr, Dickson AG, Takahashi M, Radich JA, Eisenkolb N, Asch R (2009) Elevated CO_2 enhances otolith growth in young fish. Science 324:1683

Chung WS, Marshall NJ, Watson SA, Munday PL, Nilsson GE (2014) Ocean acidification slows retinal function in a damselfish through interference with $GABA_A$ receptors. J Exp Biol 217:323–326

Deans SR (1993) Definition of the Radon transform. In: Deans SR (ed) The Radon transform and some of its applications. Dover Publications, New York, NY, p 55–61

Devine BM, Munday PL, Jones GP (2012) Rising CO_2 concentrations affect settlement behaviour of larval damselfishes. Coral Reefs 31:229–238

Doney SC, Fabry VJ, Feely RA, Kleypas JA (2009) Ocean acidification: the other CO_2 problem. Annu Rev Mar Sci 1:169–192

Forsgren E, Dupont S, Jutfelt F, Amundsen T (2013) Elevated CO_2 affects embryonic development and larval phototaxis in a temperate marine fish. Ecol Evol 3: 3637–3646

Franke A, Clemmesen C (2011) Effect of ocean acidification on early life stages of Atlantic herring (*Clupea harengus* L.). Biogeosciences 8:3697–3707

Frommel AY, Maneja R, Lowe D, Malzahn AM and others (2012) Severe tissue damage in Atlantic cod larvae under increasing ocean acidification. Nat Clim Change 2:42–46

Gagliano M, Depczynski M, Simpson SD, Moore JA (2008) Dispersal without errors: symmetrical ears tune into the right frequency for survival. Proc R Soc B 275:527–534

Goldberg JM, Wilson VJ, Cullen KE, Angelaki DE and others (2012) The vestibular system: a sixth sense. Oxford University Press, New York, NY

Hamilton TJ, Holcombe A, Tresguerres M (2014) CO_2-induced ocean acidification increases anxiety in rockfish via alteration of $GABA_A$ receptor functioning. Proc R Soc B 281:20132509

Helling K, Hausmann S, Clarke A, Scherer H (2003) Experimentally induced motion sickness in fish: possible role of the otolith organs. Acta Otolaryngol 123:488–492

Heuer RM, Grosell M (2014) Physiological impacts of elevated carbon dioxide and ocean acidification on fish. Am J Physiol Regul Integr Comp Physiol 307:R1061–R1084

Hjort (1926) Fluctuations in the year classes of important food fishes. J Cons Int Explor Mer 1:1–38

Hönisch B, Ridgwell A, Schmidt DN, Thomas E and others (2012) The geological record of ocean acidification. Science 335:1058–1063

Horne EPW, Loder JW, Naimie CE, Oakey NS (1996) Turbulence dissipation rates and nitrate supply in the upper water column on Georges Bank. Deep-Sea Res II 43: 1683–1712

Houde ED (1997) Patterns and trends in larval stage growth and mortality of teleost fish. J Fish Biol 51:52–83

Inoue M, Tanimoto M, Oda Y (2013) The role of ear stone size in hair cell acoustic sensory transduction. Sci Rep 3: 2114

IPCC (2013) Climate change 2013: the physical science basis, Chapter 6. In: Stocker TF, Qin D, Plattner GK, Tignor M and others (eds) Contribution of working group 1 to the fifth assessment report of the Intergovernmental Panel on Climate Change. Cambridge University Press, Cambridge, p 465–544

Lambert FM, Beck JC, Baker R, Straka H (2008) Semicircular canal size determines the developmental onset of angular vestibuloocular reflexes in larval *Xenopus*. J Neurosci 28:8086–8095

Lychakov DV, Rebane YT (2000) Otolith regularities. Hear Res 143:83–102

MacKenzie BR, Kiørboe T (1995) Encounter rates and swimming behavior of pause-travel and cruise larval fish predators in calm and turbulent environments. Limnol Oceanogr 40:1278–1289

Mackenzie BR, Leggett WC (1993) Wind-based models for estimating the dissipation rates of turbulent energy in aquatic environments: empirical comparisons. Mar Ecol Prog Ser 94:207–216

Maneja RH (2012) Influence of ocean acidification on otolith calcification and behavior in fish larvae. PhD dissertation, University of Kiel

Maneja RH, Frommel AY, Geffen AJ, Folkvord A, Piatkowski U, Chang MY, Clemmesen C (2013a) Effects of ocean acidification on the calcification of otoliths of larval Atlantic cod *Gadus morhua*. Mar Ecol Prog Ser 477: 251–258

Maneja RH, Frommel AY, Browman HI (2013b) The swimming kinematics of larval Atlantic cod, *Gadhus morhua* L., are resilient to elevated seawater pCO_2. Mar Biol 160: 1963–1972

Maneja RH, Frommel AY, Browman HI (2015) The swimming kinematics and foraging behavior of larval Atlantic herring (*Clupea harengus* L.) are unaffected by elevated pCO_2. J Exp Mar Biol Ecol 466:42–48

Marshall SL, Parker SS (1982) Pattern identification in the microstructure of sockeye salmon (*Oncorhynchus nerka*) otoliths. Can J Fish Aquat Sci 39:542–547

Miles FA, Lisberger SG (1981) Plasticity in the vestibuloocular reflex: a new hypothesis. Annu Rev Neurosci 4: 273–299

Mo W, Chen F, Nechiporuk A, Nicolson T (2010) Quantification of vestibular-induced eye movements in zebrafish larvae. BMC Neurosci 11:110

Mosegaard H, Svedäng H, Taberman K (1988) Uncoupling of somatic and otolith growth rates in Arctic char (*Salvelinus alpinus*) as an effect of differences in temperature response. Can J Fish Aquat Sci 45:1514–1524

Moser HG, Ambrose DA, Busby MS, Butler JL, Sandknop EM (1983) Description of early stages of white seabass, *Atractoscion nobilis*, with notes on distribution. CCOFI Rep 24:182–193

Munday PL, Donelson JM, Dixson DL, Endo GGK (2009a) Effects of ocean acidification on the early life history of a tropical marine fish. Proc R Soc B 276:3275–3283

Munday PL, Dixson DL, Donelson JM, Jones GP, Pratchett MS, Devitsina GV, Doving KB (2009b) Ocean acidification impairs olfactory discrimination and homing ability of a marine fish. Proc Natl Acad Sci USA 106:1848–1852

Munday PL, Hernaman V, Dixson DL, Thorrold SR (2011) Effect of ocean acidification on otolith development in

larvae of a tropical marine fish. Biogeosciences 8: 1631–1641

Munday PL, Watson SA, Parsons DM, King A and others (2016) Effects of elevated CO_2 on early life history development of the yellowtail kingfish, *Seriola lalandi*, a large pelagic fish. ICES J Mar Sci 73:641–649

Nilsson GE, Dixson DL, Domenici P, McCormick MI, Sorensen C, Watson SA, Munday PL (2012) Near-future carbon dioxide levels alter fish behavior by interfering with neurotransmitter function. Nat Clim Change 2: 201–204

Pannella G (1971) Fish otoliths: daily growth layers and periodical patterns. Science 173:1124–1127

Pastor AM, de la Cruz RR, Baker R (1992) Characterization and adaptive modification of the goldfish vestibuloocular reflex by sinusoidal and velocity step vestibular stimulation. J Neurophysiol 68:2003–2015

Paxton JR (2000) Fish otoliths: do sizes correlate with taxonomic group, habitat, and/or luminescence? Philos Trans R Soc Lond B 355:1299–1303

Platt C (1983) The peripheral vestibular system of fishes. In: Northcutt RG, Davis RE (eds) Fish neurobiology, Vol 1. University of Michigan Press, Ann Arbor, MI, p 89–123

Popper AN, Ramcharitar J, Campana SE (2005) Why otoliths? Insights from inner ear physiology and fisheries biology. Mar Freshw Res 56:497–504

Réveillac E, Lacoue-Labarthe T, Oberhänsli F, Teyssié JL, Jeffree R, Gattuso JP, Martin S (2015) Ocean acidification reshapes the otolith-body allometry of growth in juvenile seabream. J Exp Mar Biol Ecol 463:87–94

Riley BB, Moorman SJ (2000) Development of utricular otoliths, but not saccular otoliths, is necessary for vestibular function and survival in zebrafish. J Neurobiol 43: 329–337

Rombough PJ (1988) Respiratory gas exchange, aerobic metabolism, and effects of hypoxia during early life. In: Hoar WS, Randall DJ (eds) Fish physiology: the physiology of developing fish eggs and larvae. Academic Press, San Diego, CA, p 59–161

Simpson SD, Munday PL, Wittenrich ML, Manassa R, Dixson DL, Gagliano M, Yan HY (2011) Ocean acidification erodes crucial auditory behaviour in a marine fish. Biol Lett 7:917–920

Spencer RF, Baker R (1992) GABA and glycine as inhibitory neurotransmitters in the vestibuloocular reflex. Ann N Y Acad Sci 656:602–611

Straka H, Dieringer N (2004) Basic organization principles of the VOR: lessons from frogs. Prog Neurobiol 73:259–309

Szentagothai J (1950) The elementary vestibulo-ocular reflex arc. J Neurophysiol 13:395–407

Tseng YC, Hu MY, Stumpp M, Lin LY, Melzner F, Hwang PP (2013) CO_2-driven seawater acidification differentially affects development and molecular plasticity along life history of fish (*Oryzias latipes*). Comp Biochem Physiol A 165:119–130

Wallman J, Velez J, Weinstein B, Green AE (1982) Avian vestibuloocular reflex: adaptive plasticity and developmental changes. J Neurophysiol 48:952–967

Editorial responsibility: Stylianos Somarakis, Heraklion, Greece

Submitted: November 24, 2015; Accepted: June 4, 2016
Proofs received from author(s): June 28, 2016

Chapter 2, in full, is a reprint of materials as they appear in Shen, S.G., Chen, F., Schoppik, D.E., and Checkley, D.M., Jr. (2016) Otolith size and the vestibulo-ocular reflex of larvae of white seabass *Atractoscion nobilis* at high pCO_2. Marine Ecology Progress Series, 553:173-183. The dissertation author was the primary investigator and author of this manuscript.

Chapter 3

Spawning and mortality of Anchoveta (*Engraulis ringens*) eggs and larvae in relation to pCO_2

3.1 Abstract

The world's most productive fisheries occur in regions projected to experience intense ocean acidification. Anchoveta (*Engraulis ringens*) constitute the largest single-species fishery and live in one of the highest pCO_2 regions in the ocean. pCO_2 of the Peruvian upwelling system exceeds atmospheric CO_2 year-round. We investigated the relationship of the abundance and survival of Anchoveta eggs and larvae to pCO_2 in the spawning habitat. Anchoveta eggs and larvae, zooplankton, and data on temperature, salinity and pCO_2 were collected during a cruise off Peru in 2013. While eggs were most abundant in cool (15-16°C), lower salinity (34.85-34.90) and higher pCO_2 (1000-1100 µatm) water, larvae were most abundant in warmer (17-18°C), higher salinity (34.90-35.00) and lower pCO_2 (500-600 µatm) water. pCO_2 ranged from 167-1392 µatm and correlated positively with egg presence,

an index of spawning habitat. Zooplankton abundance explained significant variability in the abundance of small larvae. Within the cold coastal water mass, samples with highest concentrations of eggs were found at significantly higher pCO_2 than samples of larvae. Our results indicate that Anchoveta preferentially spawned at high pCO_2 and that these eggs had lower survival. Understanding the effects of ocean acidification on fish is important for the future management of fisheries.

3.2 Introduction

Naturally high-pCO_2 areas in the ocean, such as eastern boundary upwelling systems (EBUS) and CO_2 vents, offer the opportunity to study the response of marine organisms to acidified water and to contribute to our understanding of the effects of ocean acidification on marine life (Pespeni *et al.* 2013, Munday *et al.* 2014). Ocean acidification is the increase in pCO_2 and decrease in pH and $CaCO_3$ saturation state, among other changes in the inorganic carbon chemistry, due to the addition of CO_2 to the ocean from fossil fuel burning and other human activities (Doney *et al.* 2009). The response of fish to ocean acidification depends on the type of process evaluated (e.g., behavioral or physiological) and may vary between species (see review by Heuer and Grosell 2014). However, a general conclusion is that larvae are more susceptible than juveniles and adults (Heuer and Grosell 2014, Rombough 1988). Furthermore, while declining $CaCO_3$ saturation state may be the factor of greatest concern for calcifying organisms in an acidifying ocean (Doney *et al.* 2009), pCO_2 may pose the biggest threat to fish (Heuer and Grosell 2014, Rombough 1988, Kikkawa *et al.* 2004). Cutaneous gas exchange and a lack of functional gills cause early larval stages of fish to be especially vulnerable to elevated pCO_2 (Rombough 1988). Similarly, the reduction in the outward diffusion gradient of CO_2 from the fish body to the seawater as pCO_2 increases can result in an acidosis and disruption of internal pH homeostasis (reviewed in Heuer and Grosell 2014, Rombough 1988). Lastly, the highest mortality rates are incurred in the

egg and larval stages, and the dynamics of these stages are thought to greatly influence recruitment into fisheries (Houde 1987). Therefore, fisheries in naturally high-pCO_2 regions may be especially at risk from ocean acidification.

Anchovies (*Engraulis* spp.) are small pelagic fish that occur worldwide in temperate regions of high productivity, particularly in the coastal upwelling areas of EBUS (Grant and Bowen 1998, Checkley *et al.* 2009). Wind-driven upwelling brings cold, nutrient-rich, high pCO_2, low pH waters to the surface and creates a spatial and temporal environmental mosaic (Chavez and Messie 2009, Copin-Montégut and Raimbault 1994). Anchovy populations around the globe undergo large fluctuations in biomass in response to environmental changes on interannual (Ñiquen and Bouchon 2004), decadal (Lluch-Belda *et al.* 1989, Chavez *et al.* 2003, Alheit and Ñiquen 2004) and centennial (DeVries and Pearcy 1982, Finney *et al.* 2010) timescales. Notable examples are the collapse of the sardine (*Sardinops sagax*) fishery off California in 1947 and Anchoveta (*Engraulis ringens*) fishery off Peru in 1972 due to changing ocean conditions and overfishing (Checkley *et al.* 2009, Alheit and Ñiquen 2004). The low level of nucleotide diversity and shallow coalescence of mitochondrial DNA genealogies of anchovies indicate periodic regional population collapses have occurred in the past in response to oceanographic processes (e.g. upwelling intensity; Grant and Bowen 1998). Rapid evolutionary adaptation is more likely to occur in populations with high levels of existing genetic variation and large population size (Pespeni *et al.* 2013). Therefore, the strong influence of the environment on the biomass and recruitment combined with the genetic structure suggest that anchovy populations may be especially vulnerable to climate change effects such as ocean acidification, in addition to warming and deoxygenation.

The Anchoveta (*Engraulis ringens*) inhabits the Humboldt Current System and is important both ecologically and economically. Anchoveta play an important role as a midtrophic-level species, consuming phytoplankton and zooplankton, while serving as prey to higher trophic level organisms such as mackerel, hake, seabirds, and marine mammals

(Jahncke *et al.* 2004). Anchoveta also support the world's largest single-species fishery with landings of 4 million metric tons in 2012 (MMT; FAO 2015). Three distinct stocks are acknowledged: north-central Peru (4-15°S), Peru-Chile (16-24°S) and central-south Chile (33-42°S; Alheit and Ñiquen 2004). The north-central Peru (NCP) stock is located within the highly productive and high pCO_2 Peruvian upwelling system and dominates the catch. Biogeochemical models predict a decline in Anchoveta recruitment with climate change due to a reduction in primary productivity (Brochier *et al.* 2013).

The Peruvian upwelling system experiences elevated pCO_2 year-round, with concentrations exceeding those of other EBUS (Feely *et al.* 2008, Friederich *et al.* 2008, Takahashi *et al.* 2009). Measurements of pCO_2 in the coastal region of Peru can reach 1500 µatm (Friederich *et al.* 2008). The greatest disparity between sea surface and atmospheric CO_2 among EBUS globally is in the Peruvian upwelling system (Takahashi *et al.* 2009). Coastal upwelling systems, including the Peruvian upwelling system, have a lowered buffering capacity to offset acidification and are at the forefront of observable climate change (Feely *et al.* 2008, McNeil and Sasse 2016). Under IPCC RCP 8.5, hotspots of acidification (pCO_2 >1000 µatm) are projected to occur in major fishery zones by mid-century when atmospheric CO_2 is projected to reach 650 µatm (McNeil and Sasse 2016).

Anchoveta respond to environmental fluctuations by altering their habitat use and reproductive strategy. For example, during El Niño events, Anchoveta migrate further south, nearer to the coast, and into deeper water to seek refuge from warm sea surface temperatures (Ñiquen and Bouchon 2004). Fecundity and spawning frequency are reduced, and the spawning season is delayed and extended (Ñiquen and Bouchon 2004, Perea and Buitrón 2001). While adults can change their behavior to cope with suboptimal environmental conditions, the early life history stages of many fish species are planktonic and thus are largely unable to escape exposure to stressful conditions. Furthermore, the peak spawning season for Anchoveta (August-November) occurs during maximum upwelling activity

(Friederich *et al.* 2008, Lett *et al.* 2007), resulting in the spawning and development of eggs and larvae at high pCO_2. Cutaneous gas exchange and the lack of acid-base and ion regulatory mechanisms (Rombough 1988) may increase the susceptibility of eggs and larvae spawned at high pCO_2.

Exposure to naturally high and variable pCO_2 may increase the capacity of populations and species to acclimate (phenotypically change) and adapt (genetically change) to ocean acidification. For example, rearing eggs and larvae of Atlantic herring (*Clupea harengus*) and Baltic cod (*Gadus morhua*) at pCO_2 of 3000-4000 µatm had no effect on hatching success or rates of survival, growth and development. These fish spawn at a depth and time of year when pCO_2 is naturally high (>1000 µatm) in the Baltic Sea (Franke and Clemmesen 2011, Frommel *et al.*. 2013). Purple sea urchin (*Strongylocentrotus purpuratus*) from the California Current System have divergent transcriptomes along latitudinal gradients in pCO_2 associated with variations in upwelling strength (Pespeni *et al.* 2013). In addition, epigenetic transgenerational plasticity (parental conditioning) has been shown to mediate the negative effects of elevated pCO_2 on the offspring of Atlantic silverside (*Menidia menidia*) as well as Sydney rock oysters (*Saccostrea glomerata*) and cinnamon clownfish (*Amphiprion melanopus*; Murray *et al.* 2014). These results suggest that pCO_2 variability may be a strong selective force for diverse taxa.

We use the Peruvian upwelling system, with its naturally high pCO_2 and large Anchoveta population, as a natural experiment to investigate the relationship of pelagic fish eggs and larvae to pCO_2. We posed the following questions: (1) What is the surface water pCO_2 in the spawning habitat? (2) Are eggs and larvae found in areas of high pCO_2? (3) Does pCO_2 affect the mortality of eggs and larvae? To address these questions, we examined the distribution and abundance of Anchoveta eggs and larvae across an inshore-offshore gradient of pCO_2 over 10° latitude (1,112 km) off Peru during the spawning and upwelling season in August 2013.

3.3 Materials and Methods

3.3.1 Cruise Information

Eggs and larvae of the north-central Peru stock of Anchoveta (*Engraulis ringens*) and oceanographic data were collected during a 30-day cruise in August-September 2013. The cruise, Crucero Pelágico 1308-09, was conducted by the Instituto del Mar del Perú (Imarpe) on the RV José Olaya Balandra. It was comprised of parallel transects separated by 15 nm and from the coast to $\sim$ 90 nm offshore, encompassing the Anchoveta spawning habitat from Puerto Pizarro (3°S) to Callao (12°S).

3.3.2 Oceanographic Data

Temperature, salinity and pCO_2 were measured continuously and recorded at 1-minute intervals from water sampled with the vessels seawater system at 3-m depth using a thermosalinograph (Sea-Bird Electronics Inc., Bellevue, WA, Model SBE-45) and flow-through sensor based on membrane equilibration and non-dispersive infrared spectrometry (KM Contros GmbH, Kiel, Germany, Model HydroC®CO_2 FT), respectively. Ten seawater samples from a depth of 3 m were taken at selected stations for the analysis of total alkalinity and dissolved inorganic carbon (Andrew Dickson, Scripps Institution of Oceanography, La Jolla, CA) to corroborate flow-through pCO_2 measurements. In addition to these oceanographic variables measured in situ, satellite data were retrieved from the CoastWatch repository (http://coastwatch.pfeg.noaa.gov) for surface concentrations of chlorophyll *a* (mg m^{-3}). An 8-day composite of chlorophyll *a* within a 15-km radius of egg and larva stations was obtained from the AquaModis Net Primary Productivity.

3.3.3 Eggs and Larvae

Eggs were collected continuously at a depth of 3 m in 20-minute intervals using the Continuous Underway Fish Egg Sampler (CUFES) (Checkley *et al.* 1997). CUFES concentrates and filters pelagic fish eggs from a continuous flow ($\tilde{0}.5$ m^{-3} min^{-1}) of seawater through 330-µm mesh (Checkley *et al.* 1997). Concentration is reported as eggs m^{-3}. Volumetric concentration (eggs min^{-1} or eggs m^{-3}) at 3 m is highly correlated with areal abundance (eggs m^{-2}) over the range of distribution of pelagic eggs (Checkley *et al.* 1997, Checkley *et al.* 2000). Eggs were counted onboard and preserved in 2% Formalin-seawater.

Larvae were collected on station using a Hensen net of 60 cm diameter and 330-µm-mesh towed vertically from a depth of 50 m (Ayón *et al.* 2008). Larvae were counted and measured to the nearest 0.1 mm using a light microscope (Nikon Metrology, Inc., Brighton, MI, Model E600) and preserved in 70% Ethanol. Lengths were not adjusted for shrinkage during collection and preservation. The remaining zooplankton were preserved in 2% Formalin-seawater buffered with borax. Zooplankton volume (ml m^{-3}) was measured using the displacement method following the removal of large gelatinous organisms (Ayón *et al.* 2008). Maps of the concentration of eggs and larvae with pCO_2 and salinity interpolations to a 0.1° grid were created using MATLAB (The Mathworks, Inc., Natick, MA, USA).

3.3.4 pCO_2 Data Processing

The HydroC® CO_2 FT automatically performed zero gas measurements every 12 hours. These zero readings in combination with calibration information were used to apply a drift correction based on absolute sensor runtime (Fietzek *et al.* 2014). Pre- and post-deployment calibrations were performed for the range of 200-2200 µatm in July and November 2013, respectively. The response time (RT; time constant, $t_{63\%}$) of the sensor varied throughout the deployment due to a variable flow of the ship's seawater system and fouling. To account for the effect of variable RTs on the series, two corrections were

performed as described in Fiedler *et al.* (2012) and the final RT-corrected series was created from these two data sets. One correction considered a 'slow' RT of 1200 seconds and the other assumed a 'fast' RT of 300 seconds. These RT corrections represent a slow seawater flow and fouling influence as well as a fast seawater flow within an un-fouled system, respectively. The two time constants were derived as representative values from the pCO_2 data during the times of signal recovery after the regular zero gas measurements.

A linear regression ($R^2 = 0.99$) of temperature measurements at 3 m depth obtained from Niskin casts during sampling stations ($n = 50$) and temperature measurements from the thermosalinograph installed within the flow-through setup onboard was used to convert the RT-corrected pCO_2 at the sensor to pCO_2 *in situ* at 3 m (Takahashi *et al.* 1993). Time periods of variable seawater flow were removed from the final data as their quality was unknown. We estimated the uncertainty of the data by calculating the percentage difference between the RT-corrected *in situ* pCO_2 and the pCO_2 calculated from three discrete reference seawater samples analyzed for DIC and TA using the software CO_2Calc (http://pubs.usgs.gov/of/2010/1280/). pCO_2 obtained using the HydroC® CO_2 FT agreed well with pCO_2 derived from DIC and TA of the discrete seawater samples, differing by less than 1.5%. Therefore, we conservatively attribute an uncertainty of 1.5% for the majority of measurements. Over short periods and in times of large pCO_2 gradients, the uncertainty could be as high as 10% due to discrepancies in the sensors actual RT in the field and the RT assumed during processing.

3.3.5 Spatial Generalized Linear Mixed Models

We constructed a set of candidate models (SM Table 1) to evaluate the relative influence of oceanographic variables on the distribution and abundance of eggs and larvae. Specifically, we evaluated the influence of temperature, salinity, pCO_2, satellite chlorophyll *a* and zooplankton displacement volume on the presence of eggs and abundance of larvae of

SL <5 mm. Sixty percent of CUFES samples did not contain eggs, precluding the use of zero-inflated or abundance-based models. Furthermore, the full extent of where spawning occurred is better captured by using presence and absence data. Small larvae (SL <5 mm) were analyzed because they were more abundant than older and larger larvae, their collection was more contemporaneous with measurements of environmental conditions, and, since they likely would be less effective in avoiding the net, catches are probably more reflective of actual abundance than would be for larger larvae.

We performed logistic regressions with a binomial distribution and logit link to model the effects of temperature, salinity, pCO_2 and chlorophyll *a* on egg presence. Larva abundance was modeled using generalized linear models with a Poisson distribution and log link. Zooplankton displacement volume was included as an additional predictor variable. Models included either temperature or salinity, and either temperature or pCO_2 due to strong correlations between these variables (Pearsons $r > 0.6$; SM Table 3). Linear and quadratic terms were included in models because the probability of egg presence can peak across a range of conditions (Asch and Checkley 2013). Egg and larvae data were standardized by subtracting the mean and dividing by the standard deviation prior to model fitting. Spatial autocorrelation, detected by global Morans I, was accounted for through the use of spatial generalized linear mixed models (SGLMM), which consider spatial autocorrelation as a random effect (Rousset and Ferdy 2014). In R v.3.1.2 (R Core Team 2013), the function corrHLfit in the package 'spaMM' was used to obtain penalized quasi-likelihood estimates of parameters in egg and larvae models and Matérn correlation parameters.

The relative plausibility of the candidate SGLMMs to describe egg presence and larva abundance was determined using Akaikes Information Criterion adjusted for small sample sizes (AICc; SM Table 2) (Burnham and Anderson 2002). We calculated the ΔAICc and scaled the models by their Akaike weight. Parameter estimates of models with Akaike weights >10% of the model with the lowest AIC were averaged to account for model

selection uncertainty (Burnham and Anderson 2002) using the R package 'AICcmodavg.' Ninety-five percent confidence intervals were constructed around parameter estimates for each predictor variable in the model. Parameters were interpreted as significant if confidence intervals did not overlap zero (Burnham and Anderson 2002).

We constructed partial effects plots to illustrate the effect of individual predictor variables on the probability of egg capture and predicted number of larvae after removing the linear effects of other variables in the model. Partial effects were calculated by allowing the variable of interest to take on measured values while all other predictor variables in the model were fixed at their median value (Weber and McClatchie 2010). Predicted probabilities and counts were averaged within 0.5-unit bins to provide a clearer picture of the central relationships.

3.4 Results and Discussion

3.4.1 Distribution and Abundance

236,200 eggs were collected in 867 CUFES samples from the habitat of the NCP stock of Anchoveta in August and September 2013. Eggs were most abundant near the coast and found primarily between 7 and 10°S (Fig. 1), consistent with other years (Santander and de Castillo 1973, Santander and Flores 1983, Ayón 2008). Compared to the southern range ($\sim$ 15°S) of the spawning habitat, this area is characterized by a wider continental shelf, increased stability of the physical environment, higher retention rates, and better feeding conditions for larvae, all factors that likely contribute to making this area a preferred location for spawning (Lett *et al.* 2007, Santander and Flores 1983, Walsh *et al.* 1980).

Eggs were abundant, with a mean of 27 eggs m^{-3} and maximum of 2,000 eggs m^{-3} (Fig. 1). Maximal egg concentration was 1-3 orders of magnitude greater than that of the central-south Chile stock of *E. ringens* (33-42°S) in 1995 (Castro *et al.* 2000),*Engraulis*

mordax in the California Current over several years, 1998-2001 (Checkley *et al.* 2000, Asch and Checkley 2013) and *Engraulis encrasicolus* in the Benguela Current from 1986-1993 (Van der Lingen and Huggett 2003). The frequency of occurrence of eggs was maximal in water of high pCO_2 (1000-1100 µatm), cold temperature (15-16°C) and relatively low salinity (34.85-34.90) (Fig. 2). More than half of the eggs (53%) were found in this salinity range. Therefore, egg concentration was highest in the cold, coastal water mass (CCW; Swartzman *et al.* 2008), characterized by low temperature (14-18°C) and low salinity (34.9). Chlorophyll *a* estimated from satellite imagery ranged from 0.2 to 16.7 mg m^{-3}.

1,157 Anchoveta larvae were collected at 74 stations using the Hensen net. Of these larvae, 716 measured <5 mm in standard length (SL). pCO_2 data were available for 683 of these small larvae at 71 stations. The horizontal distribution of small larvae (SL <5 mm), hereafter referred to as larvae, was similar to the egg distribution, although samples with large numbers of larvae were collected further offshore (Fig. 1). Samples had a mean of 10 larvae m^{-3} and a maximum of 51 larvae m^{-3} (Fig. 1).

Compared to eggs, larvae were most abundant in lower pCO_2 (400-500 µatm), warmer (17-18°C), and more saline (34.90-35.00) water (Fig. 2). The distribution of larvae approximated that of seawater pCO_2, peaking in the mid-range of pCO_2, with 48% of larvae found between 400-600 µatm. Only 17% of larvae were found at salinity <34.90, where the majority of eggs were collected. Larvae were found within the CCW, but to a larger extent within the mixed coastal-subtropical (oceanic) water mass (MCS), characterized by salinities of 35.05-35.10 and temperatures of 14-18°C (Swartzman *et al.* 2008). Chlorophyll *a* ranged from 0.3-5.8 mg m^{-3} and zooplankton displacement volume, an index for zooplankton abundance, ranged from 0.2-13.0 mg m^{-3}.

3.4.2 pCO_2

pCO_2 ranged from 167-1392 µatm, consistent with the range of ∼150-1500 µatm measured during 2004-2006 in this region (Friederich *et al.* 2008). Approximately 74% of the measurements during 2004-2006 exceeded atmospheric pCO_2 (378 µatm; http://www.esrl.noaa.gov/gmd/ccgg/ globalview/index.html) by more than 100 µatm and 8% had values that were more than twice atmospheric pCO_2 (Friederich *et al.* 2008). In comparison, 84% of our data exceeded atmospheric pCO_2 (393 µatm; http://www.esrl.noaa.gov/gmd/ccgg/globalview/index.html) by more than 100 µatm and 23% were greater than twice atmospheric pCO_2 (756 µatm). However, the majority of high values (pCO_2 >1000 µatm) in 2004-2006 were observed further south (14-16°S) than the main spawning area and our study region. Our findings indicate that the spatial extent of high pCO_2 water in the main spawning habitat (7-12°S), as well as the maximal concentration of this water, was greater in 2013 compared to 7-9 years ago.

3.4.3 Spawning Habitat Characterization

Standardized, model-averaged parameter estimates of temperature, salinity, pCO_2 and chlorophyll *a* indicate that pCO_2 was the only statistically significant variable in predicting egg presence (Table 1). The relationship of pCO_2 to egg presence was positive and quadratic (Table 1), as seen in the partial effects plot (Fig. 3). The probability of collecting eggs increased from 0.30 to 0.97 as pCO_2 increased from the mean of 641 µatm to 1198 µatm (Fig. 3).

To our knowledge, this is the first report of pCO_2 as a variable that significantly characterizes the spawning habitat of anchovy species. Temperature and salinity, often with chlorophyll *a* concentration, have been identified as important factors in the characterization of spawning habitat for anchovy in the California Current (Checkley *et al.* 2000, Asch and Checkley 2013, Weber and McClatchie 2010, Reiss *et al.* 2008) and Benguela Current

(Twatwa *et al.* 2005). Our results are consistent with others (Reiss *et al.* 2008, Loeb and Rojas 1998) showing temperature and salinity alone do not define the spawning habitat of Anchoveta in the Humboldt Current. Furthermore, while a strong, positive relationship between egg abundance and prey availability was found for Anchoveta off Chile (Castro *et al.* 2000), we did not find a significant relationship between chlorophyll *a* and egg presence for Anchoveta off Peru.

Model estimates show a significant negative quadratic relationship between the abundance of larvae and zooplankton displacement volume (Table 1; Fig. 3). Larva abundance peaked at mean zooplankton volume of 3.0 ml m^{-3}. (Fig. 3). The zooplankton includes both predators and prey of Anchoveta larvae. Therefore, the relationship we observed may be partially explained by the match in the timing and location of first feeding by Anchoveta larvae with plankton production (Castro *et al.* 2000, Cushing 1990), as well as by predation on larvae by large zooplankton. Consistent with this explanation, the occurrence of both Anchoveta eggs and larvae off Chile and sardine eggs off California is positively correlated with zooplankton and negatively correlated with predatory zooplankton, respectively (Checkley *et al.* 2000, Castro *et al.* 2000).

3.4.4 Mortality

Samples with the highest concentrations of eggs were collected within the CCW at relatively low salinity (34.90 $\pm$ 0.01; mean $\pm$ standard deviation) and high pCO_2 (930 $\pm$ 211 µatm) waters (Fig. 4). In contrast, large concentrations of larvae were widespread within the CCW and MSC, with the centroid at a higher salinity (34.98 $\pm$ 0.06) and lower pCO_2 (552 $\pm$ 183 µatm) than that for eggs (Fig. 4). With two assumptions, our results suggest that eggs spawned at high pCO_2 (>800 µatm) suffered higher mortality than those spawned at lower pCO_2.

Our first assumption is that measurements of the environment made during the

collection of eggs and larvae reflect the conditions during the spawning and early life history development. Support for this assumption comes from a surface drifter deployed at 16°S in 2005 that recorded warming of $<$1°C and a decline in $p\mathrm{CO}_2$ of $<$150 µatm (Friederich *et al.* 2008) over the course of one week. We collected and analyzed data of eggs, which hatch in $\sim$ 2 days at 17°C (Santander and de Castillo 1973), and larvae of SL $<$5 mm, corresponding to first-feeding larvae approximately one week in age (Ware *et al.* 1981). This assumption is also important for the interpretation of the SGLMM results. Our second assumption, related to the first, is that the eggs and larvae we collected were not advected into the sampling area. Due to the effects of salinity on egg buoyancy (Sundby and Kristiansen 2015) and the weak swimming ability of small planktonic larvae (Ware *et al.* 1981), horizontal transport of eggs and larvae into water masses of differing salinities is assumed to be negligible.

Samples with abundant eggs and larvae were collected in waters of significantly different $p\mathrm{CO}_2$ (t-test, p-value $<$0.001). The expected decrease in $p\mathrm{CO}_2$ due to primary production and outgassing during the 5-7 day development of eggs into young larvae is approximately 200 µatm (Friederich *et al.* 2008). Therefore, the difference in $p\mathrm{CO}_2$ between the centers of distribution of eggs and larvae of more than 200 µatm is consistent with the hypothesis that eggs spawned within the CCW at high $p\mathrm{CO}_2$ suffered a higher mortality rate (Fig. 4). The larvae we collected were most likely survivors of eggs spawned at low-to-intermediate $p\mathrm{CO}_2$ ($<$800 µatm). Conversely, the absence of large concentrations of larvae at $p\mathrm{CO}_2$ between 700 and 1000 µatm, with one exception, suggests that eggs spawned at $p\mathrm{CO}_2$ $>$900 µatm, which constitutes the majority of eggs, did not survive to the larval stage.

3.4.5 Implications

Our data are consistent with the hypothesis that Anchoveta spawned in areas with environmental conditions that were not optimal for egg and larva survival during the austral

spring of 2013. Egg frequency of occurrence, probability of collection and concentration were maximal at high pCO_2 and low salinity, indicating Anchoveta selected water with these conditions for spawning. However, larva frequency of occurrence and concentration were highest at low pCO_2 and high salinity, consistent with high mortality rates of eggs at high pCO_2. Thus, while the majority of spawning occurred near the coast in waters of high pCO_2, eggs spawned further offshore in waters of salinity 34.91-35.0 and pCO_2 <900 µatm appear to have contributed to the majority of the survivors at the larval stage.

An alternative interpretation of our results is that temporal and spatial variation in spawning during the cruise could explain the absence of eggs at higher salinity and lower pCO_2, and of larvae at lower salinity and higher pCO_2. Histological samples of ovarian tissues from adult Anchoveta indicate a daily spawning fraction of ∼10% during the peak spawning period (Ayón and Buitron 2008). Given that our sampling encompassed the entire spawning habitat of the NCP Peru stock and occurred over several weeks, we assume that spawning was continuous, leading to a stable age distribution (Lo *et al.* 1989).

It is also important to note that there are other variables that we did not measure that may affect the distribution and abundance of eggs and larvae and whose mechanistic relationship may have been captured by the environmental variables we measured. A notable example is oxygen, which is strongly correlated with pCO_2 (Reum *et al.* 2015) and an important variable affecting fish distributions in the Humboldt Current (Bertrand *et al.* 2011). However, while the correlation of O_2 and pCO_2 is strong at depth, the surface ocean is typically high in O_2 despite elevated pCO_2. Of the 47 samples of surface (0m) oxygen taken during the cruise, 15 of these were taken in seawater with pCO_2 >800 µatm and O_2 ranged from 2.15 to 5.18 mL L^{-1}. More research on how O_2 decreases with depth in the region where eggs and larvae reside is needed to understand whether the effects we observed could have been partially explained by oxygen profiles. Lastly, variables related to water column structure and horizontal flow have increased the power of models to predict anchovy

spawning habitat in the California Current (Weber and McClatchie 2010, Asch and Checkley 2013) and had these variables been explored, they may also have contributed to a better understanding of our findings.

While Anchoveta and other small pelagic fish species generally display high spawning plasticity, there are ecological and evolutionary limits to this plasticity (Ciannelli *et al.* 2015) that may become more important as ocean acidification intensifies. Our results indicate that the ability to complete the pelagic larval life stage is a constraint (Ciannelli *et al.* 2015) that may become more severe in the future as the availability of low pCO_2 water is reduced. Presumably, Anchoveta have evolved to spawn in areas where larvae can survive since eggs hatch in approximately two days. It is possible that while the CCW is productive with optimal temperature and salinity, increasing pCO_2 will cause this habitat to become less suitable over time. The mechanism by which fish sense changes in pCO_2 is not entirely clear, and may involve changes in gene regulation via activation of a soluble adenylyl cyclase (Tresguerres *et al.* 2010). Whether Anchoveta can sense the increasing acidity of the historically optimal spawning habitat and move to lower pCO_2 waters also depends on the relative constraint of the other environmental properties to their survival.

Whether our findings are representative of other years and other species of fish in EBUS and other naturally high-pCO_2 regions is a question that merits attention. Together, Anchoveta, Alaska Pollock (*Theragra chalcogramma*), Skipjack tuna (*Katsuwonus pelamis*), sardines (*Sardinella* spp.) and Atlantic herring (*Clupea harengus*) comprise 19% of the world's global marine fish catch (FAO 2015). Due to the fact that the biological processes that produce high pCO_2 also support large fish populations (remineralization of organic matter into inorganic nutrients), the major fisheries of the world are largely found in naturally high-pCO_2 regions. These regions, such as waters off Alaska, the North Atlantic (especially near the Arctic) and EBUS, are expected to experience ocean acidification much earlier than other areas of the world's ocean (McNeil and Sasse 2016). Thus, understanding the effects

of ocean acidification on marine fish is important for the management and sustainability of fisheries in the future and requires the long-term monitoring of pCO_2, the most likely variable affecting fish response to ocean acidification (Heuer and Grosell 2014, Rombough 1988, Kikkawa *et al.* 2004), concurrent with the collection of eggs and larvae.

The management strategies of Anchoveta and Pacific sardine (*Sardinops sagax*) incorporate climate variability to some degree, and may serve as a model for the sustainable management of fisheries in the face of climate change. For example, the EUREKA Program of the Instituto del Mar del Perú enables managers and scientists to repurpose the fishing fleet for a rapid stock assessment of Anchoveta during the onset of an El Niño event (Schreiber *et al.* 2011). The harvest control rule for Pacific sardine (*Sardinops sagax*) depends on temperature in the southern California Current System (Hill *et al.* 2014). These progressive management strategies are testimony to the importance of, and ability to, consider the impacts of climate on the sustainability of commercial fisheries. In the future, EUREKA cruises and harvest control rules may be triggered by extreme upwelling or La Niña events that are characterized by high pCO_2. It is timely to consider how climate change, particularly ocean acidification, may be incorporated into fishery management strategies.

3.5 Acknowledgements

We are grateful to Dr. Dimitri Aguilar, Director of the Research in Oceanography and Climate Change Division at Imarpe, for agreeing to collaborate and allowing S.S. to participate on the cruise. We are indebted to the many scientists and personnel aboard RV José Olaya Balandra. We extend our thanks to Ron Burton and Alice Harada for fruitful conversations, and to William Watson for reviewing a draft of the manuscript.

Chapter 3, in full, is in review as Shen, S.G., Thompson, A.R., Correa, J., Fietzek, P., Ayon, P., and Checkley, D.M., Jr. Spawning and mortality of Anchoveta *Engraulis*

ringens eggs and larvae in relation to pCO_2. The dissertation author was the primary investigator and author of this manuscript.

3.6 Figures

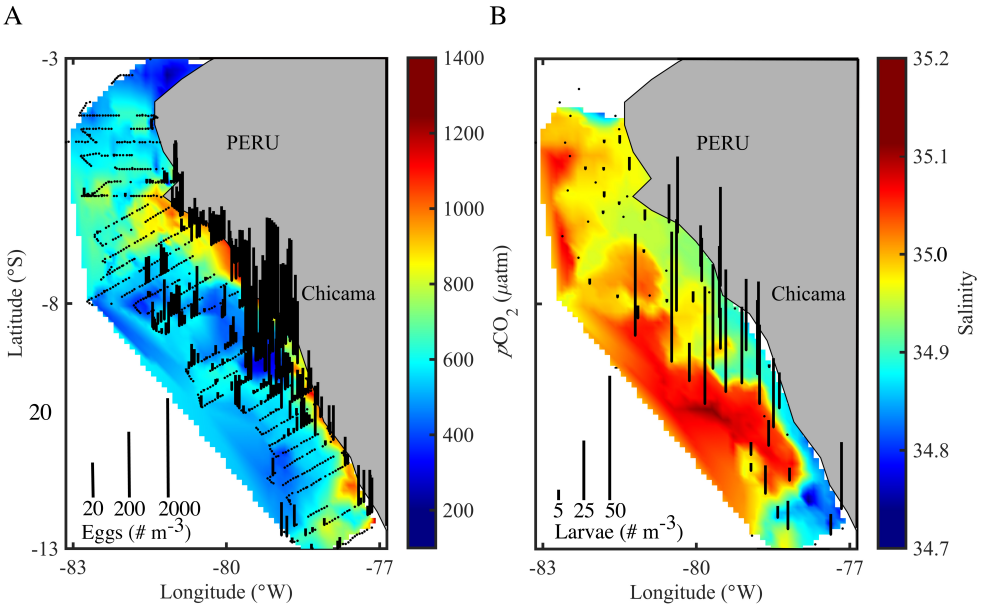

Figure 3.1: *Maps of eggs and larvae.*
Maps of the concentration of (A) eggs and (B) larvae of standard length <5 mm. Lengths of the black lines correspond to the concentration of eggs and larvae at stations where samples were collected. Interpolated measurements of (A) pCO_2 and (B) salinity are shown in the background.

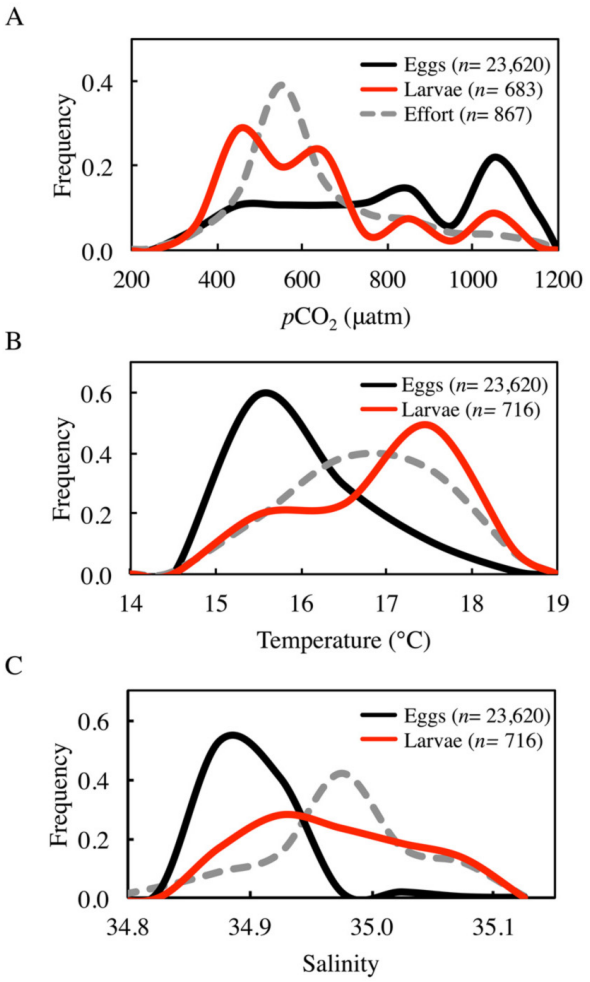

Figure 3.2: *Frequency distributions of eggs and larvae.*
Frequency distributions of eggs (black lines), larvae (red lines) and sampling effort (dashed gray lines) in relation to (A) pCO_2, (B) temperature and (C) salinity. Data for pCO_2, temperature and salinity were binned into 100-µatm, 0.5-°C and 0.05-intervals and a spline was performed to generate smooth curves.

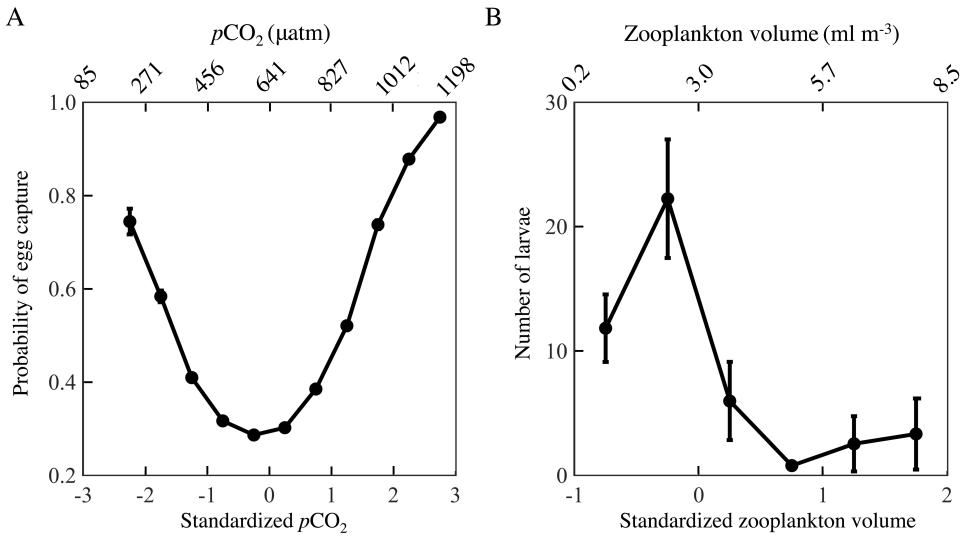

Figure 3.3: *Partial effects diagrams for egg capture and larva abundance.*
Partial effects diagrams of (A) pCO_2 on the probability of egg capture and (B) zooplankton displacement volume on the abundance of larvae. Data were standardized prior to model fitting. Mean and standard error are shown for bins of 0.5-unit.

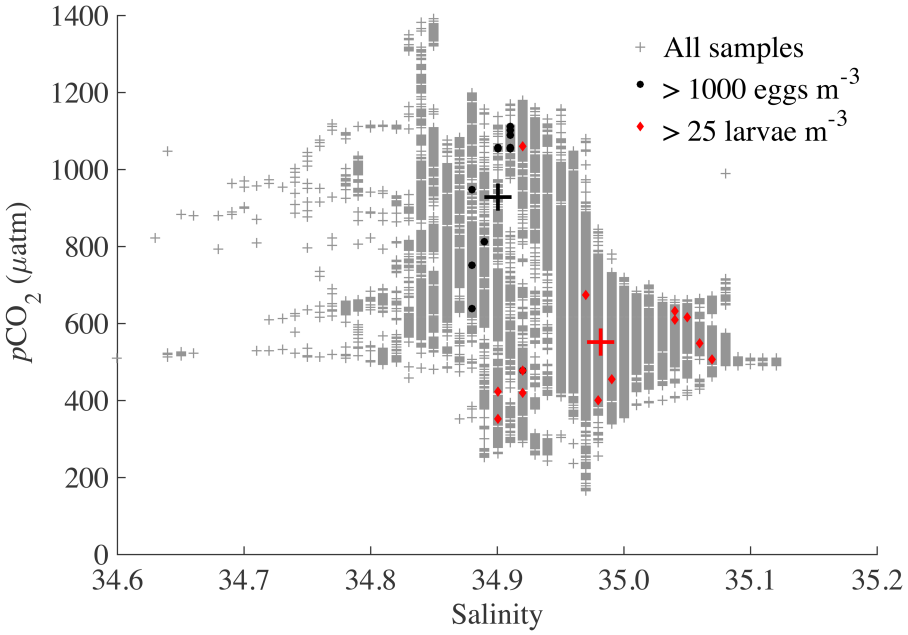

Figure 3.4: *pCO_2-salinity diagram for eggs and larvae.*
pCO_2-salinity diagram for all seawater measurements (gray plus signs), CUFES samples containing >1000 eggs m^{-3} (black circles) and samples of larvae containing >40 larvae m^{-3} (red diamonds). The centroids of the distributions are indicated by the black and red plus signs.

3.7 Tables

Table 3.1: *Parameter estimates for egg presence and larva abundance.*

Standardized, model-averaged parameter estimates and lower and upper 95% confidence intervals for candidate models that describe the relationship between egg presence and abundance of larvae, and oceanographic variables. Quadratic terms are denoted as the parameter squared. Data were standardized prior to model fitting by subtracting the mean and dividing by the standard deviation. Significant (p-value <0.05) parameter estimates are in bold.

	Eggs			**Larvae**		
Variable	**Estimate**	**LCI**	**UCI**	**Estimate**	**LCI**	**UCI**
Temp	-0.12	-0.30	0.06	0.10	-0.30	0.49
Temp^2	0.14	0.00	0.28	-0.02	-0.19	0.15
Sal	-0.06	-0.25	0.13	0.02	-0.15	0.19
Sal^2	0.02	-0.10	0.14	0.00	-0.11	0.11
pCO_2	0.19	-0.01	0.38	-0.03	-0.24	0.18
$pCO_2{}^2$	**0.52**	**0.37**	**0.68**	0.02	-0.13	0.17
Chl	0.02	-0.30	0.34	0.04	-0.33	0.41
Chl^2	-0.02	-0.10	0.06	-0.02	-0.16	0.13
Zoo				0.21	-0.44	0.85
Zoo^2				**-0.37**	**-0.73**	**-0.01**

3.8 References

Alheit J, Ñiquen M (2004) Regime shifts in the Humboldt Current ecosystem. Progress in Oceanography, 60:201-222.

Asch RG, Checkley Jr DM (2013) Dynamic height: A key variable for identifying the spawning habitat of small pelagic fishes. Deep Sea Research Part I: Oceanographic Research Papers, 71:79-91.

Ayón P (2008) Producción diaria de huevos de la Anchoveta peruana en agosto - setiembre 2003. Informe Instituto del Mar del Perú, 35:81-85.

Ayón P, Buitrón B (2008) Biomasa desovante de la anchoveta peruana. Método de producción de huevos (mph). Invierno 2003. Informe Instituto del Mar del Perú, 35:77-80.

Ayón P, Criales-Hernandez MI, Schwamborn R, Hirche H-J (2008) Zooplankton research off Peru: A review. Progress in Oceanography, 79:238-255.

Bertrand A, Chaigneau A, Peraltilla S, Ledesma J, Graco M, Monetti F, Chavez FP (2011) Oxygen: A fundamental property regulating pelagic ecosystem structure in the coastal southeastern tropical Pacific. PLoS ONE, 12:e29558.

Brochier T, Echevin V, Tam J, Chaigneau A, Goubanova K, Bertrand A (2013) Climate change scenarios experiments predict a future reduction in small pelagic fish recruitment in the Humboldt Current system. Global Change Biology, 19:1841-1853.

Burnham KP, Anderson DR (2002) Model selection and multimodel inference: a practical information-theoretic approach. Springer Scientific, New York.

Castro LR, Salinas GR, Hernndez EH (2000) Environmental influences on winter spawning of the Anchoveta *Engraulis ringens* off central Chile. Marine Ecology Progress Series, 197:247-258.

Chavez FP, Messié M (2009) A comparison of eastern boundary upwelling ecosystems. Progress in Oceanography, 83:80-96.

Chavez FP, Ryan J, Lluch-Cota SE, Ñiquen MC (2003) From anchovies to sardines and back: Multidecadal change in the Pacific Ocean. Science, 299:217-221.

Checkley DM Jr, Alheit J, Oozeki Y, Roy C (2009) Climate Change and Small Pelagic Fish. New York: Cambridge University Press, 372 p.

Checkley DM Jr, Dotson RC, Griffith DA (2000) Continuous, underway sampling of eggs of

Pacific sardine (*Sardinops sagax*) and northern anchovy (*Engraulis mordax*) in spring 1996 and 1997 off southern and central California. Deep Sea Research Part II: Topical Studies in Oceanography, 47:1139-1155.

Checkley DM Jr, Ortner PB, Settle LR, Cummings SR (1997) A continuous, underway fish egg sampler. Fisheries Oceanography, 6:58-73.

Ciannelli L, Bailey K, Olsen EM (2015) Evolutionary and ecological constraints of fish spawning habitats. ICES Journal of Marine Science, 72:285- 296.

Copin-Montégut C, Raimbault P (1994) The Peruvian Upwelling near 15°S in August 1986. Results of Continuous Measurements of Physical and Chemical Properties between 0 and 200 m Depth. Deep Sea Research Part I: Oceanographic Research Papers, 41:439-467.

Cushing DH (1990) Plankton production and year-class strength in fish populations: An update of the match/mismatch hypothesis. Advances in Marine Biology, 26:249-293.

DeVries TJ, Pearcy WG (1982) Fish debris in sediments of the upwelling zone off central Peru: a late Quaternary record. Deep Sea Research Part A, 29:87-109.

Doney SC, Fabry VJ, Feely RA, Kleypas JA (2009) Ocean acidification: the other CO_2 problem. Annual Review of Marine Science, 1:169-192.

Feely RA, Sabine CL, Hernandez-Ayon M, Ianson D, Hales B (2008) Evidence for upwelling of corrosive "acidified" water onto the Continental Shelf. Science, 320:1490-1492.

Fiedler B, Fietzek P, Vieira N, Silva P, Bittig HC, Körtzinger A (2012) In situ CO_2 and O_2 measurements on a profiling float. Journal of Atmospheric and Oceanic Technology, 30:112-126.

Finney BP, Alheit J, Emeis K-C, Field DB, Gutiérrez, Struck U (2010) Paleoecological studies on variability in marine fish populations: A long-term perspective on the impacts of climatic change on marine ecosystems. Journal of Marine Systems, 79:316-326.

Fisheries and Aquaculture topics. The State of World Fisheries and Aquaculture (SOFIA). Topics Fact Sheet. Text by Jean-Francois Pulvenis. In: FAO Fisheries and Aquaculture Department [online. Rome. Updated 19 May 2015].

Franke A, Clemmesen C (2011) Effect of ocean acidification on early life stages of Atlantic herring (*Clupea harengus* L.). Biogeosciences, 8:3697-3707.

Friederich GE, Ledesma J, Ulloa O, Chavez FP (2008) Air-sea carbon dioxide fluxes in the coastal southeastern tropical Pacific. Progress in Oceanography, 79:156-166.

Frommel AY, Schubert A, Piatkowski U, Clemmesen C (2013) Egg and early larval stages of Baltic cod, *Gadus morhua*, are robust to high levels of ocean acidification. Marine Biology, 160:1825-1834.

Grant WAS, Bowen BW (1998) Shallow population histories in deep evolutionary lineages of marine fishes: Insights from sardine and anchovies and lessons for conservation. Journal of Heredity, 89:415-426.

Heuer RM, Grosell M (2014) Physiological impacts of elevated carbon dioxide and ocean acidification on fish. American Journal of Physiology-Regulatory, Integrative and Comparative Physiology, 307:R1061-R1084.

Hill KT, Crone PR, Demer DA, Zwolinkski J, Dorval E, Macewicz BJ (2014) Assessment of the Pacific Sardine resource in 2014 for U.S.A. Management in 2014-15. http://www.pcouncil.org/wp-content/uploads/H1b_2014_FULL_Electric_PacificSardine_StockAssmnt_APR2014BB.pdf

Houde ED (1987) Fish early life dynamics and recruitment variability. American Fisheries Society Symposium Series, 2:17-29.

Jahncke J, Checkley Jr DM, Hunt Jr GL (2004) Trends in carbon flux to seabirds in the Peruvian upwelling system: Effects of wind and fisheries on population regulation. Fisheries Oceanography, 13:208-223.

Kikkawa T, Kita J, Ishimatsu A (2004) Comparison of the lethal effect of CO_2 and acidification on red sea bream (*Pagrus major*) during the early developmental stages. Marine Pollution Bulletin, 48:108-110.

Lett C, Penven P, Ayón P, Freon P (2007) Enrichment, concentration and retention processes in relation to anchovy (*Engraulis ringens*) eggs and larvae distributions in the northern Humboldt upwelling ecosystem. Journal of Marine Systems, 64:189-200.

Lluch-Belda D, Crawford RJM, Kawasaki T, MacCall AD, Parrish RH, Schwartzlose RA, Smith PE (1989) Worldwide fluctuations of sardine and anchovy stocks: The regime problem. South African Journal of Marine Science, 8:195-205.

Lo NCH, Hunter JR, Hewitt RP (1989) Precision and bias of estimates of larval mortality. Fishery Bulletin, 87:399-416.

Loeb VJ, Rojas O (1998) Interannual variation of ichthyoplankton composition and abundance relations off northern Chile, 1964-83. Fishery Bulletin, 86:1-24.

McNeil BI, Sasse TP (2016) Future ocean hypercapnia driven by anthropogenic amplification of the natural CO_2 cycle. Nature, 529:383-386.

Munday PL, Alistair JC, Dixson DL, Rummer JL, Fabricius KE (2014) Behavioural impairment in reef fishes caused by ocean acidification at CO_2 seeps. Nature Climate Change, 4:487-492.

Murray CS, Malvezzi A, Gobler CJ, Baumann H (2014) Offspring sensitivity to ocean acidification changes seasonally in a coastal marine fish. Marine Ecology Progress Series, 504:1-11.

Ñiquen M, Bouchon M (2004) Impact of El Niño events on pelagic fisheries in Peruvian waters. Deep Sea Research Part II: Topical Studies in Oceanography, 51:563-574.

Perea A, Buitrón B (2001) Aspectos reproductivos de la Anchoveta *Engraulis ringens* durante los veranos 1999 y 2000. Informe Instituto del Mar del Perú, 159:1107110.

Pespeni MH, Sanford E, Gaylord B, Hill TM, Hosfelt JD, Jaris HK, LaVigne M, Lenz EA, Russell AD, Young MK, Palumbi SR (2013) Evolutionary change during experimental ocean acidification. Proceedings of the National Academy of Sciences, 110:69376942.

Reiss C, Checkley Jr DM, Bograd SJ (2008) Remotely sensed spawning habitat of Pacific sardine (*Sardinops sagax*) and Northern anchovy (*Engraulis mordax*) within the California Current. Fisheries Oceanography, 17:126-136.

Reum CP, Alin SR, Harvey CJ, Bednarsek N, Evans W, Feely RA, Hales B, Lucey N, Mathis JT, McElhany P, Newton J (2015) Interpretation and design of ocean acidification experiments in upwelling systems in the context of carbonate chemistry co-variation with temperature and oxygen. ICES Journal of Marine Science, 73:582-595.

Rombough P (1988) Respiratory gas exchange, aerobic metabolism, and effects of hypoxia during early life. Fish Physiology, 11:59-161.

Rousset F, Ferdy J-B (2014) Testing environmental and genetic effects in the presence of spatial autocorrelation. Ecography, 37:781-790.

Santander H, de Castillo OS (1973) Estudio sobre las primeras etapas de vida de la Anchoveta. Informe Instituto del Mar del Perú, 41:1-29.

Santander H, Flores M (1983) Los desoves y distribucion larval de quarto especies pelagicas y sus relaciones con las variaciones del ambiente marino frente al Peru. FAO Fisheries Report, 291:835-867.

Schreiber MA, Ñiquen M, Bouchon M (2011) Coping strategies to deal with environmental variability and extreme climatic events in the Peruvian anchovy fishery. Sustainability, 3:823-846.

Sundby S, Kristiansen T (2015) The principles of buoyancy in marine fish eggs and their vertical distributions across the world oceans. PLoS One, 10:e0138821.

Swartzman G, Bertrand A, Gutiérrez M, Bertrand S, Vasquez L (2008) The relationship of anchovy and sardine to water masses in the Peruvian Humboldt Current System from 1983 to 2005. Progress in Oceanography, 79:228-237.

Takahashi T, Olafsson J, Goddard JG, Chipman DW, Sutherland SC (1993) Seasonal variation of CO_2 and nutrients in the high-latitude surface oceans: A comparative study. Global Biogeochemical Cycles, 7:843878.

Takahashi T, Sutherland SC, Wanninkhof R, Sweeney C, Feely RA, Chipman DW, Hales B, Friederich G, Chavez F, Sabine C, Watson A (2009) Climatological mean and decadal change in surface ocean pCO_2, and net sea-air CO_2 flux over the global oceans. Deep Sea Research Part II: Topical Studies in Oceanography, 56:554-577.

Tresguerres M, Buck J, Levin LR (2010) Physiological carbon dioxide, bicarbonate, and pH sensing. Pflugers Archiv-European Journal of Physiology, 460:953-964.

Twatwa NM, van der Lingen CD, Drapeau L, Molonet CL, Field JG (2005) Characterising and comparing the spawning habitats of anchovy *Engraulis encrasicolus* and sardine *Sardinops sagax* in the southern Benguela upwelling ecosystem. African Journal of Marine Science, 27:487-499.

Van der Lingen CD, Huggett JA (2003) The role of ichthyoplankton surveys in recruitment research and management of South African anchovy and sardine. The Big Fish Bang: Proceedings of the 26th Annual Larval Fish Conference, 303-341. Bergen, Norway, Institute of Marine Research.

Walsh JJ, Whitledge TE, Esaias WE, Smith RL, Huntsman SA, Santander H, De Mendiola BR (1980) The spawning habitat of the Peruvian anchovy, *Engraulis ringens*. Deep Sea Research Part A, 27:1-27.

Ware DM, de Mendiola BR, Newhouse DS (1981) Behaviour of first-feeding Anchoveta larvae, *Engraulis ringens*. J. Bol Inst Mar Peru Vol. Extraordinario:80-87.

Weber ED, McClatchie S (2010) Predictive models of northern anchovy *Engraulis mordax* and Pacific sardine *Sardinops sagax* spawning habitat in the California Current. Marine Ecology Progress Series, 406:251-263.

Chapter 4

Physiological resilience of white seabass (*Atractoscion nobilis*) larvae to ocean acidification

4.1 Abstract

Developmental and behavioral effects of elevated pCO_2 on the early life history stages of fish are presumed to result from compensatory processes that restore acid-base balance during respiratory acidosis. While measurements of blood chemistry are needed to address this question, measurements of aerobic metabolism and abundance of ion-transporting proteins can provide insight into the physiological changes that occur when larvae are exposed to elevated pCO_2. Oxygen consumption rate (OCR) and abundance of Na^+-K^+-ATPase (NKA) proteins were measured in 5-day-old white seabass (*Atractoscion nobilis*) reared at control (560 $\pm$ 32 µatm) and treatment (1971 $\pm$ 55 µatm) pCO_2. We hypothesized that larvae would increase production of NKA proteins to facilitate the compensation of extra- and intra-cellular fluid pH, and experience a higher OCR in response to increased NKA

protein abundance. We found no effect of elevated pCO_2 on both OCR and NKA protein abundance. OCR was 0.18 ± 0.03 μL O_2 individual^{-1} h^{-1} for control larvae (n = 45) and 0.19 ± 0.03 μL O_2 individual^{-1} h^{-1} for treatment larvae (n = 45). An approximate mass-specific OCR for control and treatment larvae of 1.06 ± 0.16 μL O_2 μg^{-1} h^{-1} (n = 16 groups of 5 larvae) was within the range reported for larvae of other fish species. The relative abundance of NKA proteins as determined by Western blot analysis did not differ significantly between control and treatment larvae. Similarly, there was no treatment effect of pCO_2 on the number of cells immunopositive for NKA. Immunostaining revealed hundreds of cells containing NKA concentrated between the head and anus of both control and treatment larvae. The lack of effect of elevated pCO_2 at the cellular level was reflected in the maintenance of growth. Larvae at high pCO_2 did not differ in length or mass from larvae at low pCO_2.The data suggest that the additional energetic costs of mitigating respiratory acidosis when larvae are exposed to elevated pCO_2 are small. Near-future concentrations of CO_2 are likely to reduce, but maintain, the outward diffusion gradient of CO_2 in young larvae. Furthermore, the presence of numerous cutaneous mitochondria-rich cells that contain NKA, the high mass-specific metabolic rate and the physiological properties of larval hemoglobin may collectively act to reduce the negative impacts of ocean acidification on the metabolism of fish larvae.

4.2 Introduction

Exposure to elevated pCO_2 within the range projected for the next several centuries with ocean acidification (∼2000 μatm; IPCC 2013) lowers the outward diffusion gradient of CO_2 and leads to respiratory acidosis in adult fish (Perry and Gilmour 2006, Esbaugh *et al.* 2012, 2016, Heuer and Grosell 2014). This is because the pCO_2 of the ocean, ranging from values undersaturated (∼150-250) to oversaturated (∼1500) with respect to the atmosphere (Friederich *et al.* 2008, Feely *et al.* 2008) is lower than the internal CO_2 in the blood of

fish, which can range from 3000 to 9900 µatm pCO_2 (Melzner *et al.* 2009b). Juvenile and adult fish compensate for this acid-base disruption through the uptake or retention of HCO_3^- and/or extrusion of H^+ using Cl^-/HCO_3^- and Na^+/H^+ exchangers and Na^+/HCO_3^- transporters (Perry and Gilmour 2006, Melzner *et al.* 2009a, Heuer and Grosell 2014). Measurements of the blood chemistry of adult estuarine red drum (*Sciaenops ocellatus*) and gulf toadfish (*Opsanus beta*) revealed elevated CO_2 and HCO_3^- concentrations within hours after exposure to 1000 and 1900 µatm pCO_2 that acted to restore internal pH (Esbaugh *et al.* 2012, 2016). For example, after a 24-hour exposure to 1900 µatm pCO_2, gulf toadfish blood CO_2 increased from about 2 to 3.5 mmHg and HCO_3^- concentrations increased from approximately 3.5 to 6.5 mM (Esbaugh *et al.* 2012).

The transport of ions is fueled by ion gradients created by Na^+-K^+-ATPase (NKA) in the mitochondria-rich cells (MRC) of the gills (Perry and Gilmour 2006, Melzner *et al.* 2009a,b). When exposed to very high pCO_2 (∼6,000-10,000 µatm), adult Atlantic cod (*Gadhus morhua*) and common eelpout (*Zoarces viviparous*) experienced a 1.5- to 2-fold increase in NKA abundance and activity (Deigweiher *et al.* 2008, Melzner *et al.* 2009b). This increase in ion transporting capacity is suggestive of the need for fish to use more energy for maintaining osmoregulation and acid-base balance. The response of NKA in adult fish exposed to lower pCO_2 (∼1000-3,000 µatm) is more varied, with observations ranging from a doubling of NKA protein activity (Esbaugh *et al.* 2016) to a transient decrease in activity and return to control levels (Esbaugh *et al.* 2012) to no change in protein abundance or activity at all (Melzner *et al.* 2009b). Regardless, there is reason to hypothesize that NKA abundance and activity may be useful indicators of the ion-regulatory capacity of fish exposed to elevated pCO_2.

The additional energetic costs of maintaining or upregulating homeostatic processes at high pCO_2 that result in increased NKA abundance may also increase oxygen consumption rate (OCR). In fact, the NKA pump itself is energetically costly and can account for

$\sim$25% of the oxygen consumption of the gills in marine fish (Stagg and Shuttleworth 1982, Morgan *et al.* 1997). Oxygen consumption is a proxy for the rate of aerobic metabolism (Fry 1971). Routine or resting metabolic rate refers to the oxygen uptake of non-fed and inactive fish, although small and infrequent movements are taken into account (Chabot *et al.* 2016). Generally, adult fish are able to maintain normal OCR under high- pCO_2 conditions (Ishimatsu *et al.* 2008, Melzner *et al.* 2009b, Couturier *et al.* 2013, Esbaugh *et al.* 2016), although changes in OCR of cardinalfish (*Ostorhinchus* spp.; Munday *et al.* 2009) and Antarctic notothenioids (*Trematomus* spp.;Enzor *et al.* 2013) exposed to 1000 µatm pCO_2 ranged from a 10% decrease to a 200% increase. The multitude of effects of elevated pCO_2 on the early life history stages of fish (reviewed by Heuer and Grosell 2014), including changes to growth (Munday *et al.* 2009a, Baumann *et al.* 2012) and biomineralization (Checkley *et al.* 2009, Bignami *et al.* 2013, Shen *et al.* 2016), could reflect changes in energy allocation and thus be associated with elevated OCR.

Due to the difficulty of measuring the blood chemistry of small fish larvae only a few millimeters in length, the physiological response of young larvae to elevated pCO_2 and mechanisms of acid-base regulation is unknown but assumed to be similar to that of juveniles and adults. In fact, many of the effects of elevated pCO_2 on young fish are presumed to be the downstream consequence of compensatory processes to restore internal pH during respiratory acidosis. While the gills, particularly the lamellae, are highly efficient organs for gas and ion exchange in juveniles and adults, they are not fully functional until metamorphosis for many species of marine fish (Rombough *et al.* 1988). The numerous NKA-containing MRCs located on the body, yolk-sac epithelium and gill wells of larvae that are morphological similar to adult gill cells are sufficient for performing ion regulation until gill MRCs become functional (Lasker and Threadgold 1968, Hiroi *et al.* 1998). Furthermore, the large surface area to volume ratio of larvae and thinness of the skin ($<$3 µm) facilitate cutaneous gas diffusion (Rombough *et al.* 1988). Lastly, 20-50% of the total energy budget

of adult marine fish is used by NKA pumps for osmoregulation (Gibbs and Somero 1990, Bœuf and Payan 2001). The fact that osmoregulation occurs during the egg and larval stages (Alderdice 1988, Lasker and Theilacker 1962, Varsamos *et al.* 2005) suggests that extant NKA pumps are also capable of performing acid-base regulation, which carries much lower energy requirements compared to acid-base regulation.

The maintenance of pH homeostasis is critical to the survival of all organisms in all stages of life because changes in pH can impact cell-to-cell signaling, cell motility, gene expression, metabolism, and whole animal performance (Putnam and Roos 1997). If more energy is required for pH and acid-base regulation in a high-pCO_2 world and the increased oxygen demand is not met, tissues can become hypoxic and slow down protein synthesis, with consequences for growth and reproduction (Pörtner *et al.* 2005). In the early life history stages of fish, even small changes in growth and mortality rates can result in order-of-magnitude changes in the recruitment and the size of adult populations (Houde 1987). Given the many effects of elevated pCO_2 on young fish and the importance of these early life history stages to the size and sustainability of adult populations, it is important to understand the physiological mechanisms underpinning the observed behavioral and developmental changes in order to better predict the impacts of future ocean acidification on fish populations.

In this study, we measured the OCR and abundance of NKA in white seabass (*Atractoscion nobilis*) larvae reared at control (560 $\pm$ 32 µatm; mean $\pm$ standard error) and elevated (1971 $\pm$ 55 µatm) pCO_2 until 5 days post fertilization (dpf). We hypothesized that rearing larvae at high pCO_2 would induce a respiratory acidosis and, in response, larvae would increase NKA production to help maintain their internal pH. Furthermore, we hypothesized that the increase in NKA abundance in treatment larvae would be evident in immunohistochemical images of larvae as a higher number of immunopositive cells for NKA. Lastly, we hypothesized that the increase in NKA abundance would correspond with

an increase in OCR, indicative of the increased demand for acid-base regulation.

4.3 Materials and Methods

4.3.1 Experimental System

The experimental system from Checkley *et al.* (2009) was expanded to include 6 (3 control, 3 treatment) water-jacketed, 5-L glass vessels with jacket water maintained at 18.0°C. Vessels were continuously bubbled with a certified air-CO_2 gas mixture of 400 µatm pCO_2 (control) and 2500 µatm pCO_2 (treatment). The average pCO_2 of control and treatment vessels was 560 $\pm$ 32 µatm and 1971 $\pm$ 55 µatm, respectively (Table 1). Control and treatment vessels had an average pH of 7.92 $\pm$ 0.02 and 7.42 $\pm$ 0.01, respectively (Table 1). The pCO_2 of treatment vessels in EX 2 was lower than in other experiments, with values near 1800 µatm.

On the morning of an experiment, newly fertilized eggs (<12 hours post-fertilization) of white seabass (*Atractoscion nobilis*) were obtained from the Leon Raymond Hubbard, Jr., Marine Fish Hatchery at the Hubbs-SeaWorld Research Institute (HSWRI) in Carlsbad, California, USA. Four-hundred eggs were transferred into each of the experimental vessels containing filtered seawater fully equilibrated at the control or experimental pCO_2 and reared for five days, resulting in 5 dpf larvae. Larvae from the first three experiments (EX 1, EX 2, EX 3) were used for microrespiration measurements, Western blot analysis and immunohistochemistry. Standard length measurements were made on live larvae following OCR measurements in EX 1 and EX 2. Larvae from the fourth experiment (EX 4) were dried on Teflon at 50°C for 24 hr to estimate dry mass, measured to the nearest 1 µg. Groups of five larvae were measured and the total mass was divided by five to obtain an estimate of individual mass.

4.3.2 Seawater Carbonate Chemistry

On the first day of each microrespiration experiment, 250 mL seawater samples were collected from each vessel and poisoned with 100 µL of mercuric chloride for the measurement of inorganic carbon chemistry. Total alkalinity (A_T) and dissolved inorganic carbon chemistry (DIC) were measured using open-cell potentiometric titration and coulometry, respectively. The software CO2Calc (http://cdiac.ornl.gov/ftp/co2sys) was used to estimate pH and pCO_2 from the measured A_T and DIC. Results for seawater samples from EX 4 are currently being processed, but are likely to be similar to those for previous experiments. HSWRI provided data for temperature and pH of the broodstock tanks on the mornings that eggs were collected for experiments, as well as the most recent measurement of A_T, which was taken no more than 2 days from the day of egg collection. pCO_2 of the broodstock environment of newly fertilized eggs was estimated from these values using CO2Calc.

4.3.3 Oxygen Consumption Rate

The oxygen consumption rate (OCR) of larvae at 5 dpf was measured using a Unisense MicroRespiration System and accompanying software, SensorTrace Rate (Unisense A/S, Aarhus, Denmark). Five larvae were removed from an individual vessel and placed into a 4 mL glass microrespiration chamber containing seawater from that vessel. The chamber was placed onto a magnetic stir rack (MR-rack) and the seawater was stirred at 600 rpm by a glass-embedded micromagnet separated from the larvae by a stainless steel mesh net. The magnetic stir rack holding the chamber was submerged in a water bath at 18.0°C. Larvae were allowed to acclimate for 10 min before oxygen measurements were recorded.

An oxygen microsensor (OX-MR) was inserted into the chamber through a capillary in the lid. The microelectrode measured the partial pressure of oxygen as it diffused across a silicone membrane to an oxygen-reducing cathode polarized against an internal Ag/AgCl anode. The resulting signal was measured by a picoammeter (Microsensor Multimeter).

Oxygen concentration was measured for 50 min, during which the larvae were visually inspected for 1 min every 15 min to observe behavior. OCR measurements were performed in duplicate using 2 chambers simultaneously, each containing 5 larvae from the same vessel and an oxygen microsensor. Oxygen measurements were also recorded in EX 3 for blanks that contained only seawater from each vessel to obtain the background microbial respiration rate ($\sim$50%), which was removed from the OCR measurements in all experiments. Following oxygen measurements, the standard lengths of larvae in EX 1 and EX 2 were measured to the nearest 0.1 mm using a dissecting microscope.

The day before the OCR measurements, the oxygen microelectrodes were pre-polarized to remove oxygen that had accumulated within the electrolyte during storage. The calibration chamber (Cal300) was filled with seawater and bubbled with air vigorously for 5 min before the microsensors were submerged. Pre-polarization was complete when the signal stabilized (40 min to 2 hr). The 0-calibration chamber was filled with an anoxic solution (0.1M sodium ascorbate and 0.1M NaOH) and the silicone tube attached to the lid was filled with seawater. The calibration chamber and the microelectrodes were stored overnight in deionized water in an 18.0°C water bath.

On the morning of OCR measurements, the microsensors were briefly polarized (10 min) as before. A two-point calibration was performed by measuring the signals of the microsensors in anoxic seawater in the 0-calibration chamber and in seawater saturated with oxygen by rigorous air bubbling for 5 min.

4.3.4 Western Blot Analysis

Following the microrespiration experiments, all larvae remaining in the vessels were harvested and flash-frozen in liquid nitrogen for Western blot analysis. Samples of frozen larvae (n = 20-60) were sonicated on ice for 20 s, homogenized in 600 µL of homogenization buffer (BHH: 12 µL, PMSF: 3 µL, and DTT: 0.6 µL), and centrifuged at 500 rcf for 10

min at 4°C to remove debris. The total protein concentration of the crude homogenate was determined by Bradford Protein Assay (BPA), a colorimetric assay based on the change in color of the Coomassie brilliant blue G-250 dye, and performed in triplicate. Samples were divided into aliquots based on protein concentration and stored at -80°C.

To prepare for Western blot analysis, samples were thawed, mixed with 90% 4x Laemmli buffer and 10% Beta-Mercaptoethanol, and heated for 5 min at 70°C. Five µg of total protein from each sample were separated by molecular weight in an Any kD, Mini-PROTEAN® TGX Stain-Free™ Precast Gel (Bio-Rad Laboratories, Inc., Hercules, CA, USA) by sodium dodecyl sulfate polyacrylamide gel electrophoresis (SDS-PAGE) at 200V for 45 min. Proteins were transferred to Polyvinylidene difluoride (PVDF) membranes using the Trans-Blot® Turbo™ System (Bio-Rad Laboratories, Inc., Hercules, CA, USA) semi-dry transfer cell for 30 min at 25V.

Western blots were blocked in Tris-buffered saline with 0.1% Tween (TBS-T) and 10% nonfat dry milk for 1 hr at room temperature, then incubated overnight with a monoclonal mouse anti-chicken NKA antibody that targeted the alpha-subunit (1:1000 dilution in blocking buffer) at 4°C on a shake table. This antibody was deposited to the Developmental Studies Hybridoma Bank by DM Fambrough and has been tested against fish (DSHB Hybridoma Product a5). After 3 washes in TBS-T for 20 min each, the blots were blocked for 1 hr and incubated with a secondary goat anti-mouse NKA antibody (1:10,000 dilution in blocking buffer) at room temperature on a shake table. Blots were washed as before.

Blots were analyzed using chemiluminescence on a ChemiDoc™ MP system with Image Lab™ software (Bio-Rad Laboratories, Inc., Hercules, CA, USA). Band fluorescence was quantified using Image Lab™ software (Bio-Rad Laboratories, Inc., Hercules, CA, USA). Protein abundance was based on the chemiluminescent signal and expressed relative to a standard that was used in all gels. The standard contained larvae from EX 1 that were reared in a cold room at 18.0°C in a 5 L beaker with bubbled air. The standard was diluted in

EX 3 and the relative abundance of NKA was multiplied by this dilution factor to facilitate comparisons among experiments.

4.3.5 Whole-body Immunohistochemistry

For each experiment, larvae from 1 control and treatment vessel each were preserved in 4% paraformaldehyde for 4 hr, transferred to 50% ethanol overnight, and stored in 70% ethanol for whole-body immunostaining. Three larvae from each experiment were immunostained with the same mouse monoclonal antibody raised against the α-unit of NKA used in Western blot analysis. Three larvae from each experiment were not incubated with the NKA antibody and served as controls. Larvae were stained with prediluted reagents of the VECTASTAIN® Universal HRP Kit (Peroxidase) R.T.U. (Ready-to-Use) (Vector Laboratories, Inc., Burlingame, CA, USA). As instructed, larvae were rinsed with 3% hydrogen peroxide for 10 min, normal goat serum (NGS; prediluted to 2.5%) for 30 min, and incubated overnight at room temperature with a mouse anti-goat NKA antibody (1:1000 dilution in 2.5% NGS). The following day, samples were rinsed three times with PBS for 5 min each before incubation in the universal pan-specific secondary antibody for 30 min, followed by another three PBS washes. Samples were immersed in peroxidase-streptavidin complex for 15 min, stained with 3,3-diaminobenzidine tetrahydrochloride for 15 min, and then rinsed in deionized water before imaging. Images of larvae were taken at each focal level using a Canon Rebel T5i camera (Canon U.S.A., Inc., Melville, NY, USA) on a Leica DMR compound microscope (Leica Microsystems, Inc., Buffalo Grove, IL, USA), stacked using the imaging software Helicon Focus 6 (Helicon Soft Ltd., Kharkov, Ukraine), and stitched using Adobe Photoshop's automated photomerge process (CS5). Measurements of standard length and counts of immunopositive cells were performed on masked images using ImageJ (https://imagej.nih.gov/ij/).

4.3.6 Data Analysis

A linear regression of oxygen concentration over time was performed and the slope of the line was estimated as the group OCR for the group of 5 larvae. The OCR of EX 3 blanks using control (treatment) seawater was subtracted from the group OCR of control (treatment) larvae to remove the contribution of bacterial respiration. The OCR of an individual larva was estimated by dividing the group OCR by five. Statistical analyses were performed on individual-based OCR (μL O_2 ind^{-1} h^{-1}). Standard-length measurements of larvae in EX 1 and EX 2 enabled the determination of length-based OCR (μL O_2 mm^{-1} h^{-1}). The averages of dry mass measurements of control and treatment larvae in EX 4 were used to calculate an approximate mass-specific OCR (μL O_2 mg^{-1} hr^{-1}) for larvae in all experiments. Length-based and approximate mass-specific OCR are available in the Supplemental Information (Table S1).

OCR, relative abundance of NKA, and larval standard length data were analyzed using Analysis of Variance (ANOVA), with pCO_2 and experiment as predictor variables. A linear regression was used to find the relationship between the standard length of larvae that were used in immunohistochemistry and the number of cells that were immunopositive for NKA in those larvae. The residuals of this model were then analyzed using ANOVA with pCO_2 and experiment as predictor variables. Lastly, dry mass measurements in EX 4 were analyzed using ANOVA with pCO_2 as the predictor variable. Model residuals for all response variables were normal distributed, as determined by Shapiro-Wilks tests. Tukey Honestly Significant Difference test (Tukey HSD) was performed for predictor variables that were significant to identify what group differed from the other groups. Results were considered significant at $p < 0.05$. Statistical analyses were performed in R version 3.1.2 (R Foundation for Statistical Computing, Wien, Austria).

4.4 Results

There was no effect of pCO_2 on the dry mass of larvae at 5 dpf (ANOVA: $F_{(1)}$ = 0.46, p = 0.51), with control larvae at 0.17 ± 0.01 mg (n = 45) and treatment larvae at 0.18 ± 0.01 mg (n = 45). There was no effect of pCO_2 on the standard length of larvae in EX 1 and EX 2 (ANOVA: $F_{(1)}$ = 0.63, p = 0.43), but there was a significant effect of experiment (ANOVA: $F_{(1)}$ = 20.21, p <0.0001) with larvae in EX 2 being significantly smaller (3.53 ± 0.01 mm; n = 59) than larvae in EX 1 (3.63 ± 0.02 mm; n = 60).

As a result of respiration by larvae, oxygen declined linearly within the microrespiration chambers (Fig. 1). Visual observations of larvae during experiments revealed that the larvae in both control and elevated pCO_2 treatments were mostly inactive, engaging in swimming bursts only to re-orient themselves. pCO_2 did not affect the OCR of 5-day-old larvae (ANOVA: $F_{(1)}$ = 0.048, p = 0.83; Fig. 2). Average OCR was 0.18 ± 0.03 μL O_2 ind^{-1} h^{-1} for control larvae and 0.19 ± 0.03 μL O_2 ind^{-1} h^{-1} for treatment larvae. Across experiments, OCR ranged from 0.09 to 0.34 μL O_2 ind^{-1} h^{-1} (Table S1). There was a significant effect of experiment (ANOVA: $F_{(2)}$ = 33.89, p <0.0001; Fig. 2) with all experiments having a significantly different mean OCR from each other (Tukey HSD p <0.05).

Western blots using an NKA antibody identified a single band at ∼100 kDA in the whole-body crude homogenates of larvae (Fig. 3; Table S2). The relative abundance of NKA was not significantly related to pCO_2 (ANOVA: $F_{(1)}$ = 2.11, p = 0.17; Fig. 4) or experiment (ANOVA: $F_{(1)}$ = 2.80, p = 0.10; Fig. 4).

Immunohistochemistry revealed an abundance of cells that were immunopositive for NKA concentrated around the middle of the larvae (Fig. 5). NKA positive cell abundance decreased between the anus and end of the caudal fin. Qualitatively, spatial distribution did not appear to differ between control and treatment larvae (Fig. 5). There was a significant positive and linear relationship between larva standard length and the number of cells immunopositive for NKA on the body (R^2 = 0.67, $F_{(16)}$ = 32.20, p <0.0001). The number

of immunopositive cells standardized to larva length did not differ significantly between control and treatment larvae (ANOVA: $F_{(1)} = 3.09$, $p = 0.10$) with an average of 565 $\pm$ 52 cells for control larvae (2.79 $\pm$ 0.09 mm) and 688 $\pm$ 19 cells for treatment larvae (2.92 $\pm$ 0.04 mm; Table S3). There was no effect of experiment (ANOVA: $F_{(2)} = 1.83$, $p = 0.20$). No cells were identified in the control larvae that were not incubated with the NKA antibody.

4.5 Discussion

White seabass larvae at 5 dpf appear to be physiologically resilient in the variables measured to pCO_2 projected for the year 2300 if carbon emissions continue unabated ($\sim$2000 µatm; IPCC 2013). We found no effect of pCO_2 on OCR or NKA abundance. Consistent with this finding, larvae did not differ in length or mass when reared at elevated pCO_2. Together, these results suggest that larvae were able to maintain acid-base regulation when exposed to elevated pCO_2 without compromising somatic growth. The high mass-specific metabolic rate and the physiological composition of the respiratory pigment of fish larvae may help to explain the relative resiliency of white sebass larvae to these pCO_2 concentrations.

The approximate mass-specific OCR of white seabass calculated using the average dry mass for control (0.17 $\pm$ 0.01 mg) and treatment (0.18 $\pm$ 0.01 mg) larvae in EX 4 ranged from 0.56 to 1.93 µL O_2 mg^{-1} h^{-1}. These values are comparable to those for the young larvae of other species of fish (Table 7 of Houde 1989). For example, OCRs range from 0.30 µL O_2 mg^{-1} h^{-1} for Atlantic herring (*Clupea harengus*) to 19.7 µL O_2 mg^{-1} h^{-1} for lined sole (*Achirus lineatus*) (Houde 1989). Since experiments were performed with groups of larvae, it is important to note that a 'calming effect' resulting in a reduction of metabolic rate has been observed for shoaling and gregarious damselfish *Chromis viridis* when groups of larvae were used for OCR measurements (Nadler *et al.* 2016). In comparison to larval OCR, the OCR of an adult tropical reef fish in warm water is around 200-300 mg O_2 kg^{-1}

h^{-1} (Munday *et al.* 2009, Couturier *et al.* 2013) and that of a fish in cold temperate or polar waters ranges from 10 to 40 mg O_2 kg^{-1} h^{-1} (Melzner *et al.* 2009b, Enzor *et al.* 2013).

We make two important assumptions in the calculation of approximate mass-specific OCR. First, we assume that the dry mass did not differ between control and treatment larvae in EX 1-3, as was shown for larvae in EX 4. Second, we assume that the average dry mass of larvae in these experiments was equal to that in EX 4. For these reasons, we use the term *approximate* mass-specific OCR and provide these results for comparison to OCR values in the literature. An important assumption in the calculation of OCR standardized to the individual is that the measured contribution of bacterial respiration to the group OCR in EX 3 is representative of that in EX 1 and EX 2.

The mass-specific metabolic demand of fish larvae is typically much higher than that of juveniles and adults (due to the rapid growth of metabolizing tissue), with OCR declining 50-80% as mass increases by four orders of magnitude (Post and Lee 1996). For the same reason, the CO_2 concentrations of the extracellular fluids and cells of larvae, while unknown, are likely to approach or exceed those of the older life stages. Blood CO_2 concentrations for adult fish range from 3000-4900 μatm during periods of inactivity to 9900 μatm following exercise (Melzner *et al.* 2009b). Therefore, adults, and presumably also larvae, are still able to maintain an outward (although reduced) gradient of CO_2 when exposed to CO_2 concentrations projected for the next several centuries with ocean acidification. Furthermore, extant NKA protein abundance and activity are adept at maintaining acid-base and pH balance when internal CO_2 is exceedingly high on a daily basis.

The chemical and physiological properties of the larva polymorph of hemoglobin may help to offset the effects of elevated pCO_2 on larval fish OCR. Larval hemoglobin has a higher oxygen affinity than the adult form for freshwater rainbow trout (*Salmo gairdnerii irideus*), marine eelpout (*Zoarces viviparous*) and many other lower, non-aquatic vertebrates (Rombough 1988, Ingermann 1992). Larval hemoglobin also has a reduced Bohr effect

and Root effect, which describe the negative effect of pH on oxygen affinity and carrying capacity, respectively (Rombough 1988). These properties of the respiratory pigments may safeguard young larvae from oxygen limitation during periods of high environment pCO_2.

Our finding that pCO_2 does not greatly affect NKA protein abundance supports the lack of an effect on OCR. The energetic cost of NKA pumping can account for ~25% of branchial oxygen consumption in adult fish (Stagg and Shuttleworth 1982, Morgan *et al.* 1997). An increase in NKA abundance and activity has only been shown for adult fish exposed to pCO_2 >5000 µatm pCO_2 (Deigweiher *et al.* 2008, Melzner *et al.* 2009b). Increasing NKA production may be too costly, especially for larvae with a high metabolic demand, and unnecessary, given the efficiency of cutaneous gas exchange and osmoregulation of eggs and larvae. Tseng *et al.* (2013) demonstrated that exposure of Japanese ricefish (*Oryzias latipes*) larvae to 1,200-4,200 µatm pCO_2 resulted in a higher expression of mRNA for genes involved in acid secretion (50-71% for Na^+/H^+ exchanger) and HCO_3^- regulation (61-123% for Na^+/HCO_3^- exchanger), and a 70% increase the expression of three NKA isoforms. Unfortunately, no measurements of NKA protein abundance or activity or metabolic rate were made to elucidate the effects of these changes.

In our study, the measured pH of the broodstock tanks on the morning of egg collection for EX 1-3 ranged from 7.24 to 7.39 (HSWRI, personal communication). We estimate that pCO_2 ranged from 1051 to 2481 µatm. This raises the question of whether the larvae we tested are adapted to high-pCO_2 and low pH conditions. Multi-generational and transplant experiments have demonstrated that some of the adverse effects of elevated pCO_2 on the growth, metabolism and survival of the larvae and juveniles of several species of fish are absent when offspring are spawned from parents living in high-pCO_2 conditions (Murray *et al.* 2013, Miller *et al.* 2012, Cattano *et al.* 2016). Similarly, the eggs and larvae of Atlantic herring (*Clupea harengus*) and Baltic cod (*Gadus morhua*), spawned in naturally high-pCO_2 conditions (>1000 µatm), are unaffected by elevated pCO_2 in ocean

acidification experiments. Our understanding of the role of epigenetic and evolutionary adaptation in shaping the response of individuals and populations to ocean acidification is far from complete.

Our results suggest that pCO_2 of 2000 µatm predicted for the world's ocean by 2300 as a result of ocean acidification do not have a detrimental effect on the physiology, metabolism and growth of young white seabass larvae. The high mass-specific metabolic rate of larvae compared to the older life stages, ability of larvae to perform energetically-expensive osmoregulatory processes using energy generated by NKA, proficiency of epithelial MRC in gas and ion exchange prior to gill development, and physiological characteristics of larval hemoglobin are consistent with the observed resiliency of white seabass larvae to elevated pCO_2. Larvae appear able to cope with elevated pCO_2, experiencing no changes in somatic growth, without having to modify cellular or metabolic processes. Our research raises many questions that highlight the need for basic research on larval fish physiology, including the mechanisms for acid-base regulation, the chemical composition of the blood and intracellular fluids, and the energetic costs of homeostatic processes (osmoregulation and acid-base regulation). A better understanding of larval fish physiology will enable ocean acidification researchers to make more informed inferences about their results and better predictions about the impacts of elevated pCO_2 on fish over their entire life cycle.

4.6 Acknowledgements

We thank the Hubbs-SeaWorld Research Institute for providing fertilized white seabass eggs and data on pH and A_T of the broodstock tanks. We are grateful to Lauren Linsmayer for her assistance with the microrespiration system and Dr. Greg Rouse for use of microscope and camera. Funding in support of this research was provided by the Scripps Institution of Oceanography at UCSD to Sara G. Shen. Support was also provided from the National Science Foundation Graduate Research Fellowship Program (NSF GRFP) to

Sara G. Shen. Animal care and experimental procedures were approved by the University of California San Diego Institutional Animal Care and Use Committee under protocol S12161. The authors declare no conflicts of interest.

Chapter 4, in full, is in preparation for publication as Shen, S.G., Kwan, G., Tresguerres, M., and Checkley, D.M., Jr. Physiological resilience of white seabass *Atractoscion nobilis* larvae to ocean acidification. The dissertation author was the primary investigator and author of this manuscript.

4.7 Figures

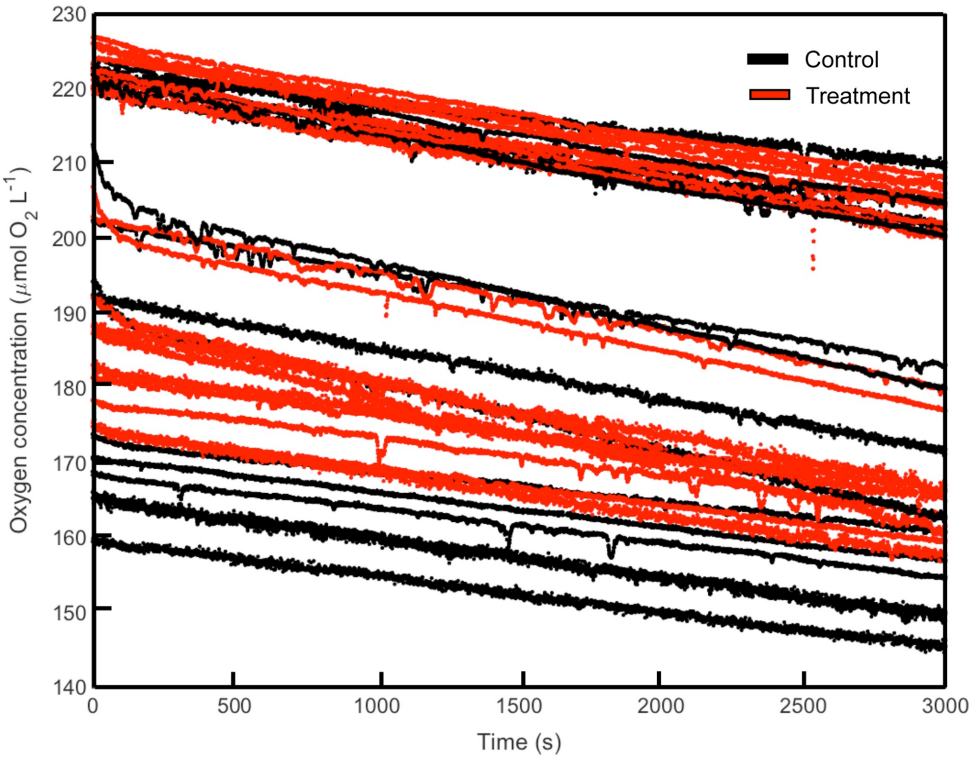

Figure 4.1: *Oxygen concentration as a function of time.*
Oxygen concentration (μmol O_2 L^{-1}) as a function of time (s). Lines show the decline in oxygen within a microrespiration chamber containing five larvae at control (black) and treatment (red) pCO_2 during EX 1-3.

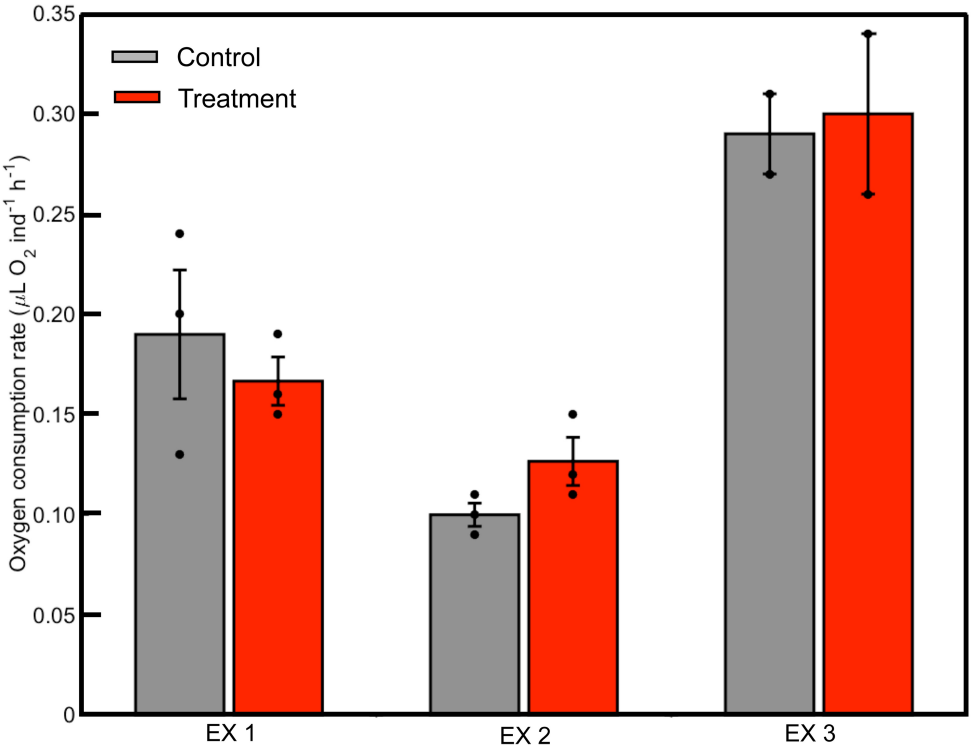

Figure 4.2: *Oxygen consumption rates of larvae.*
Bars show the oxygen consumption rates (μL O_2 ind^{-1} h^{-1} ± SEM) of thirty larvae at control (gray) and treatment (red) pCO_2. Dots are OCR values for each of the three control (C1, C2, C3) and three treatment (T1, T2, T3) vessels. The OCR dataset is available in the Supporting Information (Table S1).

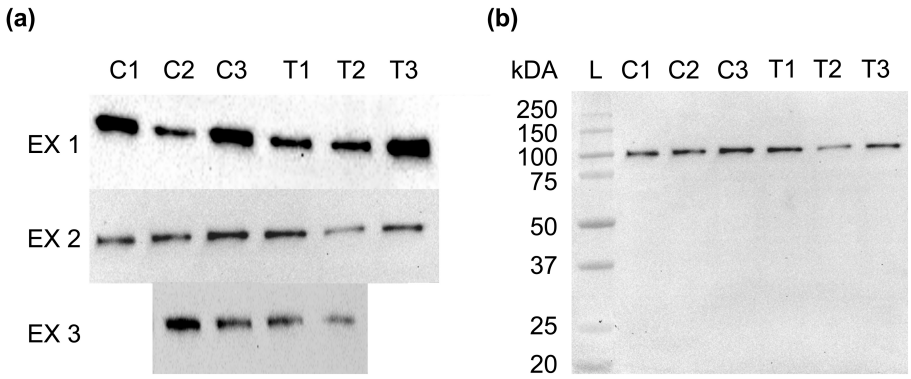

Figure 4.3: *Western blots for NKA in the crude homogenate of larvae.*
Western blots of crude homogenates of larvae at 5 dpf using an antibody against NKA. Abbreviations are as follows: EX= Experiment, C= Control pCO_2, T= Treatment pCO_2 and L= Ladder. Numbers following C and T indicate the vessel number. (a) Cut-outs of bands at $\sim$ 100 kDA pertaining to NKA. There were not enough survivors from C1 and T3 in EX 3 to perform Western blot analyses. (b) Full Western blot for EX 2 showing only bands at $\sim$100 kDA were detected.

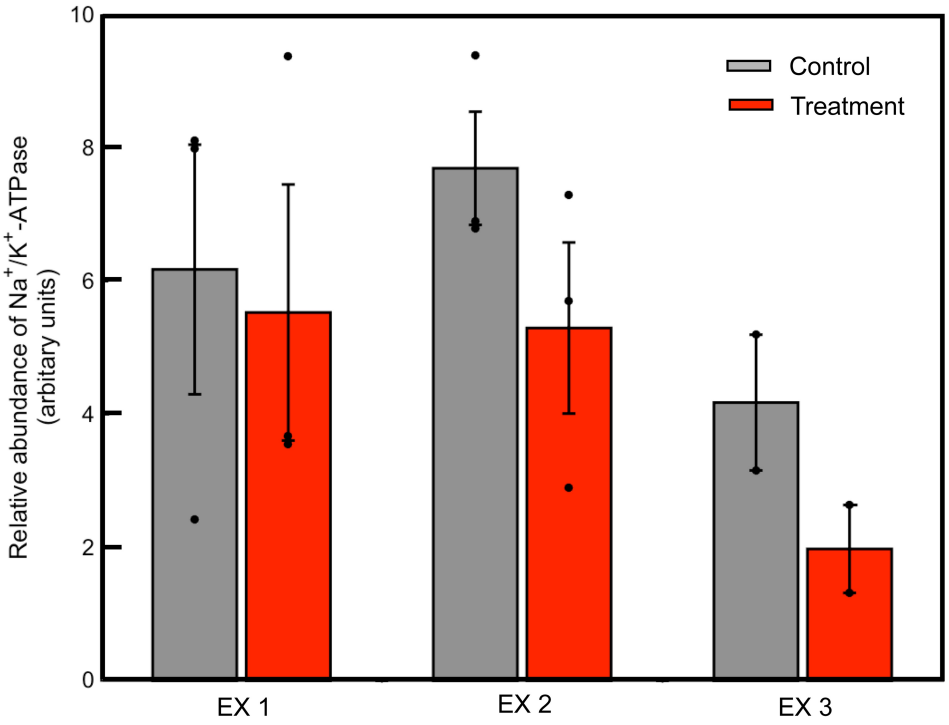

Figure 4.4: *Relative abundance of NKA in crude homogenates of larvae.*
Bars show the abundance of NKA (± SEM) in larvae at control (gray) and treatment (red) pCO_2 relative to a standard. Dots represent measurements for each of the vessels. The dataset is available in the Supporting Information (Table S2).

Figure 4.5: *Immunohistochemical staining of larvae with an NKA antibody.*
Image of larvae at 5 dpf with cells stained with an NKA antibody. Images show the distribution of cutaneous immunopositive cells for larvae at (a) control and (b) treatment pCO_2. The dataset of cell counts is available in the Supporting Information (Table S3).

4.8 Tables

Table 4.1: *Seawater carbonate chemistry measurements.*

Values are measured salinity (Sal), temperature (Temp), total alkalinity (A_T) and dissolved inorganic carbon (DIC) for each vessel within each experiment (EX). Partial pressure of CO_2 (pCO_2) and pH were estimated using the software CO2Calc.

Date	EX	Vessel	Sal	Temp (°C)	A_T (µmol kg^{-1})	DIC (µmol kg_{-1})	pCO_2(µatm)	pH
06/20/16	1	1	33.64	18.0	2262.02	2102.25	601	7.89
06/20/16	1	2	33.62	18.0	2270.18	2095.74	552	7.93
06/20/16	1	3	33.65	18.0	2269.91	2092.49	543	7.93
06/20/16	1	1	33.61	18.1	2262.51	2271.59	2097	7.39
06/20/16	1	2	33.64	18.0	2259.42	2268.87	2094	7.39
06/20/16	1	3	33.64	18.0	2264.31	2276.62	2145	7.38
07/04/16	2	1	33.61	18.0	2269.18	2061.71	454	7.99
07/04/16	2	2	33.61	18.0	2263.51	2094.85	569	7.91
07/04/16	2	3	33.64	18.0	2268.01	2078.31	503	7.96
07/04/16	2	1	33.60	18.0	2263.1	2253.03	1799	7.45
07/04/16	2	2	33.61	18.1	2269.54	2258.19	1792	7.46
07/04/16	2	3	33.62	18.0	2263.53	2251.85	1777	7.46
08/02/16	3	2	33.63	18.0	2257.87	2070.32	506	7.96
08/02/16	3	3	33.62	18.1	2247.71	2123.29	754	7.80
08/02/16	3	1	33.63	18.0	2262.57	2266.27	2005	7.41
08/02/16	3	3	33.62	18.1	2244.54	2252.21	2061	7.40

4.9 References

Alderdice DF (1988) Osmotic and ionic regulation in teleost eggs and larvae. In: Fish Physiology Volume 11, PP.163242, Academic Press, San Diego, CA.

Bœuf G, Payan P (2001) How should salinity influence fish growth? Comparative Biochemistry and Physiology Part C: Toxicology and Pharmacology, 130:411-423.

Cattano C, Giomi F, Milazzo M (2016) Effects of ocean acidification on embryonic respiration and development of a temperate wrasse living along a natural CO_2 gradient. Conservation Physiology, 4:cov073.

Chabot D, Steffensen JF, Farrell AP (2016) The determination of standard metabolic rate in fishes. Journal of Fish Biology, 88:81-121.

Checkley DM Jr, Dickson AG, Takahashi M, Radich JA, Eisenkolb N, Asch R (2009) Elevated CO_2 enhances otolith growth in young fish. Science, 324:1683-1683.

Couturier CS, Stecyk JA, Rummer JL, Munday PL, Nilsson GE (2013) Species-specific effects of near-future CO_2 on the respiratory performance of two tropical prey fish and their predator. Comparative Biochemistry and Physiology Part A: Molecular and Integrative Physiology, 166:482-489.

Deigweiher K, Koschnick N, Pörtner HO, Lucassen M (2008) Acclimation of ion regulatory capacities in gills of marine fish under environmental hypercapnia. American Journal of Physiology- Regulatory, Integrative and Comparative Physiology, 295:R1660-R1670.

Enzor LA, Zippay ML, Place SP (2013) High latitude fish in a high CO_2 world: synergistic effects of elevated temperature and carbon dioxide on the metabolic rates of Antarctic notothenioids. Comparative Biochemistry and Physiology Part A: Molecular and Integrative Physiology, 164:154-161.

Esbaugh AJ, Heuer R, Grosell M (2012) Impacts of ocean acidification on respiratory gas exchange and acidbase balance in a marine teleost, *Opsanus beta*. Journal of Comparative Physiology B, 182:921-934.

Esbaugh AJ, Ern R, Nordi WM, Johnson AS (2016) Respiratory plasticity is insufficient to alleviate blood acidbase disturbances after acclimation to ocean acidification in the estuarine red drum, *Sciaenops ocellatus*. Journal of Comparative Physiology B, 186:97-109.

Feely RA, Sabine CL, Hernandez-Ayon m, Ianson D, Hales B (2008) Evidence for Upwelling of Corrosive Acidified Water onto the Continental Shelf. Science, 13:1490-1492.

Franke A, Clemmesen C (2011) Effect of ocean acidification on early life stages of Atlantic herring (*Clupea harengus* L.). Biogeosciences, 8:3697-3707.

Friederich GE, Ledesma J, Ulloa O, Chavez FP (2008) Air-sea carbon dioxide fluxes in the coastal southeastern tropical Pacific. Progress in Oceanography, 79:156-166.

Frommel AY, Schubert A, Piatkowski U, Clemmesen C (2013) Egg and early larval stages of Baltic cod, *Gadus morhua*, are robust to high levels of ocean acidification. Marine Biology, 160:1825-1834.

Fry FEJ (1971) The effect of environmental factors on the physiology of fish. Fish physiology, 6:1-98.

Gibbs A, Somero GN (1990) Na^+-K^+-adenosine triphosphatase activities in gills of marine teleost fishes: changes with depth, size and locomotory activity level. Marine Biology, 106:315-321.

Heuer RM, Grosell M (2014) Physiological impacts of elevated carbon dioxide and ocean acidification on fish. American Journal of Physiology-Regulatory, Integrative and Comparative Physiology, 307:R1061-R1084.

Hiroi J, Kaneko T, Seikai T, Tanaka M (1998) Developmental sequence of chloride cells in the body skin and gills of Japanese flounder (*Paralichthys olivaceus*) larvae. Zoological Science, 15:455-460.

Houde ED (1987) Fish early life dynamics and recruitment variability. American Fisheries Society Symposium Series, 2:17-29.

Houde ED (1989) Comparative growth, mortality, and energetics of marine fish larvae: Temperature and implied latitudinal effects. Fishery Bulletin, 87:471-495.

Ingermann RL (1992) Maternal-fetal oxygen transfer in lower vertebrates. American Zoologist, 32:322-330.

IPCC (2013) Climate change 2013: the physical science basis, Chapter 6. In: Stocker TF, Qin D, Plattner GK, Tignor M and others (Eds.), Contribution of working group 1 to the fifth assessment report of the Intergovernmental Panel on Climate Change, PP. 465-544, Cambridge University Press, Cambridge.

Ishimatsu A, Hayashi M, Kikkawa T (2008) Fishes in high- CO_2, acidified oceans. Marine Ecology Progress Series, 373:295-302.

Lasker R, Theilacker GH (1962) Oxygen consumption and osmoregulation by single Pacific

sardine eggs and larvae (*Sardinops caerulea* Girard). Journal du Conseil, 27:25-33.

Lasker R, Threadgold LT (1968) "Chloride cells" in the skin of the larval sardine. Experimental Cell Research, 52:582-590.

Melzner F, Gutowska MA, Langenbuch M, Dupont S, Lucassen M, Thorndyke MC, Bleich M, Portner HO (2009a) Physiological basis for high CO_2 tolerance in marine ectothermic animals: pre-adaptation through lifestyle and ontogeny. Biogeosciences, 6:2313-2331.

Melzner F, G*maẗhrmo*bel S, Langenbuch M, Gutowska MA, Pörtner HO, Lucassen M (2009b) Swimming performance in Atlantic Cod (*Gadus morhua*) following long-term (4-12 months) acclimation to elevated seawater pCO_2. Aquatic Toxicology, 92:30-37.

Miller GM, Watson SA, Donelson JM, McCormick MI, Munday PL (2012) Parental environment mediates impacts of increased carbon dioxide on a coral reef fish. Nature Climate Change, 2:858-861.

Morgan JD, Iwama GK, Wilson JM (1997) Oxygen consumption and Na^+-K^+-ATPase activity of rectal gland and gill tissue in the spiny dogfish, *Squalus acanthias*. Canadian Journal of Zoology, 75:820-825.

Munday PL, Crawley NE, Nilsson GE (2009) Interacting effects of elevated temperature and ocean acidification on the aerobic performance of coral reef fishes. Marine Ecology Progress Series, 388:235-242.

Murray CS, Malvezzi A, Gobler CJ, Baumann H (2014) Offspring sensitivity to ocean acidification changes seasonally in a coastal marine fish. Marine Ecology Progress Series, 504:1-11.

Nadler LE, Killen SS, McClure EC, Munday PL, McCormick MI (2016). Shoaling reduces metabolic rate in a gregarious coral reef fish species. Journal of Experimental Biology 219: 2802-2805.

Perry SF, Gilmour KM (2006) Acidbase balance and CO_2 excretion in fish: unanswered questions and emerging models. Respiratory Physiology and Neurobiology, 154:199-215.

Pimentel M, Pegado M, Repolho T, Rosa R (2014) Impact of ocean acidification in the metabolism and swimming behavior of the dolphinfish (*Coryphaena hippurus*) early larvae. Marine Biology, 161:725-729.

Pörtner HO, Langenbuch M, Michaelidis B (2005) Synergistic effects of temperature extremes, hypoxia, and increases in CO_2 on marine animals: from Earth history to global change. Journal of Geophysical Research, 110:C09S10.

Post JR, Lee JA (1996) Metabolic ontogeny of teleost fishes. Canadian Journal of Fisheries and Aquatic Sciences, 53:910-923.

Putnam RW, Roos A (1997) Intracellular pH. In Handbook of Physiology, Cell Physiology, PP. 389-440, Oxford University Press, New York.

Rombough P (1988) Respiratory gas exchange, aerobic metabolism, and effects of hypoxia during early life. In: The Physiology of Developing Fish, PP.59-161, Academic Press, San Diego, CA.

Stagg RM, Shuttleworth TJ (1982) The effects of copper on ionic regulation by the gills of the seawater-adapted flounder (*Platichthys flesus* L.). Journal of Comparative Physiology, 149:83-90.

Tseng YC, Hu MY, Stumpp M, Lin LY, Melzner F, Hwang PP (2013) CO_2-driven seawater acidification differentially affects development and molecular plasticity along life history of fish (*Oryzias latipes*). Comparative Biochemistry and Physiology Part A: Molecular and Integrative Physiology, 165:119-130.

Varsamos S, Nebel C, Charmantier G (2005) Ontogeny of osmoregulation in postembryonic fish: a review. Comparative Biochemistry and Physiology Part A: Molecular and Integrative Physiology, 141:401-429.

Chapter 5

Conclusion

A review of the literature on the effects of ocean acidification on the early life stages of marine fish reveals a complex and somewhat contradictory picture of how fish will be impacted in the future under IPCC scenarios of climate change. The lack of a unifying response of fish to predicted concentrations of pCO_2 is also evident within my dissertation research. In Chapter 2, white seabass (*Atractoscion nobilis*) larvae reared at 2500 µatm pCO_2 experienced increased otolith growth. However, larger sized utricular otoliths did not severely impact vestibular function, as tested by the VOR. Similarly, white seabass larvae that were born and raised at 2000 µatm pCO_2 in Chapter 4 did not experience any changes in NKA protein abundance and location, OCR, or somatic growth. Together, these findings suggest that white seabass larvae may be less affected by future increases in seawater pCO_2 than the larvae of other species of fish. In contrast, Anchoveta (*Engraulis ringens*) in Chapter 3 appear to preferentially spawn in waters of high pCO_2 in the Peruvian upwelling system. The eggs and larvae may also experience higher mortality rates when born at high pCO_2, although this hypothesis requires additional years of data for a more complete and robust analysis. Therefore, Anchoveta, with an affinity for spawning in high pCO_2 waters that may have consequences for larval survival, could be considered a species that will be negatively affected by ocean acidification. The findings presented in this dissertation contribute to the

growing body of literature of the effects, including lack of effects, of ocean acidification on the early life stages of marine fish.

In an attempt to answer the question, 'How will ocean acidification affect fish?' ocean acidification scientists have performed hundreds of experiments on numerous species of fish and found themselves confronted with confusing, conflicting, and sometimes uninformative results. I too am included in this body of scientists, adding to the number of response variables and species that have been tested for ocean acidification impacts, and not finding any strong, undeniable effects in either the positive or negative direction for the two species I studied. As I near completion of my PhD research, I come to the conclusion that the answer to the question posed above, and the motivating question of my research, will depend on the species. I recognize that this fact will make it considerably more challenging for the state and federal government to prepare and potentially mitigate the ecological and socioeconomic effects of climate change and ocean acidification. I also recognize that the apparent lack of conclusive effects of ocean acidification on fish in the scientific arena can be incentive to postpone conversations between scientists, managers, fishermen, and policy makers about how to effectively consider and plan for impacts. Therefore, as I transition from the world of pure academic research to a career at the intersection of science and policy, and anticipate the challenges that will come with changing management or policy to reflect best available science, I encourage ocean acidification researchers to consider ways to synthesize existing literature results to create a more unifying picture of the overall impacts of ocean acidification on fish.

A clearer picture of the effects of ocean acidification on the early life history stages of fish may emerge from exploring and characterizing the effects of ocean acidification on 'functional groups' of marine fish (e.g., benthic vs. pelagic spawners, temperate vs. tropical species). The early life history development of fish can vary greatly between benthic-spawned and pelagic-spawned fish. For example, larvae that are born from benthic-

spawned eggs are often larger and more developed at hatch, with strong sensory and swimming abilities, compared to larvae from pelagic eggs. Furthermore, synthesizing results by geographic distribution could also yield new insights. For example, tropical reef fish have a narrower thermal window than temperate fish and their capacity for aerobic performance and growth may be impacted to a greater extent by ocean acidification due to the elevated temperatures of their environment. I also think that utilizing natural gradients (e.g., spatial and temporal) in pCO_2 will allow scientists to gain a better understanding of whole-scale (e.g., population, ecosystem) responses. The use of natural pCO_2 vents, spatial gradients in pCO_2 caused by upwelling, and temporal variability of pCO_2 has allowed ocean acidification researchers to see the long-term and cumulative effects of elevated pCO_2 on entire ecosystems. These are two suggestions that may help scientists to better predict and formulate hypotheses about the potential effects of ocean acidification.

Throughout the time it has taken me to complete my PhD research, I have come to appreciate the complexity and importance of the issue of ocean acidification. Although still in its infancy, the field of ocean acidification has shown that there will likely be serious consequences for some organisms (i.e., corals, plankton, crustaceans) while others may not be greatly affected by a future high-pCO_2 ocean. Where the early life history stages of fish reside on the spectrum of severity of ocean acidification impacts is not completely understood. Given the ecological and economic importantance of fish and fisheries, this is an increasingly important question to answer.

Appendix A

Chapter 2 Supplemental Information

A.1 Figures

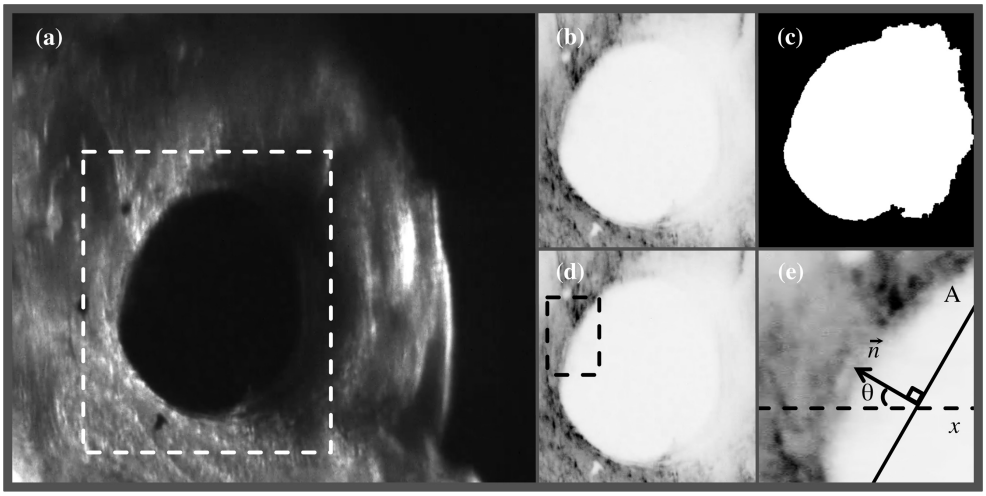

Figure A.1: *Steps to the quantification of the eye angle of fish larvae in Matlab.*
(a) Eye area is selected as ROI. (b) Grayscale threshold is applied to image. (c) Image is converted from grayscale to binary. Occlusion of the boundary of the eye by a shadow prevents the use of the whole eye to determine rotation angle. (d) A portion of the eye with a defined edge is selected and used in further analysis. (e) Angle of rotation of the eye is calculated using Radon transformation and defined as θ. Dashed boxes indicate area selection. These images are from Video S1.

A.2 Methods pertaining to Figure S1

Figure S1 illustrates the image analysis process using a sample video frame. The first step was to select the region of interest (ROI) containing the eye (Fig. S1a). Second, a threshold was used to convert the image from grayscale to binary (Fig. S1b, c). The threshold value demarcated the eye from the background and varied with illumination. However, in many videos, shadows obscured a portion of the boundary of the eye in the binary image as seen in Fig. S1c. Therefore, an unobstructed portion of the eye was selected from the grayscale image and used in further analysis (Fig. S1d). The angle of rotation of this section of the eye was calculated to represent the angle of the entire eye. The calculation was done using Radon transformation, whereby the image is projected from Cartesian coordinates (x, y) to polar coordinates (n, θ) along a series of lines (A) oriented θ (0-179°) clockwise from the x-axis (Deans1993, Fig. S1e). The Radon transform $R(n, \theta)$ was performed using the function *radon* and is the sum of the grayscale intensities of the pixels along the vector n perpendicular to A for all values of θ. When the edge of the eye has been detected, the magnitude of the vector n is maximized and the corresponding angle of the eye is known. Modifications were then made to eye data to ensure accurate measurements of eye rotation. The first step was to review the videos and remove anomalies in the eye data clearly attributed to head movement during respiration. The second step was to center the data at zero to remove the effect of variation in the position of the fish larvae in the Pasteur pipette.

A.3 Tables

Table A.1: *Data for all fish larvae in VOR experiments.*
Bottle indicates the experimental vessel in which a fish larva was reared. Fish larvae are associated with a unique ID. Gain and phase shift are defined in the text.

Date	Experiment	Bottle	pCO_2 (µatm)	ID	Gain	Phase Shift (°)
10/28/14	VOR 1	A	400	3	0.64	-8.8
10/28/14	VOR 1	A	400	12	0.26	40.2
10/28/14	VOR 1	A	400	13	0.24	-1.8
10/28/14	VOR 1	A	400	41	0.09	15.1
10/28/14	VOR 1	A	400	43	0.28	-7.9
10/28/14	VOR 1	C	2500	5	0.22	-21.9
10/28/14	VOR 1	C	2500	7	0.41	-27.6
10/28/14	VOR 1	C	2500	27	0.24	4.0
10/28/14	VOR 1	C	2500	35	0.87	36.5
10/28/14	VOR 1	C	2500	39	0.12	-5.9
11/5/14	VOR 2	A	400	25	0.40	-3.2
11/5/14	VOR 2	B	400	26	0.33	-15.7
11/5/14	VOR 2	A	400	30	0.38	-8.1
11/5/14	VOR 2	B	400	37/2	0.31	-2.6
11/5/14	VOR 2	B	400	40	0.11	-4.8
11/5/14	VOR 2	B	400	62	0.26	-30.2
11/5/14	VOR 2	C	2500	16	0.26	32.2
11/5/14	VOR 2	C	2500	19	0.23	-10.5
11/5/14	VOR 2	C	2500	33	0.19	9.2
11/5/14	VOR 2	C	2500	46	0.28	4.9
11/5/14	VOR 2	C	2500	47	0.27	-5.0
11/5/14	VOR 2	C	2500	52	0.40	8.9
11/5/14	VOR 2	C	2500	55	1.15	8.3
11/5/14	VOR 2	C	2500	59	0.34	-24.7
11/5/14	VOR 2	C	2500	61	0.35	-9.1
2/3/15	VOR 3	A	400	20	0.44	-35.3
2/3/15	VOR 3	A	400	26	0.21	38.6
2/3/15	VOR 3	A	400	27	0.45	-10.8
2/3/15	VOR 3	A	400	27/2	0.26	-40.5
2/3/15	VOR 3	A	400	36	0.23	4.7
2/3/15	VOR 3	A	400	40	0.09	0.6
2/3/15	VOR 3	A	400	41	0.53	-2.1
2/3/15	VOR 3	A	400	43	0.20	4.9
2/3/15	VOR 3	A	400	57	0.30	-28.8
2/3/15	VOR 3	C	2500	12	0.73	38.4
2/3/15	VOR 3	D	2500	15	0.35	-29.8
2/3/15	VOR 3	C	2500	18	0.34	-61.4
2/3/15	VOR 3	C	2500	31	0.40	-82.2
2/3/15	VOR 3	C	2500	33	0.85	4.5
2/3/15	VOR 3	D	2500	45	0.30	20.9
2/3/15	VOR 3	D	2500	46	0.27	35.9
2/3/15	VOR 3	C	2500	47	0.43	-10.8
2/3/15	VOR 3	C	2500	49	0.16	-8.8
2/3/15	VOR 3	D	2500	53	0.45	13.9
2/3/15	VOR 3	C	2500	62	0.19	11.5
2/3/15	VOR 3	C	2500	64	0.46	-8.9
2/3/15	VOR 3	C	2500	70	0.16	-4.0
2/3/15	VOR 3	C	2500	72	0.54	-5.0

Appendix B

Chapter 3 Supplemental Information

B.1 Tables

Table B.1: *Candidate models for egg presence and larva abundance.*

Candidate models that describe the relationship between egg presence and abundance of larvae, and oceanographic variables. Quadratic terms are denoted as the parameter squared. Data on zooplankton displacement volume were only available for larvae and therefore zooplankton displacement volume (Zoo) is not included in candidate models for egg presence. Models included temperature or salinity, and temperature or pCO_2 due to strong correlations between these variables (Pearsons r $>$0.6; SI Table 3).

Candidate Models
Eggs
Chl + Chl^2
Temp + $Temp^2$
pCO_2 + $pCO_2{}^2$
Sal + Sal^2
Temp + $Temp^2$ + Chl + Chl^2
Sal + Sal^2 + Chl + Chl^2
Sal + Sal^2 + pCO_2 + $pCO_2{}^2$
Chl + Chl^2 + pCO_2 + $pCO_2{}^2$
Sal + Sal^2 + pCO_2 + $pCO_2{}^2$ + Chl + Chl^2
Larvae
Chl + Chl^2
Temp + $Temp^2$
pCO_2 + $pCO_2{}^2$
Sal + Sal^2
Zoo + Zoo^2
Temp + $Temp^2$ + Chl + Chl^2
Temp + $Temp^2$ + Zoo + Zoo^2
Sal + Sal^2 + Chl + Chl^2
Sal + Sal^2 + pCO_2 + $pCO_2{}^2$
Sal + Sal^2 + Zoo + Zoo^2
pCO_2 + $pCO_2{}^2$ + Zoo + Zoo^2
Chl + Chl^2 + pCO_2 + $pCO_2{}^2$
Chl + Chl^2 + Zoo + Zoo^2
Temp + $Temp^2$ + Chl + Chl^2 + Zoo + Zoo^2
Sal + Sal^2 + pCO_2 + $pCO_2{}^2$ + Chl + Chl^2
Sal + Sal^2 + pCO_2 + $pCO_2{}^2$ + Zoo + Zoo^2
Sal + Sal^2 + Chl + Chl^2 + Zoo + Zoo^2
pCO_2 + $pCO_2{}^2$ + Chl + Chl^2 + Zoo + Zoo^2
Sal + Sal^2 + pCO_2 + $pCO_2{}^2$ + Chl + Chl^2 + Zoo + Zoo^2

Table B.2: *Pearson's r correlations.*

Pearson's r correlations between oceanographic, egg (n=724) and larvae (n=65) data.

	Eggs			Larvae			
Variable	**Temp**	**pCO_2**	**Chl**	**Temp**	**pCO_2**	**Chl**	**Zoo**
Sal	0.77	-0.45	-0.51	0.75	-0.36	-0.49	0.03
Temp		-0.63	-0.43		-0.69	-0.46	-0.14
pCO_2			0.25			0.26	-0.02
Chl							-0.01

Table B.3: *Model selection summary results for egg presence and larva abundance.*

Summary results of model selection for the relationships between egg presence and abundance of larvae, and oceanographic variables. Values are Akaike Information Criterion scores corrected for small sample size (AICc), the change in AICc from the lowest AICc score (ΔAICc), and the Akaike weights for candidate models.

Candidate Models

Eggs	**AICc**	**ΔAICc**	**Weight**
$pCO_2 + pCO_2^2$	881.5		0.7
$Chl + Chl^2 + pCO_2 + pCO_2^2$	884.9	3.4	0.1
$Sal + Sal^2 + Chl + Chl^2$	884.9	3.4	0.1
$Sal + Sal^2 + pCO_2 + pCO_2^2$	952.8	71.3	0.0
$Sal + Sal^2$	954.4	72.9	0.0
$Temp + Temp^2 + Chl + Chl^2$	964.4	82.9	0.0
$Chl + Chl^2$	965.2	83.8	0.0
$Temp + Temp^2$	968.6	87.1	0.0
$Sal + Sal^2 + pCO_2 + pCO_2^2 + Chl + Chl^2$	976.8	95.3	0.0

Larvae	**AICc**	**ΔAICc**	**Weight**
$Zoo + Zoo^2$	384.2	0.0	0.5
$Temp + Temp^2 + Zoo + Zoo^2$	385.6	1.4	0.2
$pCO_2 + pCO_2^2 + Zoo + Zoo^2$	387.2	3.0	0.1
$Sal + Sal^2 + Zoo + Zoo^2$	387.9	3.7	0.1
$Chl + Chl^2 + Zoo + Zoo^2$	388.2	4.1	0.1
$Temp + Temp^2 + Chl + Chl^2 + Zoo + Zoo^2$	389.1	4.9	0.0
$Sal + Sal^2 + pCO_2 + pCO_2^2 + Zoo + Zoo^2$	390.6	6.4	0.0
$Sal + Sal^2 + Chl + Chl^2 + Zoo + Zoo^2$	391.5	7.3	0.0
$pCO_2 + pCO_2^2 + Chl + Chl^2 + Zoo + Zoo^2$	391.8	7.6	0.0
$Temp + Temp^2$	392.0	7.9	0.0
$pCO_2 + pCO_2^2$	393.5	9.4	0.0
$Sal + Sal^2$	394.0	9.8	0.0
$Chl + Chl^2$	394.6	10.4	0.0
$Sal + Sal^2 + pCO_2 + pCO_2^2 + Chl + Chl^2 + Zoo + Zoo^2$	394.9	10.7	0.0
$Temp + Temp^2 + Chl + Chl^2$	396.0	11.8	0.0
$Sal + Sal^2 + pCO_2 + pCO_2^2$	396.5	12.4	0.0
$Chl + Chl^2 + pCO_2 + pCO_2^2$	398.0	13.8	0.0
$Sal + Sal^2 + Chl + Chl^2$	398.0	13.9	0.0
$Sal + Sal^2 + pCO_2 + pCO_2^2 + Chl + Chl^2$	401.1	16.9	0.0

Appendix C

Chapter 4 Supplemental Information

C.1 Tables

Table C.1: *Oxygen consumption rates of larvae.*

Oxygen consumption rates (OCR) of larvae at 5 dpf standardized to individual (ind^{-1}), standard length (mm^{-1}) and average dry mass (μg^{-1}) of control or treatment larvae in EX 4. Length-based OCR are unavailable for larvae in EX 3 because no measurements of standard length were performed. Abbreviations are as follows: C= Control and T= Treatment pCO_2.

Date	EX	pCO_2	Vessel	OCR ($\mu L\ O_2\ ind^{-1}\ h^{-1}$)	OCR ($\mu L\ O_2\ mm^{-1}\ h^{-1}$)	OCR ($\mu L\ O_2\ \mu g^{-1}\ h^{-1}$)
06/20/16	1	C	1	0.24	0.064	1.42
06/20/16	1	C	2	0.13	0.037	0.78
06/20/16	1	C	3	0.20	0.055	1.18
06/20/16	1	T	1	0.16	0.045	0.91
06/20/16	1	T	2	0.19	0.051	1.05
06/20/16	1	T	3	0.15	0.041	0.84
07/04/16	2	C	1	0.11	0.032	0.66
07/04/16	2	C	2	0.09	0.026	0.56
07/04/16	2	C	3	0.10	0.028	0.57
07/04/16	2	T	1	0.15	0.043	0.87
07/04/16	2	T	2	0.12	0.033	0.67
07/04/16	2	T	3	0.11	0.031	0.62
08/02/16	3	C	2	0.31	NA	1.84
08/02/16	3	C	3	0.27	NA	1.62
08/02/16	3	T	1	0.34	NA	1.93
08/02/16	3	T	3	0.26	NA	1.49

Table C.2: *Relative abundance of NKA proteins in the crude homogenate of larvae.*

Relative abundance of NKA proteins in crude homogenates of larvae at 5 dpf. Abundance is relative to the standard, comprised of the crude homogenate of larvae from EX 1 that were reared in a cold room at 18°C in a 5 L beaker with bubbled air.

Date	EX	pCO_2	Vessel	Relative Abundance
06/20/16	1	C	1	8.0
06/20/16	1	C	2	2.4
06/20/16	1	C	3	8.1
06/20/16	1	T	1	3.7
06/20/16	1	T	2	3.6
06/20/16	1	T	3	9.4
07/04/16	2	C	1	6.8
07/04/16	2	C	2	6.9
07/04/16	2	C	3	9.4
07/04/16	2	T	1	7.3
07/04/16	2	T	2	2.9
07/04/16	2	T	3	5.7
08/02/16	3	C	2	5.2
08/02/16	3	C	3	3.2
08/02/16	3	T	1	2.8
08/02/16	3	T	3	1.2

Table C.3: *Counts of NKA-immunopositive cells on the bodies of larvae.*
Counts of the number of cutaneous immunopositive cells stained with an anti- NKA antibody and standard lengths of larvae.

Date	EX	pCO_2	No. NKA cells	Larva SL (mm)
06/20/16	1	C	680	3.2
06/20/16	1	C	654	3.0
06/20/16	1	C	829	3.2
06/20/16	1	T	733	3.1
06/20/16	1	T	609	3.0
06/20/16	1	T	690	3.0
07/04/16	2	C	472	2.6
07/04/16	2	C	376	2.4
07/04/16	2	C	379	2.6
07/04/16	2	T	748	2.9
07/04/16	2	T	746	2.9
07/04/16	2	T	743	2.9
08/02/16	3	C	568	2.6
08/02/16	3	C	443	2.6
08/02/16	3	C	680	2.8
08/02/16	3	T	635	2.9
08/02/16	3	T	637	2.7
08/02/16	3	T	653	2.9